Author(s): Priscillia Christiani

Title: Integrating multi-source geospatial data to monitor peatland red-listed plant species, greenhouse gas dynamics, and the water table

Year: 2026

Version: Publishers version

Please cite the original version:

Christiani, P. (2026). Integrating multi-source geospatial data to monitor peatland red-listed plant species, greenhouse gas dynamics, and the water table. Nordia Geographical Publications, 55(6), 1-68. https://doi.org/10.30671/nordia.186574

Priscillia Christiani is a peatland researcher whose work focuses on using geospatial and remote sensing data to monitor peatland ecosystems. In her doctoral thesis, conducted at the University of Oulu and Natural Resources Institute Finland (Luke), she investigates how environmental and remote sensing data can be combined with statistical modelling to predict the distribution of red-listed peatland plant species, greenhouse gas sink and source patterns, and water table dynamics. Her research spans multiple spatial scales, from national-level species distribution modelling to local water table monitoring using satellite and drone data. Through her work, Christiani shows that integrating multi-source geospatial data provides a practical and scalable complement to field-based monitoring, with direct applications for peatland conservation and restoration planning.

University of Oulu Graduate School

Publication of The Geographical Society of Northern Finland & Geography Research Unit at University of Oulu

ISBN 978-952-62-5003-8 (print)
ISBN 978-952-62-5004-5 (online)

Painosalama 2026

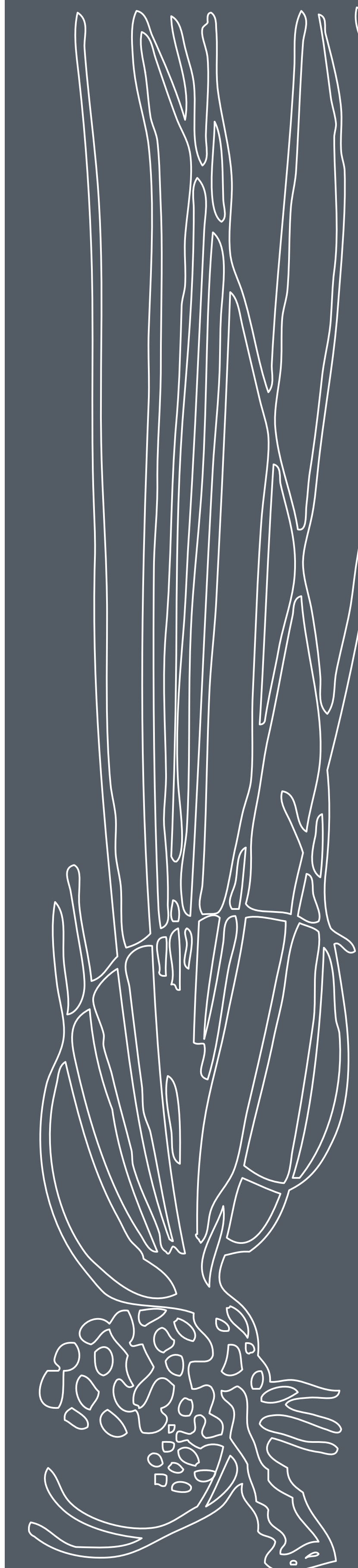

Christiani — Integrating multi-source geospatial data to monitor peatland...

nordia geographical publications 55:6

nordia geographical publications

55:6

Integrating multi-source geospatial data to monitor peatland red-listed plant species, greenhouse gas dynamics, and the water table

Priscillia Christiani

nordia
geographical
publications

volume 55 issue 6

Integrating multi-source geospatial data to monitor peatland red-listed plant species, greenhouse gas dynamics, and the water table

Priscillia Christiani

Academic dissertation to be presented with the permission of the Doctoral Training Committee for Technology and Natural Sciences of the University of Oulu Graduate School (UniOGS) for public discussion in the lecture hall L10 on the 14th of August 2026 at 12.

Supervised by

Associate Professor
Aleksi Räsänen
Geography Research Unit
University of Oulu
Finland

Professor
Anne Tolvanen
Bioeconomy and Environmental Unit
Natural Resources Institute Finland
Finland

Professor
Jan Hjort
Geography Research Unit
University of Oulu
Finland

Pre-examiners

PhD
Iuliia Burdun
Department of Earth and Environmental Sciences
KU Leuven
Belgium

Professor
Radosław Juszczak
Department of Ecology and Environmental Protection
Poznań University of Life Sciences
Poland

Opponent

Associate Professor
Martin Karlson
Department of Thematic Studies (Environmental Change)
Linköping University
Sweden

Nordia Geographical Publications is a publication of The Geographical Society of Northern Finland and Geography Research Unit at the University of Oulu. Address: PO Box 3000 FIN-90014 University of Oulu. Web: www.nordia.journal.fi. Editor-in-chief: Helena Tukiainen, helena.tukiainen@oulu.fi. Associate editors: Henriikka Salminen and Maija Toivanen. Layout editor: Oona Leppiniemi. Cover and layout design: Maija Toivanen.

ISBN 978-952-62-5003-8 (print)
ISBN 978-952-62-5004-5 (online)
ISSN 1238-2086 (print)
ISSN 2736-9722 (online)

Printed at Painosalama, Turku, 2026

Contents

Appendices are available in the printed version of this publication.

Abstract

Peatlands are important ecosystems that support biodiversity, regulate greenhouse gases (GHGs) and flooding, and help to purify water. In Finland, however, more than 50 % of peatlands have been drained to support forestry, agriculture, and peat extraction. These activities have reduced peatland biodiversity, increased GHG emissions, and altered peatland hydrology, resulting in widespread peatland ecosystem degradation. Consequently, large-scale restoration efforts have been initiated to mitigate these impacts and restore peatland functioning. As restoration progresses, regular monitoring of peatland biodiversity, GHG fluxes, and the water table (WT) is needed to track peatland conditions over time.

One approach to monitoring peatlands is field-based observation. However, this method is constrained by high costs, limited accessibility, and restricted spatial coverage. To address these limitations, this research explores the use of geospatial environmental and remote sensing (RS) data, combined with statistical modelling, as an alternative means to support peatland monitoring. First, environmental data were used to analyse whether different restoration and climate change scenarios affect the national-scale distribution of potential habitats for red-listed peatland plant species in Finland. Second, environmental data and RS data (Sentinel-1 and Sentinel-2 imagery) were compared and combined to detect national-scale patterns of potential peatland GHG sinks and sources and to evaluate which data sources provided better predictive performance. Third, environmental data were used to improve RS-based peatland WT models in three study areas ranging from 18 to 175 ha.

Environmental data were able to predict the potential habitats of peatland red-listed plant species at the national scale. Drainage and climate variables were the most important predictors. Model projections indicated that climate warming will reduce potential suitable habitats for many red-listed species, especially in the northern and middle boreal zones. However, restoration increased the amount of potential suitable habitat, reduced habitat loss, and moderated future northward shifts in species distributions. The benefits of restoration were strongest under mild climate scenarios and gradually weakened towards the end of the twenty-first century under severe warming. Although the models performed well, future studies concerning the interaction between restoration and climate change should include ecological constraints such as dispersal and species interactions to improve the realism of long-term predictions.

In detecting potential GHG sinks and sources, models combining both environmental and RS data performed best, while RS-only models had the lowest accuracy. Maps generated from environmental data alone and those from the combined dataset showed similar patterns, whereas RS-only maps displayed some differences in spatial extent. These results suggest that RS data alone are not sufficient for reliable national-scale GHG predictions and that integrating environmental and RS data is necessary to obtain accurate and realistic estimates of potential peatland GHG sink–source distributions.

At the local scale, combining RS and environmental data improved peatland WT models, both spatially and across seasons. In patterned northern boreal aapa mires, the topographic wetness index and topographic position index were important for explaining spatial WT variation. In a southern boreal drained peatland forest site, canopy height played a larger role in WT dynamics, especially across different management treatments. Uncrewed aerial vehicle data offered very high-resolution information that captured microtopography and vegetation patterns, while Sentinel-2 data allowed repeated

seasonal monitoring. These results demonstrate that multi-source RS, combined with environmental variables, can support efficient peatland WT monitoring.

Overall, this thesis shows that environmental and RS data can be used to monitor peatland red-listed species, GHG, and WT dynamics. The usefulness of environmental and RS data depends on the object being studied, the spatial scale, and site conditions, but together they provide a reliable way to observe peatland condition beyond what field measurements alone can capture. As more field data become available, and RS techniques continue to develop, these approaches will become increasingly valuable for supporting peatland conservation, restoration planning, and long-term monitoring.

Keywords: peatlands, restoration, species distribution models, water table, satellite, UAV, remote sensing

Tiivistelmä

Suot ovat tärkeitä ekosysteemejä biodiversiteetin, ilmaston ja tulvien säätelyn sekä valumavesien puhdistuksen kannalta. Suomessa kuitenkin yli 50 % soista on ojitettu metsätalouden, maatalouden ja turvetuotannon tarpeisiin, mikä on johtanut laaja-alaiseen suoekosysteemien tilan heikkenemiseen. Soiden kuivatus on heikentänyt biodiversiteettiä, lisännyt kasvihuonekaasupäästöjä ja muuttanut hydrologiaa. Tämän seurauksena on käynnistetty laajamittaisia ennallistamistoimia. Ennallistamisen edetessä tarvitaan säännöllistä soiden biodiversiteetin, kasvihuonekaasuvoiden ja pohjavedenpinnan seurantaa.

Yksi lähestymistapa soiden tilan seurantaan on maastohavainnointi, joka on kuitenkin kallista ja jonka avulla on työlästä kerätä tietoa laajoilta ja heikosti saavutettavilta alueilta. Näiden rajoitusten ratkaisemiseksi tässä tutkimuksessa tarkastellaan paikkatietopohjaisten ympäristöaineistojen ja kaukokartoituksen käyttöä yhdistettynä tilastolliseen mallinnukseen vaihtoehtoisena tapana soiden tilan seurannassa. Ensiksi ympäristöaineistojen avulla analysoitiin, miten erilaiset ennallistamis- ja ilmastonmuutosskenaariot vaikuttavat uhanalaisten suokasvien potentiaalisiin elinympäristöihin valtakunnallisella tasolla Suomessa. Toiseksi ympäristö- ja kaukokartoitusaineistoja (Sentinel-1- ja Sentinel-2-satelliittikuvat) vertailtiin potentiaalisten kasvihuonekaasunielujen ja -lähteiden valtakunnallisessa mallintamisessa. Kolmanneksi ympäristöaineistoja kokeiltiin kaukokartoituspohjaisten pohjavedenpintamallien parantamisessa kolmella tutkimusalueella, joiden pinta-ala vaihteli 18:sta 175 hehtaariin.

Ympäristöaineistojen avulla pystyttiin ennustamaan uhanalaisten suokasvien potentiaalisten elinympäristöjen esiintymistä valtakunnallisella tasolla. Tärkeimmät selittävät tekijät olivat ojitus ja ilmastomuuttujat. Malliennusteet osoittivat, että ilmaston lämpeneminen vähentää monien uhanalaisten lajien potentiaalisia soveltuvia elinympäristöjä erityisesti pohjois- ja keskiboreaalisilla vyöhykkeillä. Ennallistaminen kuitenkin lisäsi potentiaalisten soveltuvien elinympäristöjen määrää, vähensi elinympäristöjen häviämistä ja lievensi lajien levinneisyyden siirtymää pohjoiseen. Ennallistamisen hyödyt olivat suurimmat vähäisen lämpenemisen ilmastoskenaarioissa mutta heikkenivät kohti vuosisadan loppua ja voimakkaampien lämpenemisen skenaarioissa. Vaikka mallinnus toimi hyvin, tulevissa tutkimuksissa ennallistamisen ja ilmastonmuutoksen yhteisvaikutusta tulisi tarkastella ekologisten reunaehtojen kuten lajien leviämisen ja lajien välisten vuorovaikutusten avulla pitkän aikavälin ennusteiden realistisuuden parantamiseksi.

Potentiaalisten kasvihuonekaasunielujen ja -lähteiden tunnistamisessa parhaiten suoriutuivat mallit, jotka yhdistivät ympäristö- ja kaukokartoitusaineistot, kun taas pelkkiin kaukokartoitusaineistoihin perustuvat mallit olivat vähiten tarkkoja. Pelkän ympäristöaineiston ja yhdistetyn aineiston mallit tuottivat samankaltaisia alueellisia ennusteita, mutta pelkkiin kaukokartoitusaineistoihin perustuvien mallien ennustekartat erosivat muiden mallien ennustekartoista. Nämä tulokset viittaavat siihen, että kaukokartoitusaineistot yksinään eivät riitä luotettaviin valtakunnallisen tason kasvihuonekaasupäästöennusteisiin ja ympäristö- ja kaukokartoitusaineistojen yhdistäminen on välttämätöntä tarkkojen ja realististen arvioiden saamiseksi soiden potentiaalisista kasvihuonekaasunielujen ja -lähteiden sijainneista.

Paikallisella tasolla kaukokartoitus- ja ympäristöaineistojen yhdistäminen tarkensi soiden pohjavedenpinnan mallinnusta sekä alueellisesti että eri vuodenaikojen välillä. Pohjoisboreaalisilla aapasoilla topografinen kosteusindeksi ja topografinen sijainti-indeksi olivat tärkeitä pohjavedenpinnan alueellisen vaihtelun selittäjiä. Eteläboreaalisella

ojitetulla suometsäkohteella puuston latvuskorkeudella oli suurempi merkitys pohjavedenpinnan dynamiikan mallintamisessa kuin topografialla. Miehittämättömällä ilma-aluksella kerätty aineisto tarjosi tarkkaa tietoa mikrotopografiasta ja kasvillisuudesta, kun taas Sentinel-2-satelliittikuva-aineisto mahdollisti ajallisesti toistuvan seurannan. Nämä tulokset osoittavat, että monilähteinen kaukokartoitus yhdistettynä ympäristömuuttujiin mahdollistaa soiden pohjavedenpinnan tarkan seurannan.

Kaiken kaikkiaan tämä väitöskirja osoittaa, että ympäristö- ja kaukokartoitusaineistoja voidaan hyödyntää soiden uhanalaisten lajien, kasvihuonekaasuvoiden ja pohjavedenpinnan seurannassa. Ympäristö- ja kaukokartoitusaineistojen hyödyllisyys riippuu tutkittavasta kohteesta, tarkastelumittakaavasta ja kohteen olosuhteista. Yhdessä nämä aineistot tarjoavat luotettavan tavan havainnoida soiden tilaa. Maastomittausaineistojen lisääntyessä ja kaukokartoitustekniikoiden kehittyessä nämä lähestymistavat tulevat olemaan yhä arvokkaampia soiden suojelun, ennallistamissuunnittelun ja pitkäaikaisen seurannan tukemisessa.

Avainsanat: suot, ennallistaminen, levinneisyysmallinnus, pohjavedenpinta, satelliittikuvat, miehittämättömät ilma-alukset, kaukokartoitus

List of original publications

This thesis is based on the following articles, referred to by the Roman Numerals I–III.

I Christiani P, Isoaho A, Elo M, Päkkilä L, Marttila H, Aalto J, Hjort J, Tolvanen A, Rana P, & Räsänen A (2025) Negative effects of climate warming on red-listed boreal peatland plant species can be mitigated through restoration. *Biological Conservation* 306: 111126. https://doi.org/10.1016/j.biocon.2025.111126

II Christiani P, Rana P, Räsänen A, Pitkänen TP & Tolvanen A (2024) Detecting spatial patterns of peatland greenhouse gas sinks and sources with geospatial environmental and remote sensing data. *Environmental Management*, 74(3): 461–478. https://doi.org/10.1007/s00267-024-01965-7

III Christiani P, Räsänen A, Kuzmin A, Ojanen P, Minkkinen K, Korpelainen P, Rana P, Kumpula T & Isoaho A (Manuscript) Environmental variables improve remote sensing-based water table monitoring in peatlands.

Author’s contributions

I Christiani compiled datasets that were originally collected by co-authors or obtained from publicly available sources. She designed the study together with the supervisors, conducted all analyses independently, and contributed to writing the original manuscript with the co-authors.

II Christiani compiled datasets that were originally collected by co-authors or collaborators, or obtained from publicly available sources. She designed the methodology with the supervisors, conducted all analyses independently, and contributed to writing the original manuscript together with the co-authors.

III Christiani compiled datasets that were originally collected by co-authors or obtained from publicly available sources. She conducted all modelling and analyses independently and contributed to writing the original manuscript with the co-authors.

Overview of each author’s contributions to Papers I–III. Bold underlined initials denote the thesis author, Christiani.

Paper	Idea & design	Data collection & pre-processing	Analysis	Writing
I	**PC**, AR	PR (red-listed species data), JA (climate data)	**PC**	**PC**, AI, ME, LP, HM, JA, JH, AT, PR, AR
II	AR, **PC**	PO, KM (GHG data), TPP & AI (satellite data)	**PC**	**PC**, PR, AR, TPP, AT
III	AI	AI, AR, KM, PO (WT data); AK & PK (UAV data); AI (satellite data)	AI, **PC**, AR	**PC**, AR, AK, PO, KM, PK, PR, TK, AI

PC = Priscillia Christiani, AR = Aleksi Räsänen, AI = Aleksi Isoaho, PR = Parvez Rana, JA = Juha Aalto, ME = Merja Elo, LP = Lassi Päkkilä, HM = Hannu Marttila, JH = Jan Hjort, AT = Anne Tolvanen, TPP = Timo P. Pitkänen, AK = Anton Kuzmin, PO = Paavo Ojanen, KM = Kari Minkkinen, PK = Pasi Korpelainen, TK = Timo Kumpula.

I did not use generative language models in the planning or conduct of the analyses of this dissertation. Generative AI technologies were used solely to support writing tasks such as grammar and spelling checks, after which the dissertation was proofread by a professional proofreader. I take full responsibility for the content of this dissertation.

Acknowledgements

This research was funded by the Natural Resources Institute Finland (Luke), the Finnish Ministry of the Environment (EkoSuo), and the European Union (projects Hydrology LIFE, LIFE PeatCarbon, Priodiversity LIFE, ALFAwetlands), with additional support from Kone Foundation for the finalization of this thesis.

I would like to express my sincere gratitude to my supervisors, Aleksi Räsänen, Anne Tolvanen, and Jan Hjort, for their guidance and support throughout my doctoral studies. Their advice has been invaluable in developing my research skills and confidence. I also wish to thank my follow-up group, Janne Alahuhta and Jussi Peuhkurinen, for their positive and encouraging discussions during our meetings.

This thesis is the result of collective effort, and I am grateful to all co-authors for providing data and feedback that made this work possible. Special thanks go to Aleksi Isoaho for his direct contributions to the published articles. I would also like to sincerely thank the pre-examiners, Iuliia Burdun and Radosław Juszczak, for their careful reading of this thesis and their thoughtful comments, and the opponent, Martin Karlson, for his time and effort for the defence.

I am also grateful to my group manager, Anne Ojala, for her support with administrative matters at Luke, and to the Luke Oulu office for providing a collegial and motivating work environment.

Finally, I wish to thank my family and friends for their unwavering encouragement. I never expected to pursue a doctoral degree, but your support made this journey possible.

Oulu, 18 May 2026
Priscillia Christiani

Glossary

Aapa mire: A type of northern boreal peatland characterized by patterned string–flark microtopography and a mixed water supply from precipitation and groundwater.

Area under the curve (AUC): A statistical measure of model performance derived from the receiver operating characteristic (ROC) curve, indicating the ability of a model to discriminate between presence and absence, where 1 indicates perfect classification.

Canopy height model (CHM): A raster representing vegetation height, calculated as the difference between the digital surface model (DSM) and digital terrain model (DTM).

Continuous Boyce Index (CBI): An evaluation metric for presence-only species distribution models that measures how well predicted suitability values correspond to observed presences.

Drainage: The process of lowering the peatland water table through ditching or other hydrological modification, typically for forestry or agriculture.

Environmental data (ENV): Spatial GIS-based datasets describing climatic, topographic, hydrological, and soil conditions. Some environmental data may also be derived from remote sensing.

Fen: Minerotrophic peatland that receives nutrient inputs from surrounding mineral soils or groundwater, typically supporting rich vegetation.

Flark: The wetter, low-lying parts of patterned aapa mires, often dominated by sedges and mosses.

Geographic Information System (GIS): A technology for collecting, managing, analysing, and visualising spatial or geographic data.

Greenhouse gas (GHG): Atmospheric gases such as carbon dioxide (CO_2), methane (CH_4), and nitrous oxide (N_2O) that trap heat and contribute to climate change.

Growing degree days (GDD): A measure of accumulated heat used to estimate plant and insect development. GDD is calculated by summing the daily temperatures above a base threshold (commonly 5 °C). Higher GDD values indicate a warmer, longer growing season.

Light Detection and Ranging (LiDAR): A remote sensing method that measures distances using laser pulses to generate detailed three-dimensional information on surface elevation and vegetation structure.

Maximum entropy (MaxEnt): A presence-only modelling algorithm that estimates the spatial distribution of a targeted object by finding the probability distribution of maximum entropy constrained by environmental predictors.

Partial dependence plot (PDP): A graphical method showing the marginal effect of a predictor variable on a model's predicted response while holding other variables constant.

Random Forest (RF): A non-parametric machine learning algorithm that builds an ensemble of decision trees to model nonlinear and complex relationships.

Remote sensing (RS) data: Satellite- and uncrewed aerial vehicle-derived data.

Representative Concentration Pathway (RCP): A standardised greenhouse gas concentration scenario used in climate modelling to project future climate conditions.

Restoration: Management actions intended to recover the natural hydrology, vegetation, and ecosystem functions of degraded ecosystems.

Restoration level (REST): A simulated proportion of drained peatlands assumed to be restored in model scenarios (e.g. REST0–REST100).

Rewetting: A restoration method to raise the water table of drained peatlands towards natural levels, often by blocking ditches.

SAGA Wetness Index (SWI): A topographic index estimating relative soil moisture based on slope and flow accumulation derived from a digital terrain model.

Species distribution model (SDM): A statistical framework linking species occurrence data to environmental predictors to estimate or project suitable habitat.

String: The drier, elevated ridges in patterned aapa mires that alternate with wetter flarks.

Topographic Position Index (TPI): A terrain metric that describes whether a location is situated in a depression or on an elevation relative to its surroundings. TPI_5m and TPI_10m indicate the index was calculated using 5 m and 10 m neighbourhood radius, respectively.

Topographic Wetness Index (TWI): A hydrological terrain index representing the spatial distribution of potential soil moisture based on upslope contributing area and local slope.

True Skill Statistic (TSS): A model evaluation metric that balances sensitivity and specificity to measure predictive accuracy.

Water balance (WAB): An index describing the balance between water supply (precipitation) and water loss (evapotranspiration). A positive WAB means moisture surplus; a negative WAB indicates drought or moisture deficit.

Water table (WT): The vertical distance between the ground surface and the water level.

List of abbreviations

AUC	Area under the curve
BIRCH	Mean volume, birch
BLUE	Blue reflectance
CBI	Continuous Boyce Index
CHM	Canopy height model
CH_4	Methane
CO_2	Carbon dioxide
DEM	Digital elevation model
DRAINED	Proportion of drained peatlands in grid square
DSM	Digital surface model
DTD	Distance to drainage
DTM	Digital terrain model
DTW	Depth to water
ES	Early summer
EVI	Enhanced Vegetation Index
FMI	Finnish Meteorological Institute
GDD	Growing degree days
GDVI	Generalised difference vegetation index
GEE	Google Earth Engine
GHG	Greenhouse gas
GIS	Geographic information system
GNDVI	Green normalised difference vegetation index
GREEN	Green reflectance
GTK	Geological Survey of Finland
LiDAR	Light detection and ranging
LS	Late summer
Luke	Natural Resources Institute Finland
MaxEnt	Maximum entropy
MB	Middle boreal
MNDWI	Modified normalised difference water index
MS	Midsummer
MSI	Moisture stress index
MS-NFI	Multi-source National Forest Inventory
N_2O	Nitrous oxide
NB	Northern boreal
NDMI	Normalised difference moisture index
NDMI2	Normalised difference moisture index 2
NDRE	Normalised difference red edge index
NDVI	Normalised difference vegetation index
NDWI	Normalised difference water index
NIR	Near-infrared reflectance
NLS	National Land Survey of Finland
OPEN	Proportion of open peatlands in grid square
OTHER	Mean volume, other broad-leaved trees
PDP	Partial dependence plot
PINE	Mean volume, pine
RCP	Representative Concentration Pathway

RE .... Red edge reflectance
RE1–4................................. Red edge bands 1–4 reflectance
RED.................................... Red reflectance
RF.. Random forest
RMSE.................................. Root mean square error
ROCK.................................. Presence of calcareous rock in grid square
ROOT_BIOMASS .... Mean root biomass (spruce, pine, other broadleaves)
RS .... Remote sensing
SAR .... Synthetic aperture radar
SAVI .... Soil adjusted vegetation index
SB .... Southern boreal
SDM .... Species distribution model
SPRUCE .... Mean volume, spruce
ST1-HERB .... Herb-rich type
ST2-BILB .... Bilberry (*Vaccinium myrtillus*) type
ST3-LING .... Lingonberry (*Vaccinium vitis-idaea*) type
ST4-SHRUB .... Shrub type
ST6-LICHEN .... Lichen (*Cladina*) type
STR .... Shortwave infrared transformed reflectance
SWI .... SAGA wetness index
SWIR1.............................. Shortwave infrared band 1 reflectance
SWIR2 .... Shortwave infrared band 2 reflectance
Syke .... Finnish Environment Institute
TJan .... January temperature
TPI .... Topographic position index
TSS .... True skill statistics
TWI .... Topographic wetness index
UAV .... Uncrewed aerial vehicle
UNDRAINED .... Proportion of undrained peatlands in grid square
VH .... Vertical transmit and horizontal receive
VV .... Vertical transmit and vertical receive
WAB .... Water balance
WT .... Water table

1 Introduction

1.1 Peatland ecology and emerging challenges

To define peatland, it is first necessary to explain what peat is. Peat is an accumulation of incompletely decomposed plant material in the soil. Decomposition remains incomplete because it slows under long-term water-saturated, cool, acidic, and oxygen-poor conditions (Rydin & Jeglum 2006; Strack 2023). Therefore, under these conditions, organic matter accumulates over centuries and forms peat deposits. Peatland refers to land that is covered by peat, and in Finland it is usually defined as having at least 30 cm of peat (Joosten & Clarke 2002; Rydin & Jeglum 2006). The term "mire" is also used in some contexts and refers to a peatland that is still actively forming peat (Joosten & Clarke 2002).

Peatlands are often classified based on their water sources and nutrient status. Ombrotrophic peatlands (bogs) receive water only from rainfall and are nutrient-poor and acidic (usually pH < 4), while minerotrophic peatlands (fens, swamps) receive mineral-rich water from surrounding soils and therefore range from nutrient-poor to nutrient-rich (Vasander 1996). In addition to these general classifications, many countries apply region-specific peatland classification systems. For example, in Canada, peatlands are classified into bogs, fens, marshes, swamps, and shallow water according to the Canadian Wetland Classification System (Zoltai & Vitt 1995). In Finland, peatlands are divided into southern raised bogs, which are dome-shaped and ombrotrophic, and the northern aapa mire zone, characterised by shallower peat layers and a patterned surface of elevated strings and wet flarks (Figure 1; Granlund et al. 2022; Laitinen et al. 2007).

1.1.1 The ecological importance of pristine peatlands

In a pristine state, peatlands are home to plant species that are well adapted to wet, acidic, and nutrient-poor environments (Harris et al. 2015; Small 1972). Peatland are dominated by mosses, particularly *Sphagnum*, and also support vascular plants (trees, shrubs, forbs, and graminoids) and lichens. *Sphagnum* is especially important because it contributes largely to peat formation and can tolerate prolonged water saturation and low-oxygen conditions, allowing it to dominate peatland vegetation (Rydin & Jeglum 2013; Small 1972). In addition, *Sphagnum* actively modifies peatland environment by retaining water, lowering pH, and restricting nutrient availability, thereby creating conditions that are unfavourable for most vascular plants (Malmer et al. 2003; Rochefort 2000; Van Breemen 1995). Consequently, an increase in dense shrub or tree cover may indicate environmental changes such as warming and drying (Holmgren et al. 2015).

Peatlands are important for climate regulation because they store a large amount of carbon. Although they cover only 3 % of Earth's surface (Xu et al. 2018), they contain roughly 400–1000 Gt global soil carbon (Nichols & Peteet 2019; Yu et al. 2010). Natural peatlands usually act as long-term sinks for carbon dioxide (CO_2) because plant production exceeds decomposition under wet and oxygen-poor conditions (Vasander 1996). At the same time, peatlands also release methane (CH_4; Frolking et al. 2011). CH_4 emissions depend primarily on WT level, temperature, and the availability of organic substrates for microbial activity (Duan et al. 2025). CH_4 is produced in deeper, anoxic peat layers and reaches the surface by diffusion or ebullition, or through plant aerenchyma, especially in sedges and other sedge-like species (Vasander 1996). Some of the CH_4 is oxidised in the oxygen-rich upper peat layers before it reaches the

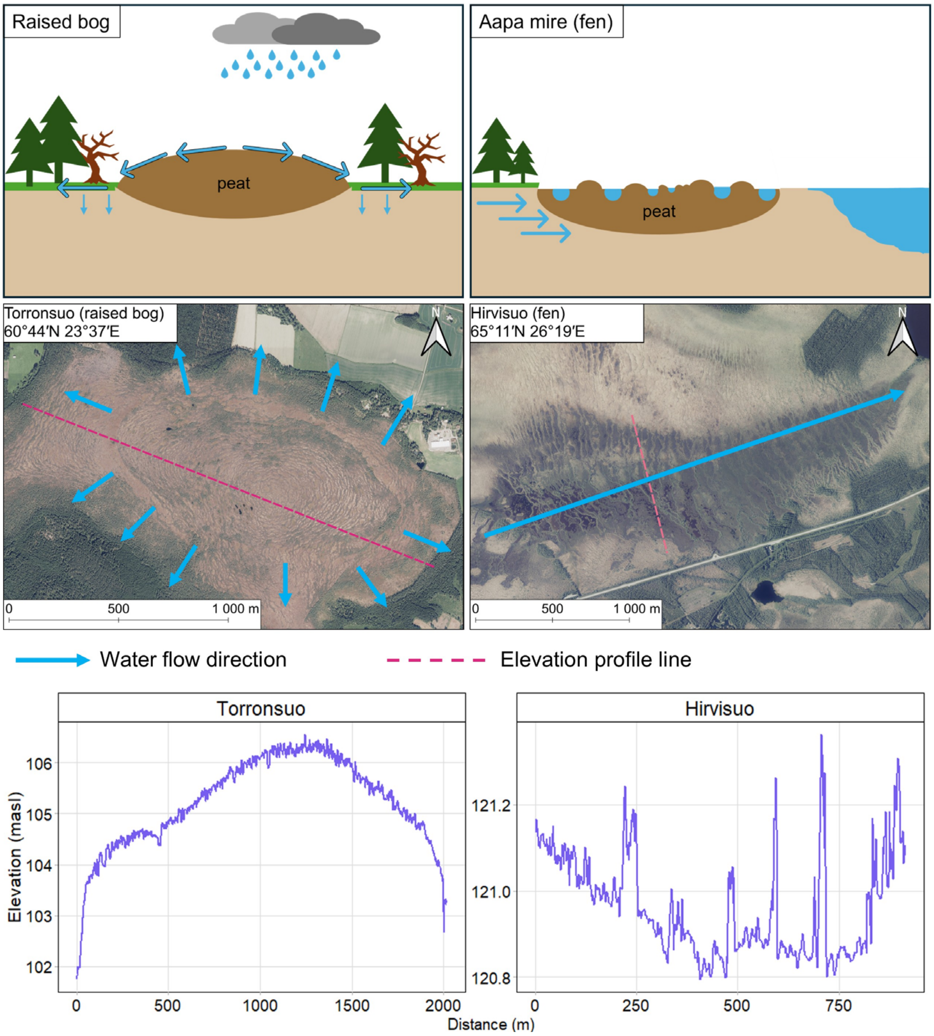

Figure 1. Conceptual and site-based illustration of raised bogs and aapa mires in Finland, with orthophotos and terrain height profiles derived from the National Land Survey of Finland (2025). Distance is in metres, and elevation is in metres above sea level.

atmosphere. CO_2 and CH_4 fluxes fluctuate diurnally and seasonally. For example, CO_2 uptake is higher during the daytime but lower during fall and winter when there is limited photosynthesis (Golovatskaya & Dyukarev 2011; Vasander 1996), and CH_4 emissions often increase during warmer periods (Long et al. 2010). In contrast to CO_2 and CH_4, nitrous oxide (N_2O) emissions from pristine peatlands are usually smaller because nitrate production is limited under acidic and waterlogged conditions (Minkkinen et al. 2020; Vasander 1996). In some cases, peatlands may even act as small sinks for N_2O due to microbial reduction processes.

1.1.2 Human pressures and degradation of peatlands

Human activity has significantly altered peatland ecosystems worldwide. Globally, peatlands cover only about 3 % of Earth's land surface, and currently 11–15 % of global peatlands are degraded (Leifeld & Menichetti 2018; UNEP 2022). Despite representing a small fraction of global peatlands, drained sites contribute disproportionately to climate change, accounting for roughly 5 % of global anthropogenic CO_2 emissions (Joosten 2009, 2016). In northern regions, including Finland, drainage pressures are particularly intense. Finland had more than 10 million hectares of peatlands in the 1950s, accounting for roughly one-third of its land area. Since then, over half of the peatlands have been drained for forestry and also for agriculture and peat extraction (Korhonen et al. 2021). Drainage has been a major driver of peatland degradation, driven largely by the need to enhance timber production (Vasander 1996). Drainage alters vegetation primarily by lowering the water table (WT). As peat becomes drier and more oxidised, peatland plant communities shift towards forest-type vegetation (Laine et al. 2006; Maanavilja et al. 2014). Species dependent on a high, stable WT and nutrient-poor conditions, such as many *Sphagnum* mosses and sedges, decline rapidly as their niches contract. Therefore, biodiversity loss is inevitable; in Finland, there are currently 85 red-listed vascular plant and bryophyte species which depend on peatlands as their primary habitats, and another 127 rely on them as secondary habitats (Hyvärinen et al. 2019).

Drainage-induced WT drawdown also disrupts peatland carbon cycling, often converting natural long-term carbon sinks into net greenhouse gas (GHG) sources (Leifeld & Menichetti 2018; Wilkinson et al. 2023). A lower WT accelerates aerobic decomposition and raises CO_2 emissions. CH_4 emissions from the peat surface typically decrease because methanogenesis is suppressed under drier conditions (Abdalla et al. 2016), but this reduction is partly offset by ditch networks, which act as significant CH_4 hotspots and may contribute 3.5 Tg CH_4 yr^{-1} globally (Peacock et al. 2021). N_2O emissions can also rise following drainage, especially in nutrient-rich peatlands where enhanced nitrification fosters elevated fluxes (Minkkinen et al. 2020).

1.1.3 Restoring and managing disturbed peatlands

Ecological restoration is an important means to return degraded ecosystems towards pristine functioning and to mitigate climate and biodiversity impacts. Restoration is implemented to protect and safeguard biodiversity (Maanavilja et al. 2014), reduce GHG emissions (Evans et al. 2021; Richardson et al. 2022), and rebuild long-term carbon sequestration and storage (Schwieger et al. 2021; Wilson et al. 2022). Global, regional, and national policies increasingly underline the urgency of such actions. For example, the Global Biodiversity Framework calls for effective restoration of 30 % of degraded peatlands by 2030, while the European Union (EU) Restoration Regulation targets restoration of 90 % of degraded ecosystems by 2050 (Regulation [EU] 2024/1991, 2024). These initiatives are expected to substantially accelerate peatland restoration across Europe in the coming decades.

For peatlands, ecological restoration focuses on restoring natural hydrology (Haapalehto et al. 2011; Menberu et al. 2017). The main method is rewetting, which usually involves raising the WT by blocking, filling, or damming drainage ditches (Andersen et al. 2017). In Finland and elsewhere, tree removal is also commonly applied where forestry-drained peatlands have dense stands which are not originally present in the native ecosystem (Vasander et al. 2003). Rewetting restores the peatland hydrological condition, which is necessary for peat-forming vegetation, especially *Sphagnum* mosses, and triggers the return of pristine-state plant communities (Haapalehto et al. 2011; Menberu et al. 2016). However, habitat specialists—especially plants that are sensitive to changes in water levels or nutrients—recover slowly or only partially. Long-term studies indicate that although restored sites recover gradually, they rarely become fully identical to pristine sites, even after many years (Elo et al. 2024; Haapalehto et al. 2017; Maanavilja et al. 2014).

WT level is a key factor regulating the biogeochemical processes that drive peatland GHG dynamics (Evans et al. 2021; Richardson et al. 2022). Studies show that restoring boreal forestry-drained peatlands can potentially bring CO_2 and CH_4 exchange back to levels similar to natural peatlands (Laine et al. 2019a; Purre et al. 2019; Urbanová et al. 2013), but the climate benefits of restoration vary greatly between peatland types and restoration measures (Laine et al. 2024; Ojanen & Minkkinen 2020). Nutrient-poor drained peatlands already have low soil CO_2, CH_4, and N_2O emissions (Alm et al. 2023; Minkkinen et al. 2020; Ojanen et al. 2013), aside from ditches (Alm et al. 2023; Ojanen et al. 2010). Restoring these sites might raise CH_4 emissions and remove the tree-based carbon sink, limiting their mitigation potential (Ojanen & Minkkinen 2020; Wilson et al. 2016). In contrast, nutrient-rich drained peatlands emit much more CO_2 and N_2O, making them better candidates for climate mitigation through rewetting (Alm et al. 2023; Minkkinen et al. 2020; Ojanen & Minkkinen 2020).

1.1.4 Peatland under a changing climate

Arctic and boreal regions are warming faster than the global average, and this includes most northern peatland areas (Post et al. 2019; Rantanen et al. 2022). Over the past decades, annual precipitation in these regions has increased, and warming is altering not only mean temperatures but also extremes, seasonality, and disturbance regimes such as fire (Box et al. 2019; Byrne et al. 2024). Climate change is already altering biodiversity, shifting species distributions and affecting population sizes, and these responses will unfold over multiple time scales from years to centuries (Campbell et al. 2021; Minayeva & Sirin 2012). As a result, northern peatlands are expected to play an increasingly important role in future climate–carbon feedback.

Rising temperatures, shifting precipitation patterns, and increasing evapotranspiration change peatland water balance (WAB; precipitation minus evapotranspiration). Warming causes plants to lose water faster through transpiration and soils to dry out more quickly. At the same time, climate projections suggest generally higher precipitation in northern regions but with strong seasonality and more frequent droughts and heavy-rain events (IPCC 2013; Lehtonen et al. 2014). Consequently, even where total precipitation increases, WAB during the growing season may decline in some areas, especially in well-drained or sloping peatlands (Gorham 1991; Roulet et al. 1992; Swindles et al. 2019). In permafrost regions, warming also deepens the active layer and promotes permafrost thaw, which can either dry peat (on raised features) or increase wetness through surface subsidence and ponding (Baltzer et al. 2014; Minayeva & Sirin 2012). Therefore, climate change is expected to increase spatial and temporal variability in peatland moisture conditions.

Climate-driven changes in hydrology and temperature also affect peatland vegetation and species composition. Many peatland plants are adapted to waterlogged and nutrient-poor conditions, yet individual species can tolerate broad ranges of pH, WT, and nutrient gradients (Minayeva & Sirin 2012; Rydin & Jeglum 2006). As climates warms, most species tend to shift towards higher latitudes and elevations (Parmesan 2006; Sun et al. 2020; Wei et al. 2021), although these shifts are often constrained by limited dispersal ability. Ma et al. (2022) showed that suitable habitat for several dominant *Sphagnum* species will expand in high-latitude peatlands north of 50°N but contract strongly at the southern edge of the boreal zone, which may become a hotspot for sink–source transitions. At the local scale, warming, WT drawdown, and increased nitrogen deposition are expected to promote invasion and dominance of vascular plants, especially graminoids and shrubs, at the expense of *Sphagnum* (Dieleman et al. 2014).

Restoration through rewetting may increase peatland resilience to climatic drying by partially re-establishing WT levels, although the net climate response remains site- and timescale-dependent due to interacting CO_2 and CH_4 fluxes (Laine et al. 2024). In contrast, both drainage and climate warming tend to lower the WT, and even a modest WT decline can increase ecosystem respiration and alter the net CO_2 balance (Laine et al. 2019b; Mäkiranta et al. 2018). Previous projections estimated WT declines of around 8–22 cm under warmer conditions, mainly due to higher evapotranspiration (Gorham 1991; Roulet et al. 1992), but more recent work points to regionally variable outcomes because precipitation is also increasing and droughts and floods may both become more frequent (Wu & Roulet 2014). In fens, which are adapted to continuous throughflow of mineral-rich water, a WT drop tends to cause faster and stronger ecological and biogeochemical responses than in ombrotrophic bogs (Komulainen et al. 1999; Wu & Roulet 2014). Drying generally favours deeper aeration, higher CO_2 emissions and lower CH_4 emissions, while rewetting or permafrost thaw can raise WTs, maintain anoxic conditions and promote CH_4 release (Evans et al. 2021). Thus, future WT trajectories will largely determine whether peatlands dry and emit more CO_2 or become wetter with higher CH_4 emissions.

1.2 Statistical analysis using environmental and remote sensing data in peatland studies

Monitoring peatland red-listed species, GHG fluxes, and the WT at the scales needed for management is challenging. Traditional field-based monitoring becomes labour-intensive, time-consuming, and costly (Besson et al. 2022; Kays et al. 2015) if we aim to record all occurrences of red-listed plant species and measure GHG sinks and sources and the WT at many points, especially in large peatland areas that are often remote and far from road access. These challenges are expected to intensify with the implementation of the EU Nature Restoration Law, which places strong emphasis on large-scale peatland restoration and requires regular assessment of restoration outcomes. Consequently, there is a growing need for simplified, scalable monitoring approaches. Spatial modelling that integrates environmental and remote sensing (RS) data can complement field measurements and support regular, large-scale monitoring of peatland restoration (Lees et al. 2018).

1.2.1 Modelling approaches for peatland studies

Peatland red-listed plant species and GHG fluxes prediction can be built on the framework of species distribution models (SDMs). Although often referred to as SDMs, these modelling techniques can be applied to other spatial ecological variables, including the location of peatlands (Wu et al. 2025) and specific peatland types, such as fens (Raney & Leopold 2018) and palsa mires (Leppiniemi et al. 2025), and GHG balances (Parkkari et al. 2017). SDMs explain how the occurrence or abundance of a species or other variable is related to environmental conditions and then use these relationships to predict where suitable conditions occur in space. They are usually rooted in a niche-based view, where a species persists where environmental conditions allow births to balance or exceed deaths, and they combine ecological knowledge with statistical and geographic information system (GIS) tools (Araújo & Guisan 2006; Elith & Leathwick 2009). In practice, SDMs work in environmental space: They relate species records to climate, topography, soils, or habitat variables and then project these relationships back into geographic space to obtain maps of potential habitat or distribution.

Building an SDM involves several linked steps: assembling species occurrence (and, if available, absence) data; selecting predictors that are ecologically meaningful for the target species; dealing with spatial bias and correlations among predictors; choosing a modelling algorithm; fitting the model; evaluating its performance with independent or withheld data; and mapping predictions, sometimes after converting continuous suitability to binary presence–absence (Araújo et al. 2019; Elith & Leathwick 2009). Conceptually, important issues include the choice of spatial scale, the distinction between modelling the niche versus the realised geographic distribution, and the different aims of explanation versus prediction (Araújo & Guisan 2006). SDMs are also subject to several sources of uncertainty: sampling biases, model parameterisation, model selection and evaluation, and differences among species, for example the tendency for specialist species to appear better predicted than generalists (Jiménez□ Valverde et al. 2008). Despite these limitations, SDMs provide a robust framework for integrating field, environmental, and RS data, making them a useful tool for modelling species or other variable distributions in peatland studies.

SDMs increasingly draw on machine learning algorithms because these methods offer flexible, data-driven ways to learn complex relationships between species occurrences and environmental predictors. The conceptual foundation of SDMs fits naturally with machine learning's strength in pattern recognition and prediction (Elith & Leathwick 2009). Among the available machine learning algorithms, maximum entropy (MaxEnt) and random forest (RF) are widely used in peatland studies for modelling species distributions and other spatial ecological variables (Hamedianfar et al. 2025; Keränen et al. 2024; Leppiniemi et al. 2025; Oke & Hager 2017; Räsänen et al. 2022).

MaxEnt treats the species distribution as a probability distribution over all sites in the landscape and estimates this distribution under a set of constraints derived from the observed presences (Phillips & Dudík 2008; Phillips et al. 2017). In practice, MaxEnt represents the true, unknown distribution by another probability distribution that matches the empirical averages of a set of environmental "features" at the presence locations. Because these constraints usually do not uniquely determine the distribution, MaxEnt selects, among all distributions that satisfy them, the one with maximum entropy, i.e. the most spread-out or least constrained distribution consistent with the data (Elith et al. 2011; Phillips et al. 2017). MaxEnt implements several feature classes derived from continuous and categorical predictors, including linear, quadratic, product, threshold, hinge, and categorical indicator features, allowing the model to capture means, variances, covariances, and more complex responses to environmental gradients (Phillips & Dudík 2008). Working with presence-only data and a set of background points, MaxEnt produces continuous suitability values ranging from 0 (least suitable) to 1 (most suitable), which are commonly interpreted as indices of relative habitat suitability (Merow et al. 2013; Phillips & Dudík 2008). However, the interpretation of MaxEnt outputs depends on strong assumptions about how presence data have been sampled, and this has been widely debated (Merow et al. 2013). If presences are treated as a random sample of individuals, it is natural to interpret predictions as relative occurrence rates, but this requires assuming that sampling intensity is proportional to local population density, which is often unrealistic (Merow et al. 2013). Alternatively, if grid cells are assumed to have been sampled at random, then logistic output can be interpreted as probability of presence, but this rests on assumptions that have been criticised and may not hold in practice, especially when sampling bias or multiple individuals per cell are likely (Merow et al. 2013; Phillips & Dudík 2008). Despite its limitations, MaxEnt has been widely used in ecological modelling due to its ability to handle small sample sizes, nonlinear relationships, and complex interactions among predictors (Elith et al. 2011; Phillips & Dudík 2008).

RF is a flexible ensemble learning algorithm that can be used for both classification and regression, allowing it to model categorical and continuous response variables. RF builds a large number of decision trees using bootstrap samples of the data and combines their predictions following Breiman's framework for regression and classification (Breiman 2001). At each split, only a random subset of predictors is considered, which decorrelates the trees and reduces overfitting. For regression tasks, predictions are obtained by averaging the outputs of all trees in the ensemble, while for classification tasks, predictions are based on majority voting or class probabilities (Breiman 2001). RF can capture complex nonlinear relationships and interactions among predictors, handle large datasets, and provide measures of variable importance, while being relatively robust to multicollinearity (Belgiu & Drăguţ 2016).

1.2.2 Remote sensing data for peatland monitoring and prediction

To build prediction models for any variable of interest, a set of predictor variables describing the environmental characteristics of the study area is required. RS data are particularly well suited for this purpose, as they offer consistent, spatially explicit measurements over large spatial extents. RS data refers to information acquired about objects or areas without direct contact, using sensors operating at a distance. RS sensors can be broadly classified into passive sensors, which measure naturally emitted or reflected electromagnetic radiation (e.g. optical and thermal sensors), and active sensors, which transmit their own signal and record the backscattered response (e.g. radar and light detection and ranging [LiDAR]). RS data range from satellite observations to low-altitude uncrewed aerial vehicle (UAV) data.

Passive optical satellite sensors with moderate to high spatial resolution, including MODIS (250–1000 m), Landsat (30 m), and Sentinel-2 (10–20 m), provide repeated imagery suitable for regional monitoring of vegetation and surface conditions (Bechtold et al. 2018; Harris et al. 2015; Räsänen et al. 2020, 2022). Active radar satellites, for example Sentinel-1, provide C-band synthetic aperture radar (SAR) data that are sensitive to surface roughness, vegetation structure, and moisture and are largely independent of cloud cover and illumination conditions (Asmuß et al. 2019; Bechtold et al. 2018; Lees & Artz & et al. 2021). At finer spatial scales, UAVs equipped with optical (RGB and multispectral), thermal, or active LiDAR sensors deliver ultra-high-resolution data that capture peatland microtopography and vegetation patterns in detail (Dronova et al. 2021; Ikkala et al. 2022; Räsänen & Virtanen 2019).

RS data provide spectral indices that can be used as proxies for vegetation, moisture, and other surface conditions. In the optical domain, spectral bands across the visible (red, green, blue), near-infrared (NIR), and shortwave infrared (SWIR) respond sensitively to changes in peatland hydrology, as increasing moisture generally reduces reflectance (Harris & Bryant 2009; Isoaho et al. 2023; Räsänen et al. 2022; Sadeghi et al. 2015). NIR and SWIR each consist of multiple individual bands capturing different portions of the infrared spectrum, while visible bands capture the range detectable by the human eye. From this set of optical bands, vegetation and moisture indices such as normalised difference vegetation index (NDVI; Rouse et al. 1974), normalised difference moisture index (NDMI; Gao 1996), and normalised difference water index (NDWI; McFeeters 1996) are derived and have been used to characterise greenness, vegetation cover, and wetness.

While RS cannot directly observe belowground wetness, surface soil moisture is often closely linked to the WT via capillary connectivity, and vegetation patterns also respond to long-term hydrological conditions (Breeuwer et al. 2009; Lafleur et al. 2005; Potvin et al. 2015, 2015; Strack & Price 2009). Both moisture and vegetation can be tracked with optical, thermal, and radar data (Meingast et al. 2014; Pang et al. 2023; Räsänen & Virtanen 2019). Trapezoid-based models such as the optical trapezoid model, which relies solely on optical reflectance, and the temperature vegetation dryness index, which combines optical and thermal information, have shown strong relationships with soil moisture and water table level (Burdun et al. 2020a, 2020b; Holidi et al. 2019; Räsänen et al. 2022). Furthermore, several studies have reported strong correlations between optical reflectance or indices and the WT or soil moisture, often outperforming passive and active microwave and thermal variables (Burdun & Bechtold & Sagris & Lohila & et al. 2020; Burdun et al. 2023; Kolari et al. 2022; Räsänen et al. 2022). At the same time, combining optical and SAR features in multi-sensor models can further improve WT predictions (Lees et al. 2021a; Räsänen et al. 2022). These approaches have been applied both with UAV data, which enable ultra-high-resolution modelling of WT patterns in open peatlands (Isoaho et al. 2023), and with satellite data, which allow spatiotemporal analyses of restoration impacts and long-term hydrological change at landscape scales (Burdun et al. 2020b; Isoaho et al. 2024; Kalacska et al. 2018; Räsänen et al. 2022).

RS is increasingly used to monitor GHG dynamics in peatlands. Räsänen et al. (2021) showed that continuous RS-derived predictors—particularly VH-polarised (vertical transmit, horizontal receive) Sentinel-1 backscatter, Sentinel-2 predictors (such as water vapour, blue, and coastal aerosol bands), the topographic wetness index (TWI), and other digital terrain model (DTM) features—explained up to 76 % of the variance in CH_4 fluxes, and that modelling sinks and sources separately improved the representation of spatial patterns compared to land-cover maps. For CO_2, optical and thermal satellite data have been used to estimate gross primary productivity, ecosystem respiration, and net ecosystem exchange through empirical relationships, for example using light-use-efficiency or temperature–greenness models that combine vegetation indices (e.g. NDVI, EVI) with land surface temperature (Junttila et al. 2021; Lees et al. 2021b). Additionally, RS-derived proxies related to vegetation structure and composition—used to estimate canopy height, biomass, species richness, and species composition—have been linked to belowground carbon stocks using structural equation models and UAV or hyperspectral data, improving predictions compared with purely data-driven models (Lopatin et al. 2019). Proximal visible and near-infrared spectroscopy combined with high-resolution LiDAR-derived digital elevation models (DEMs) has also enhanced mapping of soil organic carbon and total nitrogen in peat soils (Mendes & Sommer 2023; Mendes et al. 2022), while land-use classifications from Sentinel-2 have been used together with Intergovernmental Panel on Climate Change emission factors to estimate CO_2 emissions from degraded raised bogs at the national scale (Habib et al. 2024).

1.2.3 GIS-based environmental data as ecological predictors

RS can be used to generate GIS-based environmental datasets that serve as ecological predictors in statistical models. These data typically include topographic variables (elevation, slope, TWI), climatic variables (temperature, growing degree days [GDD], WAB), soil and geological variables (soil type, peat depth, fertility, bedrock type), and land-cover and land-use variables (peatland type, forest type, drained vs. undrained area, human influence; Figure 2). GIS-based environmental data can provide full spatial coverage, often nationally or globally, enabling field measurements of species distributions, GHG sinks and sources, and WT at plots to be upscaled to local or national scales. However, many environmental datasets are static or represent long-term averages and thus cannot capture short-term dynamics associated with extreme events or rapid management changes. Some variables (e.g. drainage intensity, the TWI, land-cover class) serve only as indirect proxies for ecological processes and may oversimplify complex local conditions. Moreover, adding numerous environmental layers does not automatically improve model performance; instead, careful selection of ecologically meaningful predictors is required (Bucklin et al. 2015).

In many SDMs, climate-only predictor sets are still commonly used, and they often perform well in quite coarse spatial resolution (Stickley & Fraterrigo 2023). However, climate-only SDMs have been criticised as incomplete representations of species' niches, because they ignore other important drivers, such as land cover, soils, and human impacts (Araújo & Peterson 2012; Heikkinen et al. 2006). Land cover and human influence, for example, are often included to better capture habitat constraints (Junker et al. 2012; Pearson et al. 2004), and more dynamic predictors, such as extreme weather events, may become increasingly relevant under climate change (Parmesan et al. 2000; Seabrook et al. 2014).

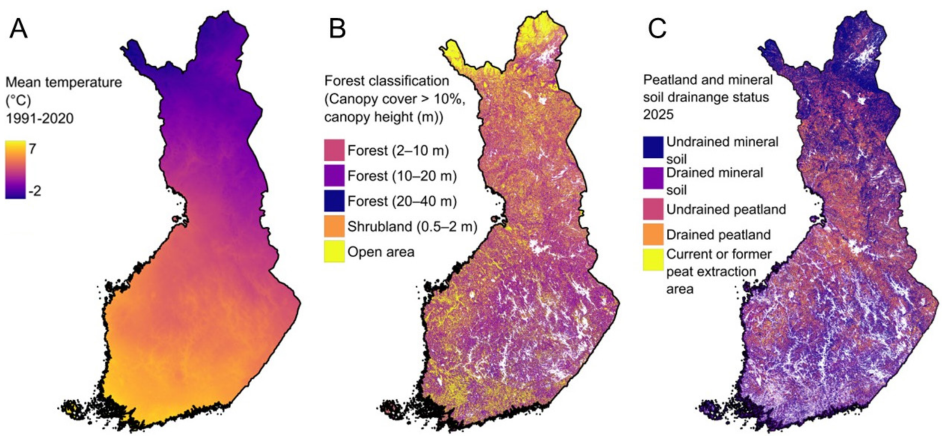

Figure 2. Examples of environmental data. (A) Mean annual air temperature (1991–2020) from Aalto and Pirinen (2023). (B) Forest classification based on canopy height and cover from the Finnish Environment Institute (2022). (C) Peatland and mineral soil drainage status from the Finnish Environment Institute (2025).

Several studies have shown the value of using environmental data in peatland contexts. Wu et al. (2025) identified the TWI, elevation, and soil pH as key determinants of peatland suitability, while Raney and Leopold (2018) highlighted elevation, canopy height, and the topographic position index (TPI) as important predictors of fen occurrence. In cold-region peatlands, Leppiniemi et al. (2025) found that palsa and peat plateau distributions were strongly controlled by thawing and freezing degree days in combination with the TWI. For predicting the occurrence of red-listed peatland plant species in Finland, Saarimaa et al. (2019) found that the proportions of drained peatland, open peatland, and undrained peatland, together with the TWI and WAB, had the highest importance. Moreover, Parkkari et al. (2017) showed that drainage intensity and nutrient-related variables were key predictors of GHG balance patterns and that drainage-related variables could act as practical proxies for the WT at the landscape scale where direct WT maps are lacking.

1.3 Objectives of the thesis

GIS-based environmental and RS data have been widely used in peatland studies and in SDMs, particularly to assess the effects of climate change on plant and animal species. However, relatively few studies have explicitly incorporated restoration scenarios alongside future climate projections when assessing the distributions of the modelled species. Consequently, there is limited understanding of how restoration and climate change together may affect the availability and spatial distribution of potential suitable habitats for red-listed peatland species at the national scale.

Peatland GHG sinks and sources and WT dynamics exhibit strong spatial and temporal variability and therefore require frequent monitoring. Although RS data have shown potential for detecting peatland vegetation patterns and surface characteristics, no studies have demonstrated how environmental data combined with RS data can be used to model the spatial distribution of potential peatland GHG sinks and sources. In addition, WT dynamics are often assessed using field measurements and RS data alone, but the potential of integrating environmental data with RS-based models to improve WT prediction at the local scale has not been sufficiently investigated.

I analysed potential peatland red-listed plant species distributions and potential GHG sinks and sources at the national scale and modelled WT dynamics at the local scale. The differences in spatial scale reflect both the availability and resolution of environmental and RS datasets along with the need to evaluate whether they can be used across scales for peatland monitoring and restoration planning. I introduce approaches to support peatland biodiversity conservation, management, and restoration planning—all of which rely on spatial information. I use environmental and RS data to predict the distribution of red-listed peatland plant species, detect potential peatland GHG sinks and sources, and model the peatland WT (Figure 3). Ultimately, this thesis encourages reflection on what environmental and RS data can detect and monitor, beyond—or in combination with—traditional field-based measurements and how this knowledge can support future peatland monitoring and restoration planning. The overarching goal of this thesis is to investigate how different environmental and RS datasets, combined with statistical modelling, can be used to detect and map potential suitable habitat for red-listed species, potential GHG sink and source patterns, and the WT in Finnish peatlands.

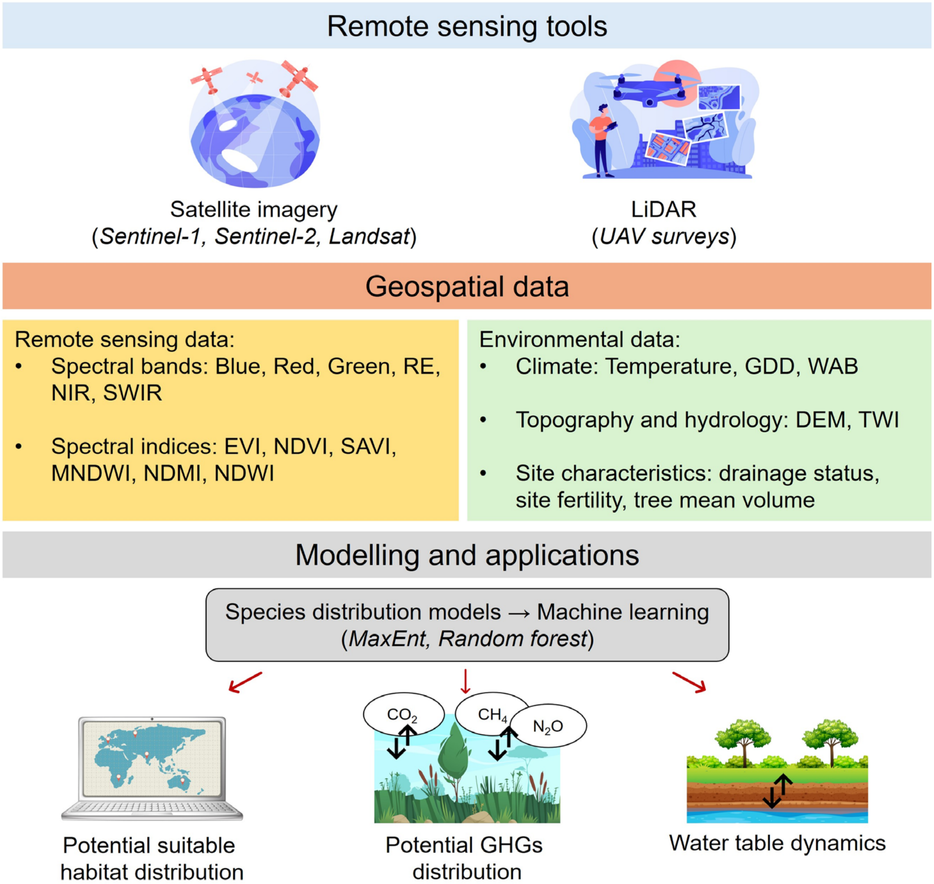

Figure 3. Framework of multi-source geospatial data and modelling applications. Abbreviations used in this figure are defined in the list of abbreviations. Illustrations sourced from Freepik (www.freepik.com), used under the Freepik Free License.

Given the broad scope of this aim, the thesis is divided into three specific objectives (**O1–O3**), each addressed by a total of 10 research questions (**RQs**):

O1: To evaluate whether environmental data can be used to predict how restoration and climate change together affect the distribution of Finland's red-listed peatland plant species at the national scale (Paper I).

Based on previous modelling studies on peatland restoration (e.g. Tolvanen et al. 2020), increasing restoration extent is expected to enhance potential habitat suitability for red-listed peatland plant species, although responses may vary among species groups. Environmental variables related to drainage and climate are expected to be key predictors of species occurrence (Saarimaa et al. 2019). While restoration is generally expected to increase habitat suitability, climate change may have mixed or negative effects depending on the species. Species distributions are also expected to shift geographically under future climate scenarios (Ma et al. 2022). Therefore, I addressed the following research questions:

RQ1: How well do models based on environmental data perform in predicting the occurrence of red-listed peatland plant species?
RQ2: Which environmental data are the most important in explaining the occurrence of red-listed peatland plant species?
RQ3: How do restoration scenarios and projected climate change affect the availability of potential suitable habitats for red-listed peatland species?
RQ4: How do species' latitudinal distribution patterns and richness change under different restoration and future climate scenarios?

O2: To evaluate whether environmental and satellite data can be used to detect potential peatland GHG sinks and sources at the national scale (Paper II).

Based on previous studies using environmental and RS data to model peatland GHG dynamics (e.g. Parkkari et al. 2017; Räsänen et al. 2021), both environmental and RS datasets are expected to provide meaningful predictive power for detecting GHG sinks and sources at the landscape scale. Environmental variables related to site conditions, such as drainage intensity and fertility, are expected to play a key role in explaining GHG balances (Parkkari et al. 2017), while RS variables capturing surface moisture and topography are also expected to be important predictors (Räsänen et al. 2021). Therefore, I addressed the following research questions:

RQ5: How does model performance differ among environmental, RS, and combined datasets?
RQ6: Which environmental and RS variables are most important for predicting potential GHG sinks and sources?
RQ7: How do prediction maps differ between models using environmental, RS, and combined datasets?

In this study, the term "GHG sinks/sources" is used to describe gas-specific fluxes rather than an aggregated GHG balance. CO_2, CH_4, and N_2O fluxes were modelled separately, and peatlands may simultaneously function as CO_2 sinks and CH_4 sources.

O3: To investigate whether environmental data improve RS-based models of the WT at the local scale (Paper III).

Based on previous studies applying RS to model peatland WT (e.g. Isoaho et al. 2023; 2024), RS data are expected to provide meaningful predictive power for estimating WT at the local scale. Variables derived from RS, particularly those related to surface moisture and vegetation characteristics, are expected to contribute substantially to WT model performance. Environmental variables describing site conditions, such as topography, may further improve WT model performance when combined with RS data. Therefore, I addressed the following research questions:

RQ8: Do environmental data improve the performance of RS-based WT models at the local scale?
RQ9: Which environmental and RS variables contribute most to model performance?
RQ10: How do prediction maps differ between RS-only models and models that clude environmental data?

2 Materials

2.1 Study sites

Papers I and II were conducted at the national scale across Finnish peatlands (Figure 4). The country was divided into a spatial grid, excluding cells with less than 10 % peatland cover based on the peatland drainage status map from the Finnish Environmental Institute (2009). In Paper I, the grid resolution was 25 ha (500 m × 500 m), while in Paper II, the resolution was 1 ha (100 m × 100 m) due to the high resolution of RS data used.

Paper III was carried out at the local scale in two regions of Finland (Figure 4). In northern Finland, the Pallas region includes two aapa mire complexes, Matorovansuo and Välisuo, which were partially drained in the 1960s but still contain wet open areas with typical northern mire vegetation, such as *Carex magellanica*, *Eriophorum vaginatum*, and *Sphagnum lindbergii*. The sites have flark–string microtopography. In southern Finland, Lettosuo is a nutrient-rich drained peatland forest that was first drained in the 1930s–1960s and experimentally harvested in 2016 with three treatments: clearcut, partial cut, and control (Korkiakoski et al. 2023). The site is dominated by *Picea abies*, *Pinus sylvestris*, and *Betula pubescens*.

2.2 Field data

Datasets on red-listed peatland plant species occurrences, GHG sinks and sources, and water table dynamics were used in this thesis (Table 1). In Paper I, presence-only records of 27 red-listed peatland vascular plant and bryophyte species were obtained from the national database (Hyvärinen et al. 2019), which compiles observations from professionals, amateurs, herbaria, and scientific literature. Records were filtered to include only records with (i) collection dates from 2000 onwards, (ii) spatial accuracy of ≤ 100 m, (iii) at least 10 records per species, and (iv) occurrences located in undrained peatlands. The filtered data were classified into northern boreal, middle boreal, and southern boreal zones according to the dominant occurrence of each species.

In Paper II, field-based measurements of annual CH_4, CO_2, and N_2O fluxes were compiled from long-term monitoring sites across Finland, representing drained, rewetted, and undrained peatlands (Korkiakoski et al. 2019; Minkkinen et al. 2018, 2020; Ojanen et al. 2010, 2013, 2018, 2019). Measurements were conducted mainly during the snow- and frost-free seasons. Each site was classified as a GHG sink (negative or zero annual balance) or source (positive annual balance), separately for each gas (CO_2, CH_4, and N_2O). At sites equipped with eddy covariance systems, ecosystem CO_2 exchange was derived directly from continuous flux measurements. At chamber-only sites, ecosystem-scale CO_2 balance was reconstructed by combining modelled soil CO_2 net exchange and tree stand carbon accumulation. Soil CO_2 net exchange was estimated based on annual decomposition and litter input following Ojanen et al. (2012), while CO_2 uptake by vegetation was quantified from tree stand biomass increment derived from forest inventory measurements (Ojanen et al. 2010, 2013, 2019). The total ecosystem CO_2 balance was then calculated as the difference between tree stand CO_2 uptake and soil CO_2 emissions. Sites were classified as CO_2 sinks or sources based on the sign of this combined annual balance. In total, the dataset included 47 sinks and 56 sources for CH_4, 39 sinks and 37 sources for CO_2, and 1 sink and 102 sources for N_2O.

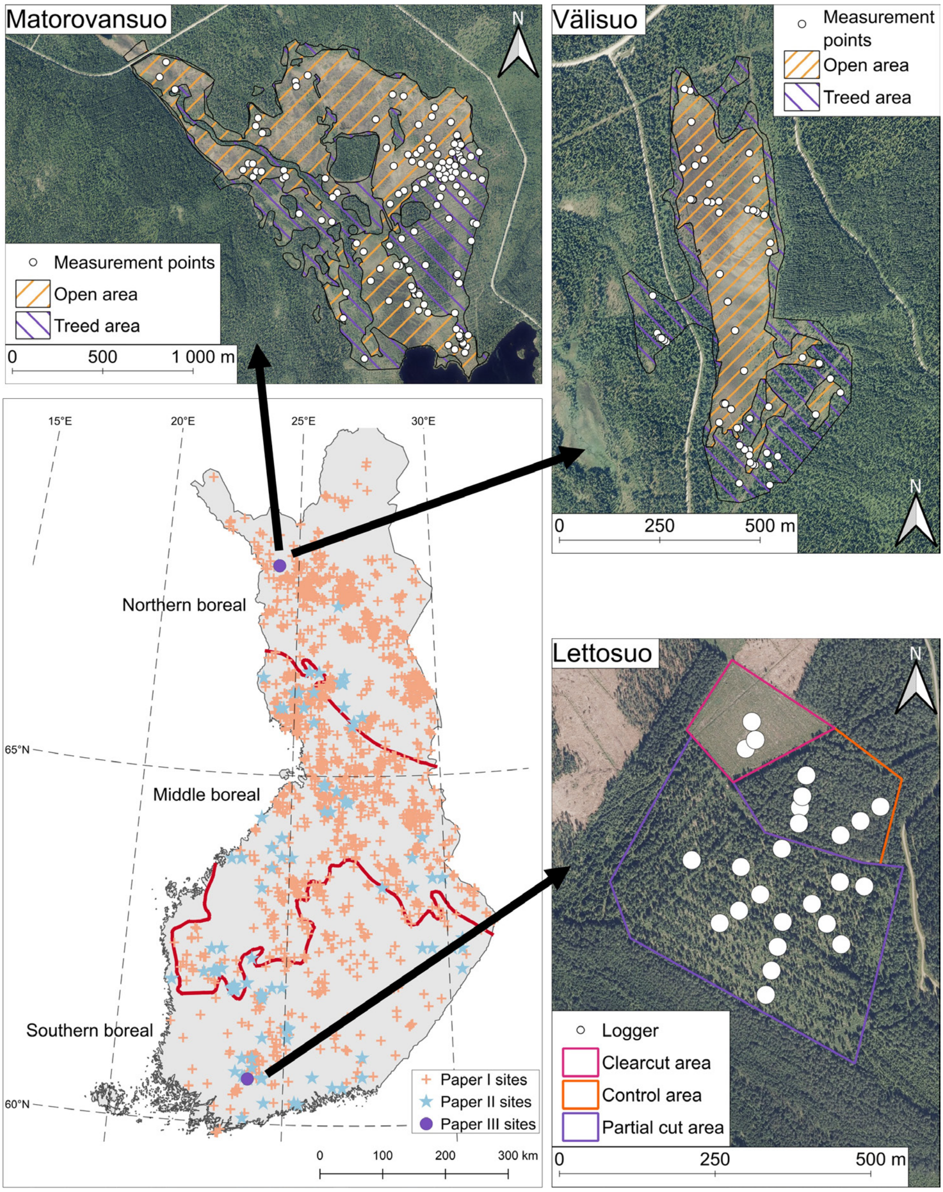

Figure 4. Study sites across Finland used in Papers I–III. Orthophotos were obtained from the National Land Survey of Finland (2025).

In Paper III, WT data were collected from both Pallas and Lettosuo. In the Pallas region, the WT was manually measured at 169 plots (72 in open and 97 in treed areas) from 23–25 July, 2023. In Lettosuo, continuous WT data were collected with 25 automatic loggers (3 in clearcut, 15 in partial cut, and 7 in control areas) during the 2017–2023 growing seasons. Data were recorded hourly and aggregated to daily averages. The WT was expressed relative to the local peat surface, with negative values indicating below-surface levels and positive values indicating above-surface levels.

Table 1. Summary of the field data. CH_4 = methane; CO_2 = carbon dioxide; N_2O = nitrous oxide; WT = water table.

Paper(s)	Variable	Unit	Number of observations	Measurement / Inventory method
I	Red-listed peatland plant species	-	8734	National red-list database (Hyvärinen et al., 2019); field and herbarium observations.
II	CH_4	g m^{-2} yr^{-1}	103	Static (closed) chambers, with fluxes determined from gas samples collected from chamber headspace at regular intervals.
II	CO_2	g m^{-2} yr^{-1}	76	Eddy covariance (ecosystem-scale net CO_2 exchange) and closed chamber techniques (soil and forest floor respiration).
II	N_2O	g m^{-2} yr^{-1}	103	Static (closed) chamber method, with gas samples analysed from chamber headspace.
III	WT	cm	194	Manual measurements in Pallas, where WT depth was measured using perforated plastic tubes installed in the peat. The water level inside each tube was equalised by gently blowing through an elastic hose, and the distance from the water surface to the peat surface was measured with a ruler. Automatic loggers were used in Lettosuo.

2.3 Environmental data

Environmental data used as predictors in Papers I–III represented climatic, hydrological, topographic, and site characteristics (Table 2 and Table 3). In Paper I, baseline climatic variables (GDD, WAB, and January temperature [TJan]) from 1981–2010 and future projections for 2040–2069 and 2070–2099 under Representative Concentration Pathways (RCPs) 2.6, 4.5, and 8.5 were obtained from the Finnish Meteorological Institute (Aalto 2023; Heikkinen et al. 2020) in 50 m resolution. Hydrological and topographic conditions were represented by the TWI (Beven & Kirkby 1979). Site characteristics were described by the proportions of undrained, drained, and open peatlands; site fertility types (ST); and mean tree volumes of pine, spruce, birch, and other broad-leaved species. The presence of calcareous rock was included, as many red-listed peatland plant species require calcareous substrates. In addition, four restoration scenarios were simulated for all grid cells containing drained peatlands. These scenarios represented 0 %, 30 %, 50 %, and 100 % restoration of drained peatlands (REST0–REST100) by proportionally adjusting the drained and undrained peatland cover to reflect potential restoration outcomes (Tolvanen et al. 2020). The continuous variables were resampled to a 500 m resolution using the average method, while the categorical variables were resampled using the majority rule to preserve dominant class.

In Paper II, climatic variables (GDD, WAB) were derived from the Finnish Meteorological Institute for 1990–2013 (Pirinen et al. 2012) in 1 km resolution. Topography was represented by the TWI, while site characteristics were represented by the proportions of undrained and drained peatlands, four site fertility types, and mean root biomass of spruce, pine, and other broad-leaved trees. The variables were resampled from the original resolution to 100 m resolution by using nearest neighbour interpolation.

Table 2. Environmental data used as predictors in Papers I–II. Abbreviations used in this table are defined in the list of abbreviations.

Variable	Unit	Spatial resolution (m)		Data source
		Paper I	Paper II	
Climatic				
Mean GDD	°C days	50	1000	FMI
Mean annual WAB	mm	50	1000	FMI
Mean TJan	°C	50	–	FMI
Projected mean GDD	°C days	50	–	FMI
Projected mean annual WAB	mm	50	–	FMI
Projected mean TJan	°C	50	–	FMI
Hydrological and topographic				
TWI	–	10	10	NLS, DEM
Site characteristics				
UNDRAINED	%	25	25	Syke
DRAINED	%	25	25	Syke
OPEN	%	16	–	Syke
ST1-HERB	%	16	16	Luke, MS-NFI
ST2-BILB	%	16	16	Luke, MS-NFI
ST3-LING	%	16	16	Luke, MS-NFI
ST4-SHRUB	%		16	Luke, MS-NFI
ST6-LICHEN	%	16	16	Luke, MS-NFI
ROCK	–	1:200 000	–	GTK
PINE	m^3/ha	16	–	Luke, MS-NFI
SPRUCE	m^3/ha	16	–	Luke, MS-NFI
BIRCH	m^3/ha	16	–	Luke, MS-NFI
OTHER	m^3/ha	16	–	Luke, MS-NFI
ROOT_BIOMASS	10 kg/ha	–	16	Luke, MS-NFI

Table 3. Environmental data used as predictors in Paper III. DTM = digital terrain model; UAV = uncrewed aerial vehicle; LiDAR = Light Detection and Ranging; NLS = National Land Survey of Finland.

Variable	Abbreviation	Unit	Source, spatial resolution			
			Pallas	Resolution (m)	Lettosuo	Resolution (m)
Canopy height model	CHM	m	UAV LiDAR	1	Airborne LiDAR, NLS and Finnish Forest Centre	1
SAGA wetness index	SWI	–	DTM (UAV-LiDAR)	1	DTM (NLS airborne LiDAR)	2
Slope	-	°	DTM (UAV LiDAR)	1	DTM (NLS airborne LiDAR)	2
Aspect	-	°	DTM (UAV LiDAR)	1	DTM (NLS airborne LiDAR)	2
Topographic position index	TPI	–	DTM (UAV LiDAR)	1	DTM (NLS airborne LiDAR)	2
Distance to closest drainage	DTD	m	Topographic database (NLS)	–	Topographic database (NLS)	–
Depth to water	DTW	cm	DTM (UAV LiDAR)	1	DTM (NLS airborne LiDAR)	2

In Paper III, canopy height model (CHM) for Pallas was generated from UAV LiDAR data, whereas CHM for Lettosuo was obtained from the Finnish Forest Centre (Table 3). The Lettosuo CHM had an original resolution of 1 m and was derived from the 0.5 points m^{-2} airborne LiDAR data collected by the National Land Survey of Finland (NLS) in 2019. The Pallas CHM was resampled to one-metre resolution using the averaging method, after which a three-cell radius mean filter was applied to represent a more generalised canopy height around the WT plots. The SAGA Wetness Index (SWI), a topographic wetness index, was calculated from DTM following the methodology of Ikkala et al. (2022), and a 5 x 5 cell median filter was applied to the SWI to remove noise. Slope and aspect were also calculated from DTM using a 3 x 3 cell neighbourhood. TPI was calculated from DTM using 5 and 10 m neighbourhood radiuses (Guisan et al. 1999; Weiss 2011). Distance to the closest drainage (DTD) was calculated from the topographic database provided by the NLS. Environmental data were then extracted using buffers with a 15 cm radius for Pallas and a 15 m radius for Lettosuo. For DTD, the exact distance values from each WT plot were used. For Pallas, depth to water (DTW; Murphy et al. 2009) index was calculated from the UAV-derived DTM using stream network initiation thresholds of 0.5, 1, 2, 4, and 10 ha. For Lettosuo, DTW was obtained from the Natural Resources Institute Finland (Salmivaara 2023) using the same thresholds as for Pallas.

2.4 Pre-processing satellite imagery (II–III)

For Paper II, Sentinel-1 and Sentinel-2 imagery was derived from the European Space Agency for the years 2019–2023 and processed on Google Earth Engine platform (Gorelick et al. 2017). To minimise noise in single-date images, representative composites were generated for three periods of the snow- and frost-free season: early summer (1 May–15 June), midsummer (1 July–15 August), and late summer (1 September–15 October). These periods correspond to different stages of the growing season: Early summer reflects high water table conditions following snowmelt, midsummer represents the peak vegetation biomass under reduced water availability, and late summer marks vegetation senescence and a renewed rise in water levels. Multi-year averages were calculated to represent typical seasonal conditions, aligning with the multi-year field data. Because of frequent late-summer cloud cover, Sentinel-2 composites were limited to early summer and midsummer periods.

Sentinel-1 Ground Range Detected products (ascending orbit) were used after standard pre-processing (thermal noise removal, radiometric calibration, and terrain correction using ASTER DEM). For each period, median composites were produced for the VV (vertical transmit, vertical receive) and VH (vertical transmit, horizontal receive) polarisation bands, and their ratio (VV/VH; hereafter Polarisation ratio) was included as an additional variable.

Sentinel-2 Level-2A surface reflectance data were filtered to a maximum cloud cover of 20 %. Remaining clouds, shadows, and snow were masked using the Scene Land Cover classification. From the unmasked areas, mosaics were produced using the 40th percentile reflectance value per band, which reduced haze and cloud remnants more effectively than median compositing (Pitkänen et al. 2024). The CloudScore+ algorithm (Pasquarella et al. 2023; see Paper III) was not used because it was not available at the time of the analysis. Nine spectral bands were retained, excluding bands 1, 9, 10 (60 m resolution) and 8A (narrow NIR). Four spectral indices were then calculated (Table 4). To harmonise with the 100 m resolution of the environmental predictors, all Sentinel-based layers (Sentinel-1: 20 m; Sentinel-2: 10 m) were resampled using the nearest-neighbour method.

For Paper III, Sentinel-2 Level-2A surface reflectance data were processed for the growing seasons of 2017–2023 using Google Earth Engine. Images with cloud cover exceeding 30 % were discarded, and the CloudScore+ algorithm (Pasquarella et al. 2023) was applied to mask remaining clouds and shadows using a threshold value of 0.7 on the CloudScore+ cs_cdf layer. Snow cover was removed using the Scene Land Cover classification. All Sentinel-2 spectral bands at 10 m and 20 m resolutions were included, from which a set of spectral indices was calculated (Table 4). Mean reflectance and index values were then extracted within a 15 m radius buffer around each logger location to represent local conditions. Outlier observations (e.g. SWIR transformed reflectance [STR] < 10, NDVI < 0, EVI outside −1 to 1) were removed, and only dates providing valid data for all loggers were retained to minimise residual cloud effects.

Table 4. Remote sensing variables that are used in Papers II and III. Equations and references are in Papers II–III. UAV = uncrewed aerial vehicle.

Variable	Abbreviation	Source	
		Paper II	Paper III
SAR			
Vertical–Vertical polarisation	VV	Sentinel-1	–
Vertical–Horizontal polarisation	VH	Sentinel-1	–
VV/VH polarisation	POL	Sentinel-1	–
Optical			
Blue reflectance	BLUE	Sentinel-2	UAV and Sentinel-2
Green reflectance	GREEN	Sentinel-2	UAV and Sentinel-2
Red reflectance	RED	Sentinel-2	UAV and Sentinel-2
Red edge reflectance	RE	–	UAV
Red edge reflectance 1-3	RE1-3	Sentinel-2	Sentinel-2
Red edge reflectance 4	RE4	–	Sentinel-2
Near infrared reflectance	NIR	Sentinel-2	UAV and Sentinel-2
Shortwave infrared reflectance 1-2	SWIR1	Sentinel-2	Sentinel-2
SWIR Transformed reflectance	STR	–	Sentinel-2
Vegetation indices			
Enhanced Vegetation Index	EVI	–	UAV and Sentinel-2
Green Difference Vegetation Index	GDVI	–	UAV and Sentinel-2
Green Normalised Difference Vegetation Index	GNDVI	–	UAV and Sentinel-2
Normalised Difference Red Edge Index	NDRE	–	UAV and Sentinel-2
Normalised Difference Vegetation Index	NDVI	Sentinel-2	UAV and Sentinel-2
Soil Adjusted Vegetation Index	SAVI	–	UAV and Sentinel-2
Water / moisture indices			
Modified Normalised Difference Water Index	MNDWI	Sentinel-2	Sentinel-2
Moisture Stress Index	MSI	–	Sentinel-2
Normalised Difference Moisture Index	NDMI	Sentinel-2	Sentinel-2
Normalised Difference Moisture Index 2	NDMI2	–	Sentinel-2
Normalised Difference Water Index	NDWI	Sentinel-2	UAV and Sentinel-2

2.5 Collecting and processing UAV imagery (III)

UAV data were collected in the Pallas region (Välisuo and Matorovansuo) between 22 and 24 July, 2023 using a DJI Matrice 300 RTK platform equipped with a MicaSense Altum-PT multispectral camera and a YellowScan Mapper+ LiDAR sensor. The flights were performed in terrain-following mode, with the UAV referencing the National Land Survey of Finland 2 m DEM to maintain an altitude of approximately 120 m for multispectral flights and 100 m for LiDAR flights.

Multispectral flights were conducted with 70 % forward and 75 % side overlap, resulting in a ground sampling distance of approximately 5 cm. Radiometric normalisation was performed using reflectance panels and the onboard irradiance sensor to ensure spectral consistency, and trajectory corrections were obtained in real time via the Trimble VRS network. The Altum-PT imagery was processed in Agisoft Metashape (v. 2.0.4) using a Structure-from-Motion workflow to produce ultra-high-resolution orthomosaics with ~5 cm spatial resolution. From the spectral bands, a set of moisture- and vegetation-related indices was derived (Table 4). To link the spectral data with field measurements, 15 cm-radius buffers were created around each WT monitoring point, from which area-weighted mean values of spectral bands and indices were extracted.

LiDAR data were collected using the YellowScan Mapper+ system equipped with an Applanix APX-15 IMU. Flights were carried out at low altitude with high line overlap, resulting in point densities of approximately 385 pulses m^{-2} in Välisuo and 400 pulses m^{-2} in Matorovansuo. Standard trajectory correction and pre-processing steps were applied, including ground classification and generation of 20 cm DTMs and DSMs.

3 Methods

3.1 Maximum entropy (I–II)

To model potential suitable habitat based on presence-only data, MaxEnt (Phillips et al. 2006) was run in R using the dismo package (version 1.3.5; Hijmans et al. 2010). In Paper I, MaxEnt was used to predict current and future potential habitat suitability for red-listed peatland plant species in Finland. Each species was modelled individually using an identical set of environmental data to enable direct comparison. To reflect limited dispersal capacity, a 20 km dispersal constraint was applied (O'Connell et al. 2013). Models were run for the baseline period (1981–2010) using historical climate data, and for two future periods (2040–2069 and 2070–2099) under three GHG concentration trajectories (RCP2.6, RCP4.5, and RCP8.5) and four restoration scenarios—0 %, 30 %, 50 %, and 100 % (REST0, REST30, REST50, REST100)—to predict changes in potential suitable habitat for each species.

In Paper II, the MaxEnt was used to predict the spatial distribution of CO_2, CH_4, and N_2O sinks and sources across Finnish peatlands. Following Parkkari et al. (2017), each measured sink or source was treated as an occurrence point. To reduce pixel-level noise, mean values of all predictors within a 50 m buffer around each observation and background point were extracted prior to modelling. Separate models were developed for CO_2, CH_4, and N_2O sinks and sources (the N_2O sink was excluded due to limited data). Three predictor sets were tested: (1) environmental, (2) satellite, and (3) combined.

For both Papers I and II, 10,000 randomly located background points were generated to account for sampling bias (Barbet-Massin et al. 2012). Although MaxEnt is considered relatively robust to correlated predictors due to its regularisation framework, multicollinearity was still reduced by selecting variables with pairwise |Spearman correlation| < 0.7 to improve interpretability. Model performance was assessed using cross-validation (fivefold in Paper I, tenfold in Paper II). In Paper I, performance was quantified using the area under the receiver operating characteristic curve (AUC), the continuous Boyce index (CBI), and the true skill statistic (TSS), whereas in Paper II, only the AUC was calculated. The difference in the choice of evaluation metrics between Papers I and II was due to criticism of the AUC as a sole performance measure in SDM (Fernandes et al. 2019; Manzoor et al. 2018). Model stability in Paper II was further evaluated by comparing training and testing AUC values (Parviainen et al. 2013).

The importance of predictors in Papers I and II was evaluated using permutation importance, which measures the decrease in model performance when the values of a predictor are randomly permuted. This approach was chosen because it reflects the independent contribution of each variable to model accuracy and is less influenced by correlations among predictors compared to MaxEnt's default variable contribution. For Paper II, predictor importance was further refined using backward stepwise variable selection due to the larger number of predictors compared to Paper I, to reduce model complexity and remove variables with little contribution without compromising model performance. The final models were used to generate spatial prediction maps.

Continuous suitability maps from MaxEnt were converted to binary maps using the maximum training sensitivity plus specificity threshold (Liu et al. 2013). In Paper I, the binary maps were used to quantify potential habitat loss and gain between current and future conditions and to estimate potential latitudinal shifts, calculated as the north–south displacement between potential habitat centroids. To assess species richness, binary maps of all modelled species were stacked and summed, and potential suitable habitat change was quantified as the difference between current and projected richness. In Paper II, the binary maps were used to visualise the distributions of potential GHG sinks and sources across the study area.

3.2 Random forest (III)

For Paper III, RF regression (Breiman 2001) was done in R (R Core Team 2025). Prior to model development, variable selection using random forests (VSURF; Genuer et al. 2015) was applied to identify the most relevant predictors. VSURF performs a three-step procedure—thresholding, interpretation, and prediction—to iteratively remove irrelevant and redundant variables based on variable-importance metrics. The selection process was repeated 10 times, and all variables that were selected in any iteration were retained to ensure stability (Putkiranta et al. 2024).

Final RF models were trained with 500 trees, and the optimal number of variables randomly sampled at each split (mtry) was determined using the tuneRF function in the caret package (Kuhn, 2008). Separate models were constructed for each study region and data combination. In Pallas, a combined model including all area types was built, as well as separate models for the treed and open areas using UAV-based data alone and UAV plus environmental data (UAV–ENV). In Lettosuo, models were developed for each harvesting treatment (clearcut, partial cut, control) using satellite (SAT) and combined SAT–ENV data.

Model performance was evaluated using cross-validation methods that matched the data structure at each site. At Pallas, each location had a single WT measurement. Therefore, to account for spatial autocorrelation, spatial block cross-validation was used. The area was divided into 100 m blocks, based on variogram analysis and a block-size sensitivity test. Blocks were randomly assigned to five folds. Models were trained on four folds and tested on the remaining fold. This procedure was repeated 100 times using different random seeds.

At Lettosuo, WT was measured repeatedly at the same locations over several years, while environmental variables are constant. To avoid information leakage due to this spatiotemporal structure, spatiotemporal cross-validation was applied. Test folds were defined by unique plot–year combinations, and training data included all other plots and years. The cross-validation was repeated ten times using different random seeds. Variable-importance scores for both Pallas and Lettosuo were averaged and scaled to sum to 100.

The effects of individual predictors on the WT were examined using partial dependence plots. For each predictor, partial dependence plots were computed on a regular grid of predictor values while averaging over all other variables. Ensemble-level partial dependence plots were obtained by aligning results across all model runs and summarising the mean effects and 95 % intervals.

Finally, spatially continuous WT maps were produced by upscaling the RF predictions to raster grids. Prior to upscaling, anthropogenic features such as roads and duckboards were masked out. All optical and environmental layers were resampled to 1 m resolution in Pallas and 10 m resolution in Lettosuo. For Lettosuo, cloud-free Sentinel-2 images from early summer (18 May, 2019), midsummer (15 July, 2018), and autumn (10 September, 2019) were used to generate prediction maps, capturing seasonal variation in WT depth during the growing season.

4 Results

4.1 Predicting climate and restoration effects on red-listed peatland species with environmental data (I)

Models for 21 of 27 species performed well with average test AUC = 0.93, CBI = 0.84, TSS = 0.77 (Figure 5A). Six species with low model performance (TSS < 0.5, CBI < 0.6) were excluded from further analyses. On average, species occurrence was most strongly explained by proportion of undrained peatlands (28.8 %), followed by mean January temperature (15.6 %) and mean growing degree days (13.7 %; Figure 5B). Proportion of undrained peatlands was the top predictor for 14 species, while mean January temperature and growing degree days were most important for only two species each.

Restoration increased the predicted potential suitable habitat for all species groups, reflecting the strong influence of drainage-related variables. Middle boreal species showed the largest gains in predicted potential suitable habitat from REST0 to REST100, northern boreal species showed moderate gains, and southern boreal species showed the smallest increases (Figure 6A).

Climate change scenarios further affected the availability of predicted potential suitable habitat expansion and loss. Under REST0, middle boreal species had the highest expansion across all climate change scenarios but also substantial predicted potential habitat losses. Northern boreal species showed moderate predicted potential habitat gains but experienced large losses under RCP4.5 and RCP8.5. Southern boreal species showed smaller, more stable predicted potential suitable habitat changes with relatively limited losses. Predicted potential habitat losses intensified under more severe climate scenarios, particularly for northern and middle boreal species.

When restoration and climate change effects were combined, restoration clearly mitigated potential habitat losses. Under RCP2.6, all species groups showed consistent patterns, with greater restoration (REST100) leading to higher potential habitat expansion and slightly reduced loss compared to REST0. Under RCP8.5, restoration still increased potential suitable habitat and reduced loss, but its effectiveness diminished towards 2070–2099—especially for northern and middle boreal species, for which expansion decreased and loss increased. Southern boreal species, unlike northern and middle boreal species, showed greater potential habitat expansion under RCP8.5 in 2080–2099.

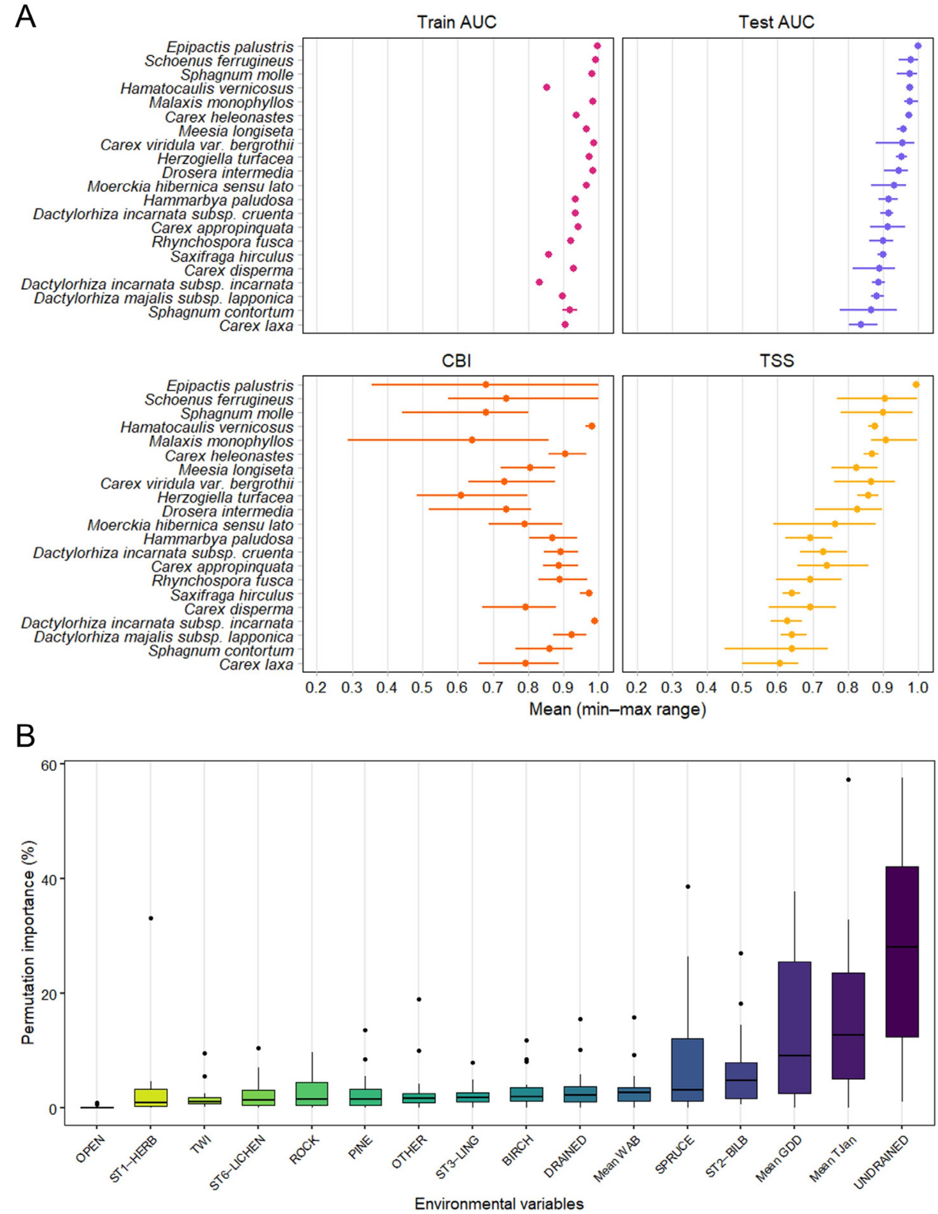

Figure 5. (A) Model performance for the 21 red-listed peatland plant species included in Paper I, shown as mean ± min–max range for training and test AUC, CBI, and TSS. (B) Permutation importance of environmental data used in the species distribution models. Boxes show the median and interquartile range across species. Abbreviations used in this figure are defined in the list of abbreviations.

A clear south-to-north gradient was observed in migration distances (Figure 6B). Southern boreal species showed the largest northward shifts (≤ 142 km), while northern boreal species shifted ≤ 80 km. Without restoration, extreme climate change scenarios (RCP4.5 and RCP8.5) produced greater northward movements than RCP2.6. Restoration generally reduced the magnitude of these shifts. For instance, under

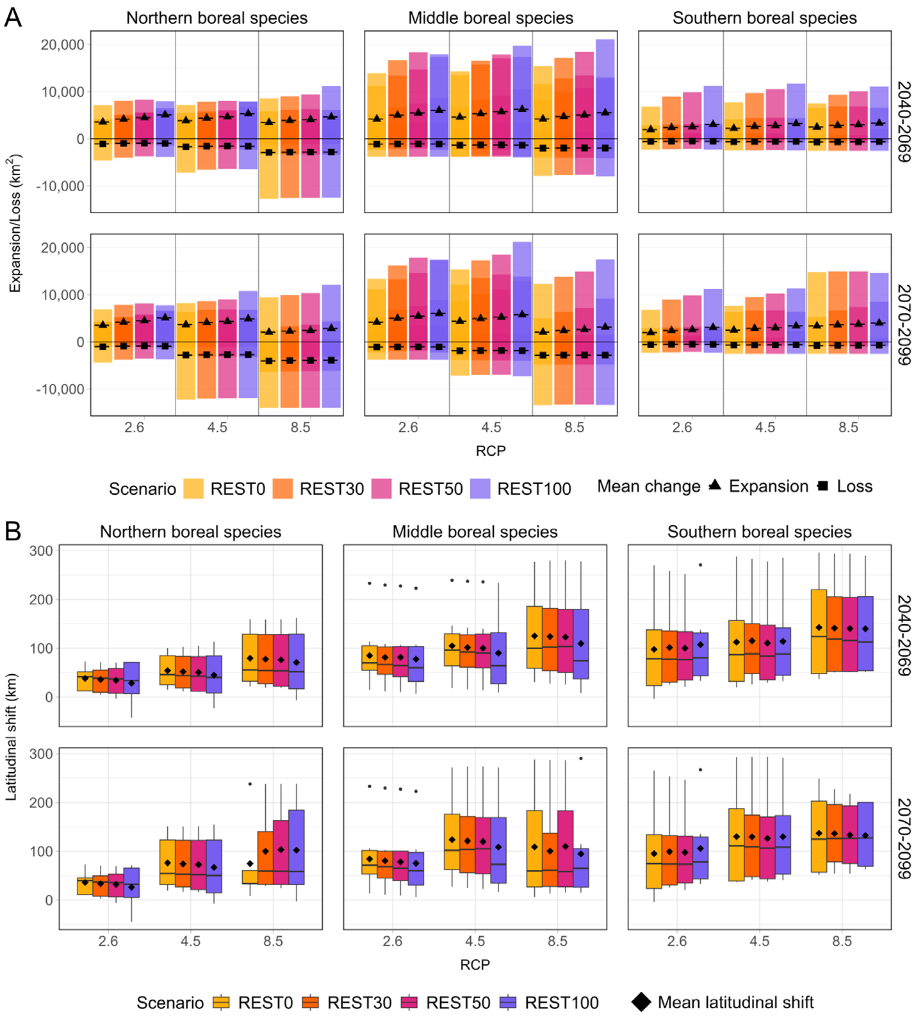

Figure 6. (A) Projected changes in potential suitable habitat area for northern, middle, and southern boreal species under different Representative Concentration Pathway (RCP) scenarios and restoration levels (REST0–REST100) for 2070–2099 compared to the current distribution. Bars represent minimum and maximum values across individual species, with positive values (above zero) indicating potential habitat expansion and negative values (below zero) indicating potential habitat loss. Dashed lines with markers show mean values for all species for both expansion and loss. (B) Projected latitudinal shifts (km) for northern, middle, and southern boreal species under different RCP and restoration scenarios for 2040–2069 to 2070–2099 compared to the current distribution. Positive values indicate northward movement, while negative values indicate southward movement.

REST100 and RCP2.6, middle boreal species shifted 77.5 km in 2040–2069 compared to 84.9 km under REST0. Under RCP8.5, the reduction was notable, particularly for northern boreal (from 79.5 km under REST0 to 70.7 km under REST100 in 2040–2069) and southern boreal species (from 137.1 km under REST0 to 132.3 km under REST100 in 2070–2099).

Across both 2040–2069 and 2070–2099, moderate increases in species richness were most pronounced in the northern and middle boreal regions under RCP2.6 (Figure 7A). However, by 2070–2099, under RCP8.5, richness declines emerged in northern boreal zone, and this negative trend persisted even with restoration. In other cases, restoration consistently increased red-listed species richness across all boreal zones (Figure 7B).

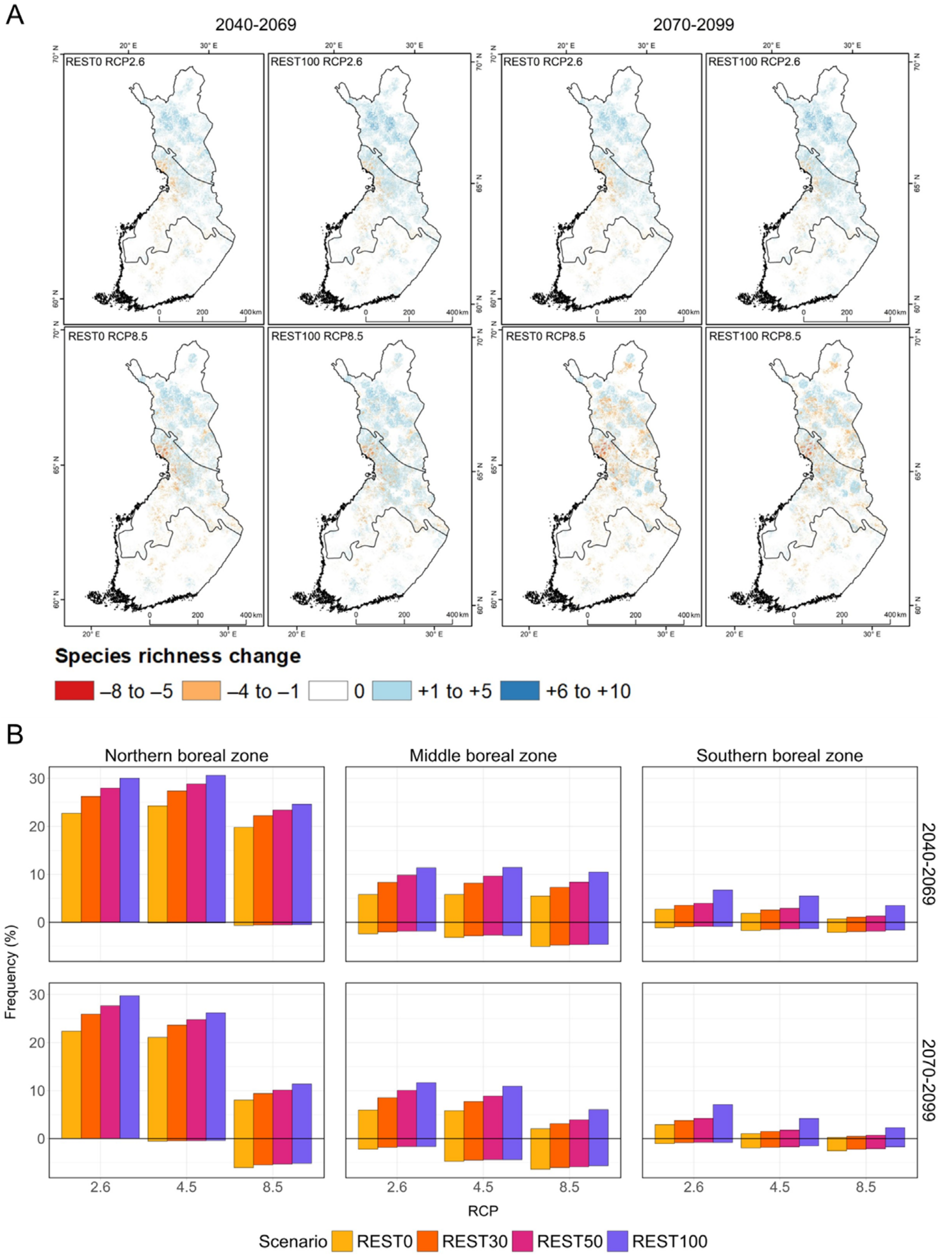

Figure 7. (A) Predicted changes in species richness of red-listed peatland plant species under different Representative Concentration Pathway (RCP) scenarios and restoration levels (REST0–REST100) for 2040–2069 to 2070–2099 compared to the current distribution. Different colours (from red to blue) indicate the magnitude of richness change. (B) Frequency of grid cells showing richness changes under different RCP and restoration scenarios for 2040–2069 to 2070–2099 compared to the current distribution. Positive values (above zero) indicate potential habitat expansion, and negative values (below zero) indicate potential habitat loss.

4.2 Detecting potential peatland GHG sinks and sources using environmental and satellite data (II)

The combined models (ENV–SAT) consistently performed the best, with average AUCs of 0.91 for training and 0.85 for test data (Table 5). Models based solely on environmental data performed almost similarly to the ENV–SAT models, with mean AUCs of 0.88 and 0.81 for the training and test sets, respectively. By contrast, models using only satellite variables had lower AUCs, with mean AUCs of 0.82 (training) and 0.76 (test). Model stability, assessed using AUC stability across folds, was similar across all models with an average AUC stability of 0.93.

Table 5. Model performance based on area under the receiver operating characteristic curve (AUC) values for detecting greenhouse gas (GHG) sinks and sources using environmental (ENV), satellite (SAT), and combined (ENV–SAT) data. Best performance per row is shown in bold.

Metric	GHG Type	ENV	SAT	ENV–SAT
Train AUC	CH_4 sink	0.88	0.82	**0.91**
	CH_4 source	0.88	0.85	**0.92**
	CO_2 sink	0.86	0.74	**0.90**
	CO_2 source	0.87	0.85	**0.91**
	N_2O source	0.90	0.85	**0.92**
Test AUC	CH_4 sink	**0.84**	0.75	**0.84**
	CH_4 source	0.83	0.81	**0.87**
	CO_2 sink	0.74	0.66	**0.78**
	CO_2 source	0.78	0.80	**0.85**
	N_2O source	0.86	0.81	**0.88**
AUC Stability	CH_4 sink	**0.95**	0.91	0.93
	CH_4 source	0.95	**0.96**	0.95
	CO_2 sink	0.87	**0.89**	0.87
	CO_2 source	0.90	**0.93**	**0.93**
	N_2O source	**0.96**	0.95	**0.96**

Variable importance analysis showed clear differences among environmental, satellite, and combined models (Table 6). In models using only environmental predictors, GDD was consistently the most influential variable, particularly for CH_4 sinks and N_2O sources, and also ranked highly in other GHG models. Proportion of undrained and drained peatlands and water balance were important across CH_4 and CO_2 sources, while site fertility contributed moderately.

In SAT models, Sentinel-2 variables were generally dominant, except for the CO_2 sink, where Sentinel-1 VH backscatter (late summer VH) was the most important predictor. Among individual bands and indices, early summer Blue band and midsummer RE1 band were most influential for CH_4 sinks and CO_2 sources, respectively, while midsummer NDMI and early summer MNDWI were key predictors for CH_4 and N_2O sources (Table 6).

When environmental and satellite variables were combined, the models selected both data types among the top predictors. Proportion of undrained peatlands was the most influential variable for CH_4 and CO_2 sinks, water balance for N_2O sources, and early summer MNDWI and midsummer RE1 for CH_4 and CO_2 sources, respectively. The top three most important variables in most cases comprised a mixture of environmental and satellite data, except for CO_2 sinks, which relied entirely on environmental variables. These patterns highlight the complementary roles of environmental and satellite data in explaining spatial variability in potential peatland GHG sinks and sources.

Table 6. Top three environmental (ENV) and satellite (SAT) variables in the final models of each greenhouse gas sink and source (CH_4, CO_2, N_2O) based on permutation importance values. Abbreviations used in this table are defined in the list of abbreviations.

Model	ENV	Permutation importance (%)	SAT	Permutation importance (%)	ENV–SAT	Permutation importance (%)
CH_4 sink	Mean GDD	35.4	ES_Blue	18.8	UNDRAINED	23.2
	UNDRAINED	27.6	MS_RE1	18.8	Mean GDD	17.7
	ST4-SHRUB	15.8	MS_NDWI	16.5	MS_NDWI	14.9
CH_4 source	DRAINED	30.6	MS_NDMI	17.9	ES_MNDWI	13.4
	Mean GDD	18.8	ES_RED	13.8	Mean GDD	11.7
	Mean WAB	17.2	MS_NDVI	13.5	MS_NDVI	11.1
CO_2 sink	ST2-BILB	19.1	LS_VH	63.5	UNDRAINED	15.4
	UNDRAINED	17.4	MS_Blue	15.1	Mean GDD	12.3
	ST3-LING	17.1	ES_Blue	9.5	DRAINED	10.9
CO_2 source	UNDRAINED	35.4	MS_RE1	33.5	MS_RE1	18.1
	DRAINED	27.3	ES_NIR	18.9	UNDRAINED	17.1
	Mean GDD	14.7	ES_RE2	15.5	Mean GDD	14.1
N_2O source	Mean GDD	28.8	ES_MNDWI	17.8	Mean WAB	17.0
	Mean WAB	27.3	ES_RED	11.8	Mean GDD	16.5
	DRAINED	19.8	MS_MNDWI	8.4	ES_NIR	15.8

Across all GHGs, prediction maps from ENV and ENV–SAT models showed similar occurrence patterns. SAT-based models tended to extend predicted GHGs occurrence northward relative to ENV and ENV–SAT models. For CH_4, all models predicted sink occurrence mainly in central to southern Finland (Figure 8A–C), with SAT data predicted slightly larger sink extents and pushing predicted source areas farther north than ENV and ENV–SAT models (Figure 8B and E). For CO_2, ENV and ENV–SAT models predicted strong sink and source occurrence primarily in western, middle, and southern Finland (Figure 9A, C, D, F), whereas SAT models additionally showed high-probability sink and source occurrence in the northwest and northeast region (Figure 9B and E). For N_2O, ENV and ENV–SAT models showed source predictions in western to southern Finland (Figure 10A, C), while SAT models predicted a more dispersed pattern extending from northern to southern regions (Figure 10B).

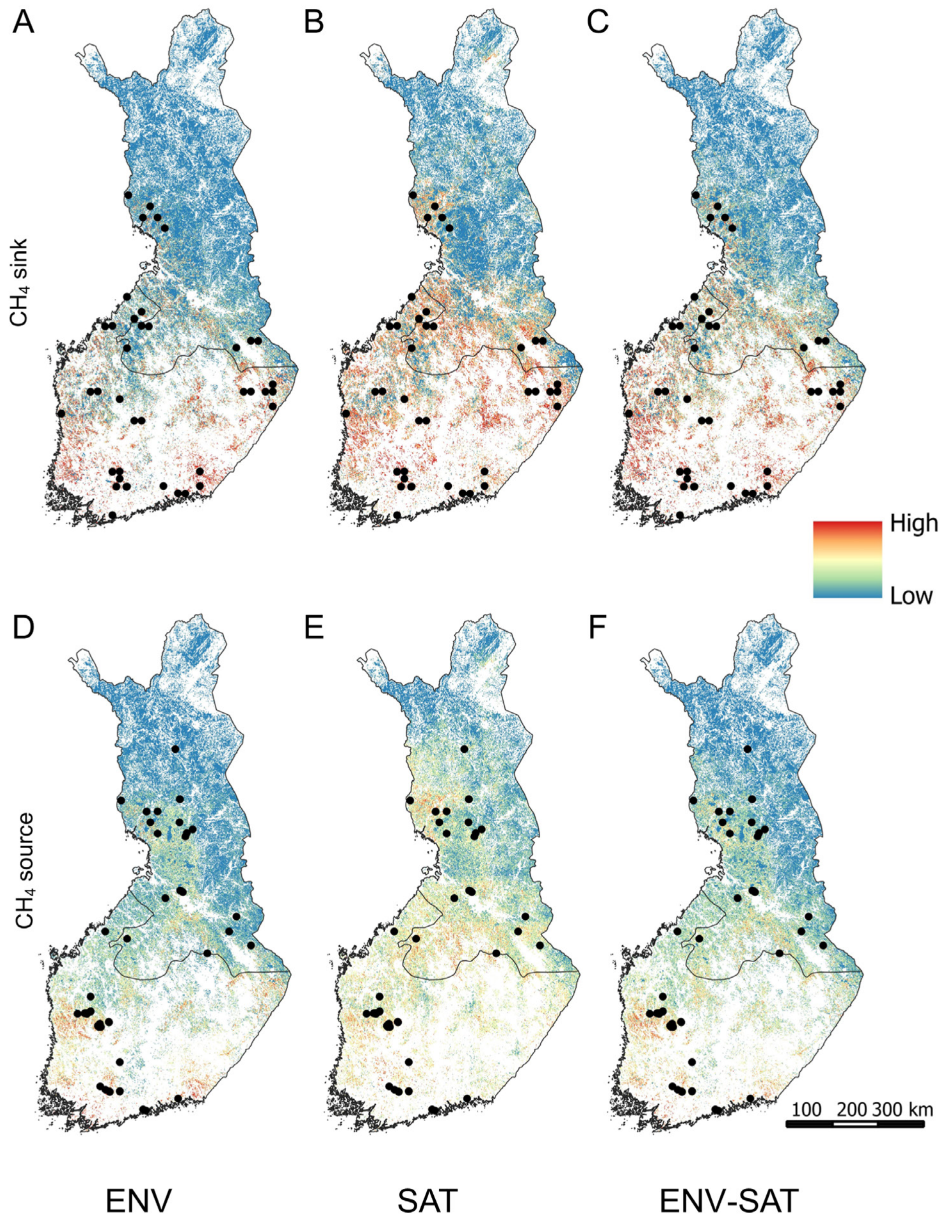

Figure 8. Predicted probability of CH_4 sinks (A–C) and sources (D–F) from environmental (ENV), satellite (SAT), and combined (ENV–SAT) variables. Black dots represent field measurement sites of CH_4 fluxes.

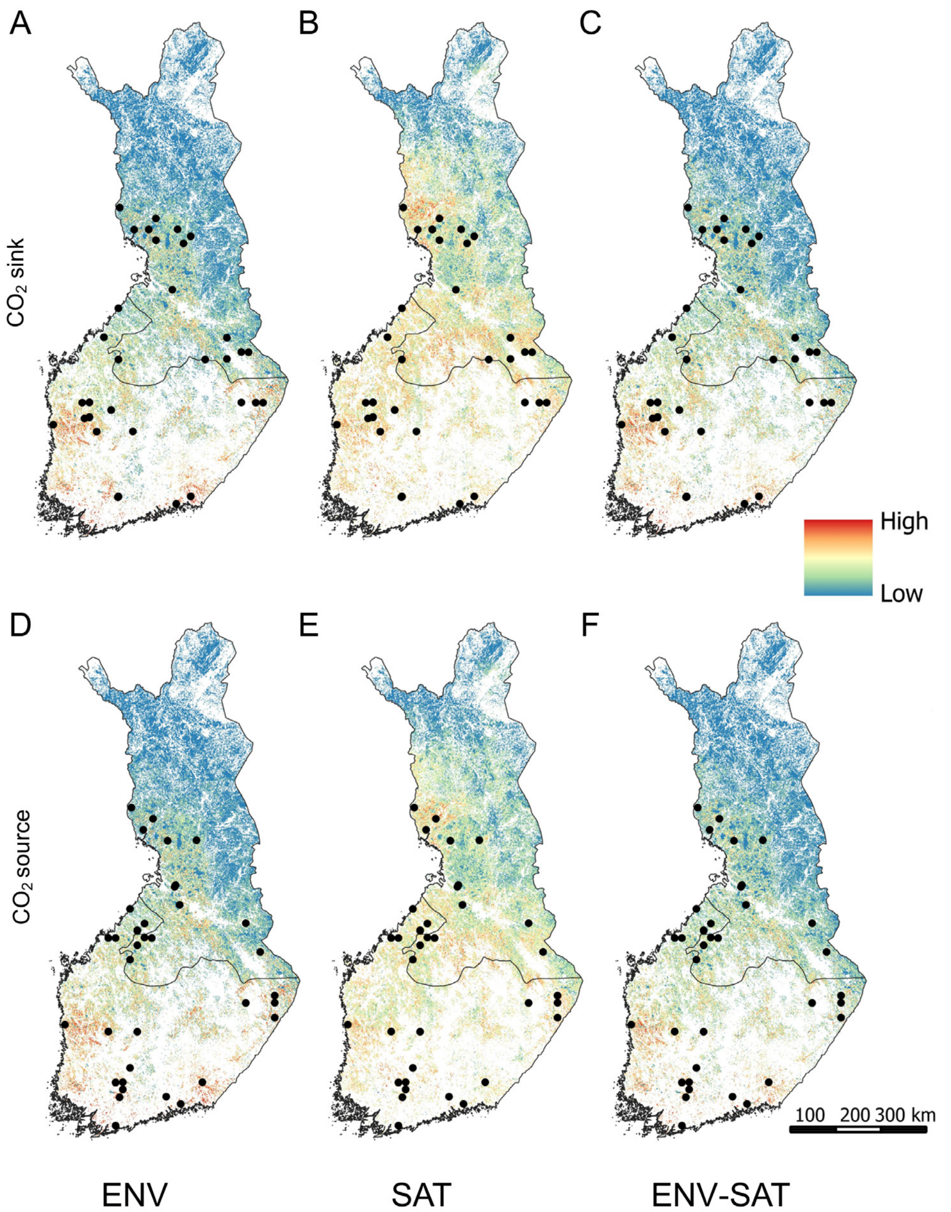

Figure 9. Predicted probability of CO_2 sinks (A–C) and sources (D–F) from environmental (ENV), satellite (SAT), and combined (ENV–SAT) variables. Black dots represent field measurement sites of CO_2 fluxes.

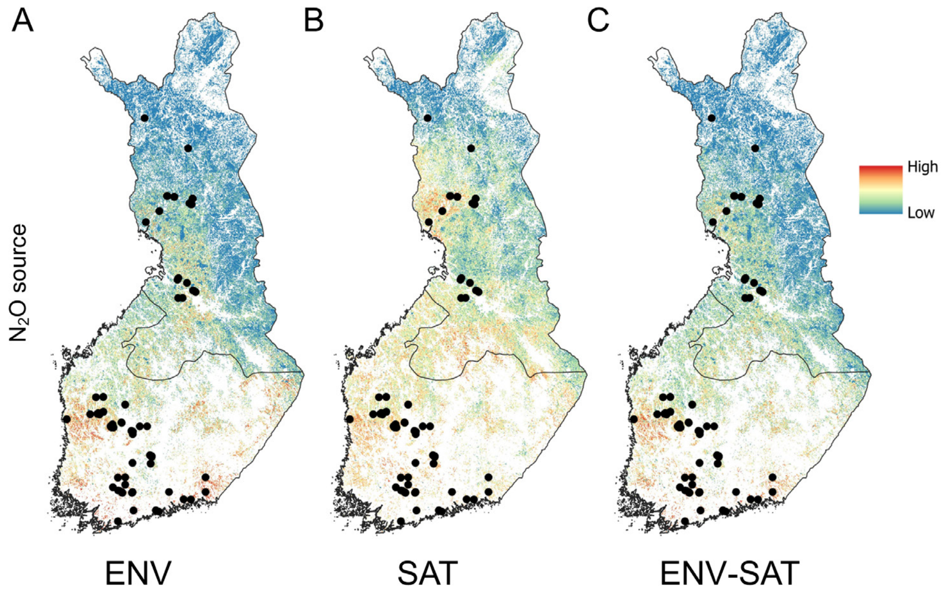

Figure 10. Predicted probability of N_2O sources (A–C) from environmental (ENV), satellite (SAT), and combined (ENV–SAT) variables. Black dots represent field measurement sites of N_2O sources.

4.3 Improving RS-based WT models with environmental data (III)

The inclusion of environmental data generally improved the predictive performance of RS-based WT models in both study sites (Table 7). In Pallas, incorporating environmental predictors substantially increased the mean R^2 in the combined area from 0.34 to 0.50, while also reducing RMSE from 12.25 cm to 10.74 cm. Similar improvements were observed in the open and treed areas, where mean R^2 increased from 0.29 to 0.41 and from 0.23 to 0.42, respectively, accompanied by consistent decreases in RMSE.

In Lettosuo, SAT–ENV models also generally showed the highest accuracy. Mean R^2 increased from 0.39 to 0.49 in the combined area and from 0.42 to 0.51 in the partial cut area, accompanied by decreases in RMSE (13.63 to 12.04 cm and 12.87 to 10.99 cm). SAT–ENV WT model in control area showed the highest R^2 (0.59) but also the highest RMSE (12.19 cm) among SAT–ENV WT models. In the clearcut area, the improvement in R^2 was minimal, with an increase of 0.01 from 0.16 to 0.17.

In Pallas, the NDVI was the most influential predictor in the combined and SAVI in open area and SWI in treed areas (Figure 11). From the ENV data, TPI_10m was an important predictor in both combined and open area, whereas DTW_10 ha was also among the important predictors in the treed areas. From the UAV data, vegetation indices (GDVI, EVI, BLUE) and the water index (NDWI) were among the most important predictors. The SWI showed a positive dependence with predicted WT, with values increasing steadily across its range. NDWI also showed a positive dependence,

Table 7. Model performance (mean R^2 and RMSE) of water table models in Pallas and Lettosuo. UAV refers to uncrewed aerial vehicle, ENV refers to environmental data, and SAT refers to satellite data.

Location	Area type	Model	Mean R^2	Mean RMSE (cm)
Pallas	Combined	UAV	0.34	12.25
		UAV-ENV	0.50	10.74
	Open	UAV	0.29	12.00
		UAV-ENV	0.41	10.96
	Treed	UAV	0.23	12.86
		UAV-ENV	0.42	11.19
Lettosuo	Combined	SAT	0.39	13.63
		SAT-ENV	0.49	12.04
	Clearcut	SAT	0.16	8.57
		SAT-ENV	0.17	8.26
	Control	SAT	0.49	16.71
		SAT-ENV	0.59	12.19
	Partial cut	SAT	0.42	12.87
		SAT-ENV	0.51	10.99

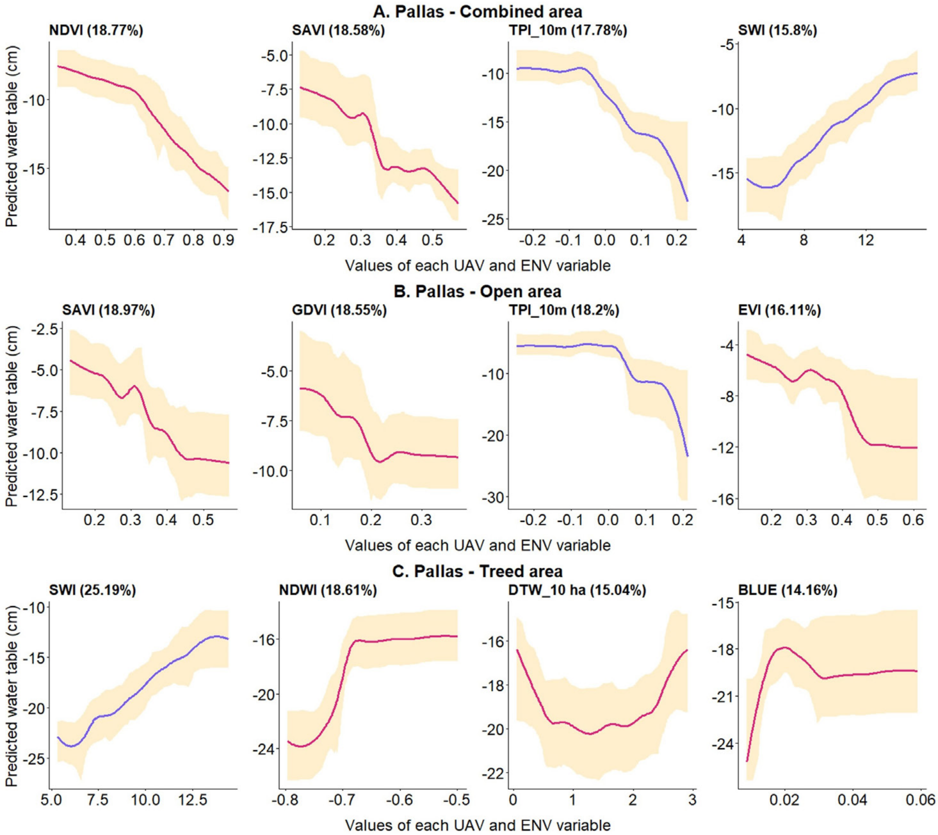

Figure 11. Partial dependence plots for the most influential predictors in the Pallas site based on UAV–ENV models. Each panel shows the marginal effect of a single UAV (pink line) or ENV (purple line) variable on the predicted WT (cm). The blue line represents the average partial dependence, illustrating how changes in each predictor are associated with a higher or lower WT. Shaded green areas indicate the 95 % confidence intervals. Percentages in parentheses next to each subplot title show the relative importance of the variable within the model. Only the four most important predictors per model are shown for A) combined, B) open, and C) treed areas. Full sets of partial dependence plots are provided in Paper III.

but the curve became flat at higher NDWI values. In contrast, both TPI variables and all vegetation indices showed non-linear negative dependences.

In Lettosuo, CHM was the most influential predictor in the combined and partial cut areas, while SAVI and red-edge bands (RE2, RE3, RE4) contributed most in the clearcut area and DTW_10 ha in the control area (Figure 12). NDMI2 and NDVI were also important across the models. CHM showed relatively stable responses followed by a sharp decline at higher values. In the clearcut area, SAVI and red-edge bands showed consistent negative relationships with predicted water table. Notably, NDMI2 showed decreasing predicted WT with increasing values, while DTW showed increasing predicted WT with increasing values.

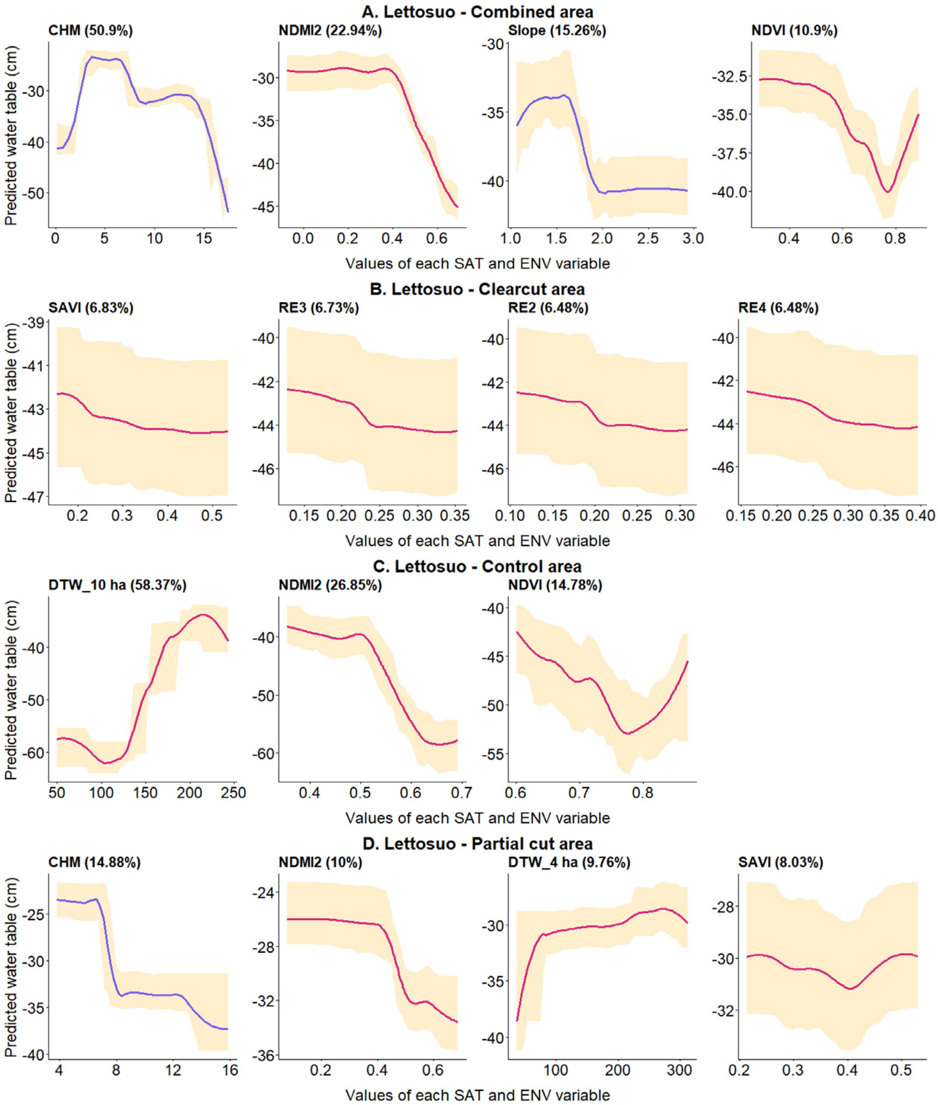

Figure 12. Partial dependence plots for the most influential predictors in the Pallas site based on SAT–ENV models. Each panel shows the marginal effect of a single SAT (pink line) or ENV (purple line) variable on the predicted WT (cm). The blue line represents the average partial dependence, illustrating how changes in each predictor are associated with a higher or lower WT. Shaded green areas indicate the 95 % confidence intervals. Percentages in parentheses next to each subplot title show the relative importance of the variable within the model. Only the four most important predictors per model are shown for A) combined, B) clearcut, C) control, and D) partial cut areas. Full sets of partial dependence plots are provided in Paper III. Abbreviations used in this figure are defined in the list of abbreviations.

The upscaled WT maps in Pallas showed distinct spatial heterogeneity (Figure 13). Strings exhibited lower WT values than the wetter flarks, and treed areas appeared consistently drier than open areas. The UAV–ENV models captured this fine-scale variability more realistically than UAV-only models, showing a lower predicted WT and higher spatial heterogeneity, particularly in treed areas.

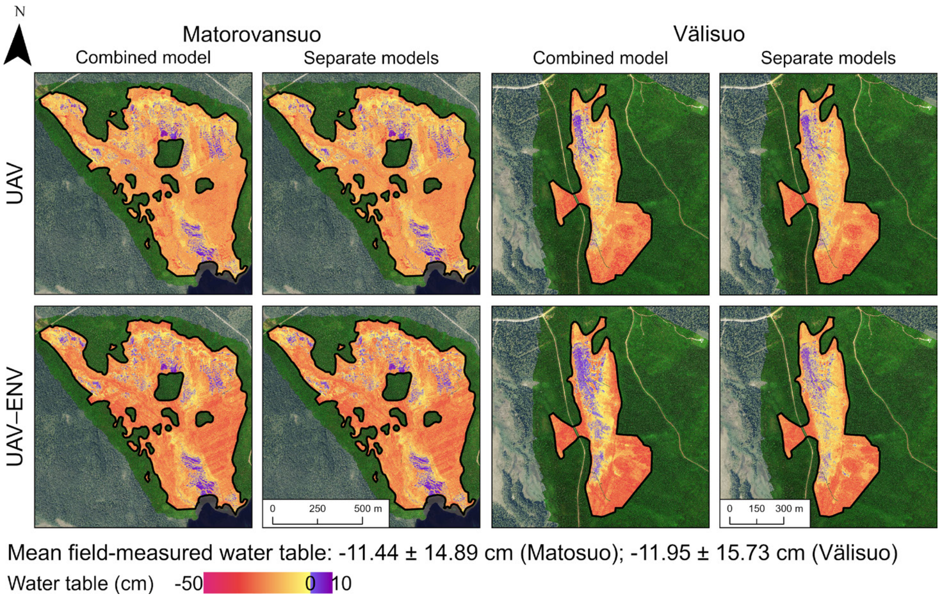

Figure 13. Spatially upscaled water table in Pallas region based on UAV models (columns 1–2) and UAV–ENV models (columns 3–4), with either combined models for all areas or separate models for open and treed peatlands. UAV = uncrewed aerial vehicle data; ENV = environmental data. Orthophotos were obtained from the National Land Survey of Finland (2025).

Upscaled WT maps in Lettosuo showed spatial and temporal variation (Figure 14). Across all seasons, the control area remained the driest, while the partial cut and clearcut areas were consistently wetter. Temporal variation was evident as WT generally declined from early summer to midsummer and autumn. Including environmental variables increased spatial heterogeneity and enhanced differentiation among treatments, particularly during midsummer and autumn..

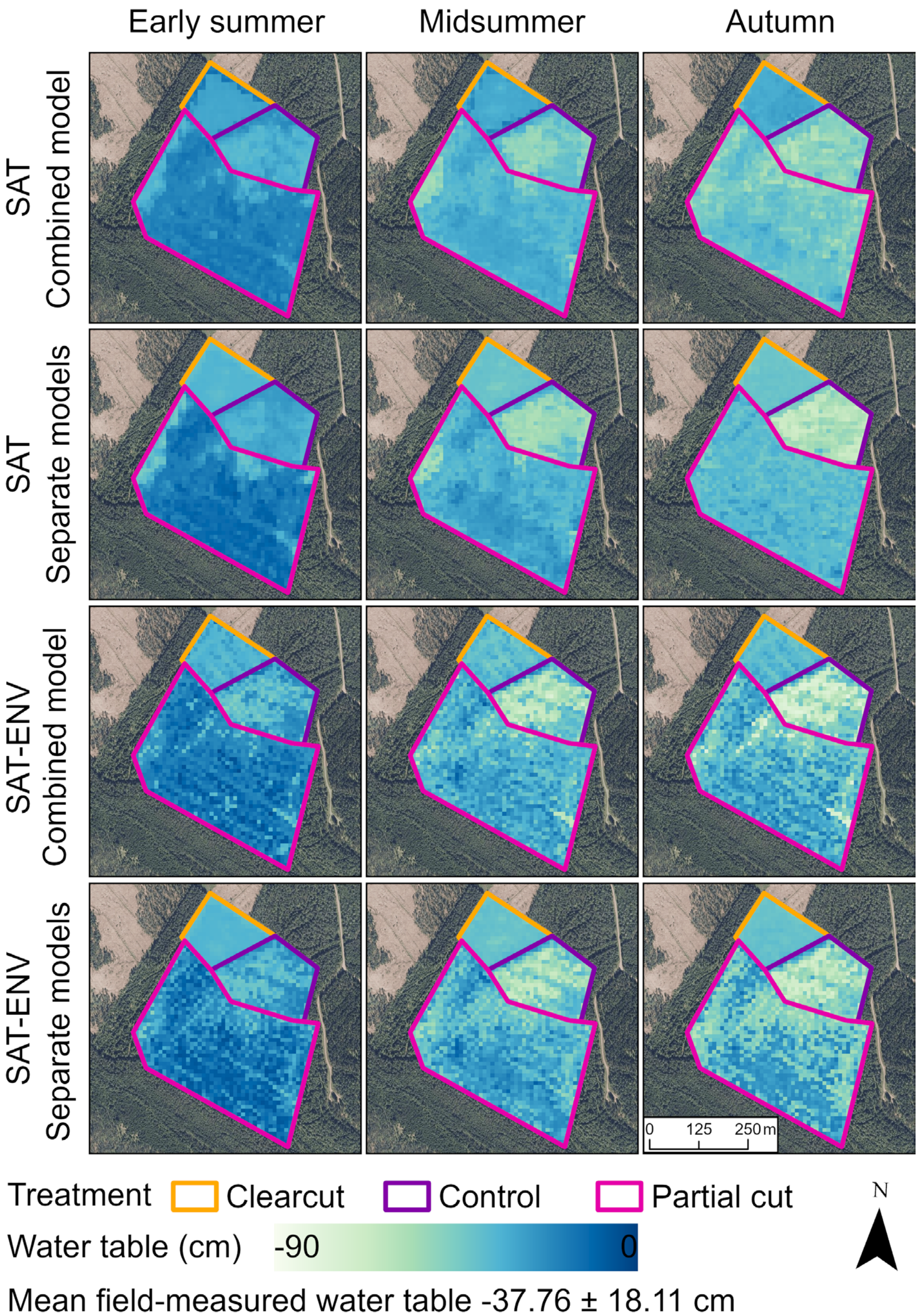

Figure 14. Spatially upscaled water table in Lettosuo across three seasonal periods (early summer, midsummer, and autumn) based on SAT and SAT–ENV models with combined models for all areas or separate models for the different treatments (clearcut, control, partial cut). SAT refers to satellite data, and ENV refers to environmental data. Orthophotos were obtained from the National Land Survey of Finland (2025)

5 Discussion

Multi-source geospatial data can be used to monitor various aspects of peatlands at national and local scales. In Paper I, models using environmental data were able to predict potential suitable habitats for red-listed species at the national scale and to show, through climate and restoration scenarios, how their potential distributions may change in the future (**O1**). In Paper II, models using environmental and satellite data could detect potential peatland GHG sinks and sources at the national scale (**O2**). However, models based solely on satellite data showed lower predictive performance than models using environmental data. This likely reflects the fact that the satellite variables used in this paper do not adequately represent key environmental characteristics, such as wetness conditions and drainage status, which are important proxies for potential GHG sinks and sources at this spatial scale. Contrary to initial expectation, combining satellite and environmental data did not substantially improve model performance compared with environmental-only models, suggesting that environmental data captured most of the relevant information for predicting potential peatland GHG sink and source patterns. Paper III showed that the inclusion of environmental variables improves RS-based model performance for spatial and spatiotemporal WT dynamics (**O3**). Both UAV- and satellite-based models achieved higher R^2 and lower RMSE with environmental predictors included, indicating that multi-source datasets better capture WT variability across scales. Model differences between the two sites (Pallas and Lettosuo) were driven by data characteristics: Pallas WT data represented a single measurement during the peak of a growing season, while Lettosuo logger data spanned multiple years.

5.1 The role of environmental data in peatland monitoring

As expected based on previous studies, the proportion of drained and undrained peatlands was the most important environmental predictor in both Papers I and II, indicating that it serves as a strong proxy for explaining both potential habitat suitability for red-listed peatland plant species (Saarimaa et al. 2019) and the distribution of potential GHG sink and source areas (Parkkari et al. 2017). Although the drainage-related variables used here represent peatland status rather than direct hydrological measurements (e.g. WT depth or surface soil moisture), the modelling results suggest that drainage status is directly linked to both potential habitat suitability and potential GHG sinks and sources. Undrained peatlands, which have not been used for intensive forestry or agriculture, maintain high water levels, diverse site fertility, and complex microtopography. These saturated conditions provide suitable habitats for many specialist species (Saarimaa et al. 2019) and suppress aerobic decomposition and CO_2 release, which might promote CH_4 production. In contrast, drained peatlands experience lowered water levels, increased oxygen availability, enhanced aerobic decomposition, and increased shrub and tree invasion. These changes lead to habitat degradation for red-listed plant species (Similä et al. 2014) and result in greater CO_2 and N_2O emissions (Hyvönen et al. 2013; A. M. Laine et al. 2019a; Laine et al. 1996).

As hypothesised, higher restoration levels in Paper I led to greater potential habitat availability for red-listed peatland plant species (Tolvanen et al. 2020). In other words, increasing the undrained peatlands corresponded to more potential suitable habitat. However, the assumption that restored sites immediately regain undrained characteristics oversimplifies the gradual and heterogeneous nature of ecological recovery. Restored peatlands often remain incomplete in their vegetation recovery even after 10–30 years, with full recovery seldom achieved (Atkinson et al. 2022; Elo et al. 2024; Kreyling et al. 2021). Therefore, in this case, environmental data cannot yet represent time-dependent hydrological or vegetation dynamics, and the modelled outcomes should be interpreted as potential rather than realised restoration effects.

Consistent with the initial assumption that climatic variables would be important predictors, climatic variables were also important in Papers I and II. In Paper I, mean January temperature and growing degree days were among the important predictors, indicating that temperature plays a significant role in defining potential suitable habitats (Thuiller et al. 2005). GDD reflects the duration and intensity of the growing season, while TJan represents the severity of winter conditions affecting plant survival (Heikkinen et al. 2020; Körner 2007). Together, these variables effectively delineate the thermal limits of peatland plant distributions. Furthermore, as assumed, climate change was found to have mixed effects on potential suitable habitats: while some species benefited from projected warming, others experienced reductions in suitable habitat. Additionally, geographical shifts in species distributions were detected under future climate scenarios, consistent with the expectations outlined in the objectives. At the same time, the climate projections showed the limits of environmental data: Although the inclusion of temperature-related variables allowed the models to depict broad-scale latitudinal shifts and species richness changes, the climate datasets cannot capture transient or extreme phenomena such as drought, soil subsidence, or complex feedback between warming and hydrology.

In Paper II, mean GDD and WAB were important in explaining spatial patterns of CH_4 and N_2O. Thus, the variables reflecting regional climate and moisture regimes can increase model accuracy when combined with drainage-related variables. WAB captures variation in effective precipitation, which might be linked to peatland wetness. This aligns with the importance of the WT in regulating peatland GHG fluxes (Evans et al. 2021; Heikkinen et al. 2024; Koch et al. 2023). Because nationwide WT data are not available, broad-scale climatic proxies such as WAB help to compensate for this gap by approximating moisture conditions. In contrast, CO_2 fluxes are more strongly determined by site-specific characteristics such as drainage status and site fertility. Of the climate variables, GDD could explain photosynthetic activity and CO_2 uptake (Zhu et al. 2022), but it may primarily influence the strength rather than whether a specific area acts as a net sink or source CO_2 (Groendahl et al. 2007; Kroner & Way 2016).

Site fertility also contributed to model performance in both Papers I and II. In Paper I, moderately fertile sites (ST2-BILB) was among the top five most important variables for predicting the occurrence of peatland red-listed plant species. In Paper II, nutrient-poor sites (ST4-SHRUB) tended to support CH_4 sinks, whereas moderately fertile (ST2-BILB) and moderately poor (ST3-LING) sites were associated with CO_2 sinks. These relationships likely result from interactions between nutrient limitation, microbial decomposition, and plant productivity (Bhullar et al. 2013; Hommeltenberg et al. 2014; Ojanen et al. 2013). Fertile sites release more CO_2 due to higher respiration rates and organic matter turnover (Jauhiainen et al. 2016; Maljanen et al. 2010; Ojanen et al. 2013; Renou-Wilson et al. 2014).

The contribution of topographical variables varied across Papers I–III. In Papers I and II, the influence of the TWI was minimal. This may partly reflect redundancy with other environmental predictors, as variables such as drainage status, site fertility, and climate already capture major gradients in moisture availability relevant for potential species distributions and potential GHG sinks and sources. When such variables are included, the TWI may therefore provide limited additional explanatory power. In addition, the relatively coarse spatial resolution of the nationwide models likely reduced the sensitivity of the TWI at the national scale, where fine-scale wetness patterns are averaged out.

As assumed, environmental variables describing site conditions, such as topography, improved RS-based WT model performance when combined with RS data. In Paper III, topography-related predictors were more informative. In Pallas, the SWI showed a positive relationship with the WT, consistent with theoretical expectations, as it is derived from topographic modelling of water flow routes and terrain flatness (Böhner & Selige 2006). The TPI was also important in Pallas. Negative TPI values (depressions) corresponded to a higher WT, whereas elevated areas (positive TPI) were drier—consistent with the string–flark topography typical of northern aapa mires (Heiskanen et al. 2021; Maanavilja et al. 2011). DTW was an important predictor in most WT models, except in the combined area of Lettosuo. However, the relationship between DTW and WT was not always as expected. Theoretically, higher DTW values indicate greater elevation above the nearest surface water, and are thus generally associated with drier conditions and deeper water tables (Murphy et al. 2008, 2009), though this relationship is not necessarily linear and may vary depending on the flow initiation threshold used. However, in this study, this expected pattern was observed only for DTW_0.5 ha in Pallas combined and open areas.

CHM did not emerge as an important predictor in Pallas, likely due to sparse tree cover and the greater influence of macro- and microtopographical variation typical of northern aapa mires. In contrast, CHM was among the most important variables in Lettosuo. CHM acts as a proxy for forest structure and stand volume, both of which directly influence evapotranspiration rates. Previous studies have demonstrated that WT is closely linked to stand volume, as evapotranspiration from mature and dense tree stands regulates WT depth during the growing season (Hökkä et al. 2008; Sarkkola et al. 2010, 2013). Thus, CHM captures not only canopy presence but also the hydrological influence of vegetation on peatland water balance.

Distance to the nearest ditch contributed little to the models in Paper III. In the Pallas combined area, WT increased with distance from the ditch but showed little change beyond ~50 m. This pattern is consistent with Nimr et al. (2026), who found that drainage effects on peatland WT extend over several tens of metres, reflecting ditch spacing needed for effective drainage. The weak influence of this variable in the models may reflect local heterogeneity in peat properties and hydrological connectivity. In particular, the hydraulic conductivity of peat decreases sharply with increasing peat humification (Päivänen 1969), which likely weakens simple distance-based relationships. In addition, ditch density may play an important role, as the cumulative effect of multiple ditches located farther away can exceed the influence of a single nearby ditch. As a result, distance to the nearest ditch alone may be an insufficient predictor of the WT in landscapes where drainage networks are dense or unevenly distributed.

5.2 The contribution of remote sensing to peatland monitoring

Consistent with the assumption that RS variables capturing surface moisture and vegetation characteristics would contribute to model performance, Sentinel-2 data proved useful in explaining spatial patterns of both potential GHG sinks and sources and peatland WT dynamics across the study sites (Papers II and III). Sentinel-2 variables were generally more important than Sentinel-1 in explaining spatial patterns of potential GHG sinks and sources (Paper II), and several vegetation- and moisture-related indices derived from Sentinel-2 (e.g. NDVI, NDMI, MNDWI, SAVI, NDRE, and RE indices) also emerged as important predictors of the WT in Paper III. This aligns with previous work demonstrating that multispectral optical data can delineate peatlands and wet areas, capture vegetation and land-cover variation, and approximate soil moisture conditions (Bourgeau-Chavez et al. 2017; Isoaho et al. 2024; Kolari et al. 2022; Minasny et al. 2019; Räsänen et al. 2022)—features that are closely linked to GHG flux patterns, as vegetation composition, productivity, and surface wetness influence CH_4, CO_2, and N_2O emissions. Furthermore, SWIR, NIR, and red reflectance are often found to be sensitive to changes in peatland hydrology (Harris and Bryant, 2009; Räsänen et al. 2022; Isoaho et al. 2023), as they respond to variations in surface moisture. Increased surface moisture and reduced oxygen availability constrain plant productivity and alter vegetation composition, leading to lower values of greenness-based indices such as NDVI and EVI, while moisture-sensitive indices such as NDMI and MNDWI increase until saturation, after which their response plateaus. Conversely, when the WT drops below a certain threshold, the capillary connection between the peat surface and deeper water table weakens, reducing the sensitivity of shorter-wavelength RS signals—including optical and C-band SAR— to further WT drawdown (Asmuß et al. 2019; Bechtold et al. 2018; Burdun et al. 2023; Räsänen et al. 2022).

Sentinel-1 variables were generally less influential in most GHG models (Paper II), which is consistent with findings from studies showing that Sentinel-1 C-band SAR typically shows lower explanatory power than optical data for representing peatland wetness and WT position, particularly in forested or structurally complex peatlands (Isoaho et al. 2024; Räsänen et al. 2022). In these environments, C-band SAR backscatter responds not only to moisture conditions but also to surface roughness and vegetation structure, which can confound the hydrological signal (Räsänen et al. 2022). Tree cover and canopy density have further been shown to strongly affect the sensitivity of satellite-derived signals to peatland WT dynamics, reducing the ability of RS predictors to capture moisture-driven gradients in more densely vegetated peatlands (Burdun et al. 2023). These factors may explain the lower importance of Sentinel-1 variables for CH_4 and N_2O fluxes, which are closely linked to fine-scale hydrological variation.

Although Sentinel-2 was generally more important than Sentinel-1 in most GHG models, the CO_2 sink model showed the opposite pattern: Late-summer VH backscatter was the strongest remote-sensing predictor, while optical variables were less influential. Previous peatland studies have shown that Sentinel-1 backscatter in boreal environments can be particularly sensitive to vegetation structure and biomass rather than soil moisture alone (Räsänen et al. 2020). The strong contribution of VH backscatter in the CO_2 sink model therefore likely reflects sensitivity to canopy structure and surface conditions that are closely linked to photosynthetic capacity and carbon uptake during peak growing season. Therefore, Sentinel-1 provides complementary structural information that is not fully captured by optical data, and combining optical and SAR observations might improve the representation of peatland environmental gradients relevant for potential GHG sinks and sources. Despite this complementarity, the overall contribution of RS data in Paper II remained limited. Additionally, Sentinel-1 data were not included in the WT analysis because previous multi-sensor studies have shown that, although combining SAR and optical data can slightly improve WT estimates, optical variables alone explain most of the WT-related variability in boreal peatlands, while SAR-only models perform substantially worse (Isoaho et al. 2024).

At finer spatial scales, UAV-based RS can be used to model the WT at Pallas (Paper III). UAV imagery provided ultra-high-resolution multispectral data, enabling us to capture microtopography and small-scale vegetation patterns that are related to the WT. Vegetation and moisture indices derived from UAV data (such as the NDVI, SAVI, GDVI, EVI, and NDWI) were among the most important predictors in the Pallas models, and partial dependence plots showed clear patterns: Vegetation indices decreased as the WT became higher and conditions more waterlogged, while the NDWI increased with higher WT until saturation, after which the relationship plateaued. These results indicate that UAV-based optical indices can be used to model WT dynamics in boreal aapa mires (Isoaho et al. 2023).

However, the performance of UAV-based optical models varied within Pallas depending on vegetation structure. Model performance (R^2) was lower in treed areas than in open peatlands, consistent with previous findings that dense canopy cover reduces the sensitivity of optical sensors to surface moisture and ground-layer vegetation signals (Burdun et al. 2023). In these treed areas, the inclusion of topography data such as the SWI, DTW and the TPI helped maintain moderate model performance, indicating that ancillary environmental information can partially compensate for the limitations of optical data under dense canopy cover.

5.3 Implications for practice and future research: Data and methodological reflections

Environmental data are increasingly available as open-access products in many parts of the world, including global datasets on climate, topography, and land cover, as well as more detailed regional or national inventories in some countries. In Finland, such environmental data are generally reliable and readily accessible online, although they are not always freely available. While such datasets enable large-scale modelling, they often vary in spatial resolution and temporal representativeness, which can be difficult for local-scale applications. Freely available satellite products (such as Sentinel-1 and Sentinel-2) are also easy to access, can be processed with open-source tools, and provide consistent temporal coverage, allowing repeated monitoring across seasons and years. In addition, UAV-based data, although limited to smaller areas, can offer very high-resolution information for local studies or detailed monitoring. However, UAV data collection requires good weather and can be relatively costly. Thus, the selection of data sources can be adjusted according to the size of the study area and the purpose of the activity.

This thesis also shows that geospatial approaches always depend on the quality and representativeness of the available field data. Environmental and RS predictors can only describe peatland conditions accurately when there is enough ground reference information to calibrate them. In practice, species records, GHG sinks and sources, and WT measurement data are often geographically unevenly distributed, especially because many intact or remote peatlands are difficult to access. This may cause predictions to be biased towards areas that have been surveyed more often, which are usually drained peatlands close to roads, particularly in the national-scale analyses presented in Papers I and II. Increasing field sampling in undrained, rewetted, and restored areas would therefore improve future models and help reduce these biases. In addition, systematic validation with ground reference data remains important for all RS applications, especially when new sensors or processing methods are used.

The used of spatial resolution also affects how well environmental conditions are captured. In Paper I, most environmental data resolution had to be aggregated to 500 m grid cells resolution to match other predictors, which inevitably smooths out small-scale variation. As a result, species observations from fully undrained microhabitats may be linked to mixed grid cells that also contain drained areas. This might lead to underestimation of potential habitat suitability of the red-listed species in the most intact sites. In addition, the chosen spatial scale influences the relevance of individual predictor variables. For example, the contribution of the TWI was relatively weak in the national-scale models in Papers I and II, whereas in the local-scale study in Pallas (Paper III), the TPI was as an important predictor. This indicates that fine-scale topographic controls become more influential at local scales, while their effects may be obscured in coarser-resolution, national-scale analyses.

The ecological assumptions in the models also can be improved. In Paper I, the SDMs used a general 20 km dispersal limit, which may overestimate how far some specialist peatland species can move, especially after restoration. Species-specific dispersal studies or genetic analyses would help produce more realistic projections and identify species that might need assisted colonisation (Kyrkjeeide et al. 2016; Zanatta et al. 2020). Similarly, most SDMs do not yet explicitly include fine-scale microclimate, species interactions, or physiological traits, even though these factors can influence species distributions (Kolstela et al. 2024; Urban et al. 2016; Virtanen et al. 2010). This is partly a matter of data availability and modelling choices rather than conceptual constraint, as methods such as joint species distribution models can account for species co-occurrence and potential biotic interactions. However, such approaches typically require detailed occurrence data and substantially increase model complexity. Similarly, incorporating microclimate or trait-based variables is often limited by the lack of spatially explicit datasets at appropriate scales. As these data and methods continue to develop, their integration into SDMs could lead to more robust predictions of species responses to restoration and climate change

For GHG modelling in Paper II, a major limitation arises from the strong spatial and temporal variability of CO_2, CH_4, and N_2O fluxes, which are driven by interacting hydrological, biological, and climatic processes that are difficult to capture using sparse field measurements. As a result, model predictions are sensitive to the representativeness of the available flux data, which in this study were geographically unevenly distributed across peatland types and seasons. In particular, the limited coverage of undrained and rewetted sites, as well as the lack of winter and shoulder-season measurements, likely contributes to uncertainty in the predicted magnitude and spatial patterns of potential GHG sinks and sources. In addition, upscaling approaches based on environmental and RS proxies rely on indirect relationships rather than explicit process representation (Levy et al. 2022). While such approaches are useful for identifying broad spatial patterns, the use of annually aggregated GHG sink and source data means that short-term flux dynamics and episodic responses to WT fluctuations, temperature extremes, or events such as droughts or heatwaves cannot be resolved or assessed in this study. Future studies could use expanded and more systematic flux measurements across peatland condition gradients, improved temporal coverage, and closer integration of multi-sensor RS data with process-based understanding. Combining correlative spatial models with targeted field experiments or process-based modelling frameworks—such as CARDAMOM (Bloom et al. 2016), ORCHIDEE (Qiu et al. 2018, 2019), LPJ-GUESS (Smith et al. 2014) —could be applied to further help constrain uncertainties and improve accuracy in landscape-scale GHG assessments.

In WT modelling (Paper III), future studies could test the use of higher-spatial-resolution optical data, such as UAV imagery, in treed peatlands like Lettosuo to better separate canopy and ground vegetation signals and clarify WT–vegetation relationships, which were less clear with Sentinel-2 data in this study. In addition, larger sample sizes and more structured sampling designs—particularly in post-harvest and clearcut areas—would improve model generalisability and help capture spatial WT variability more reliably. Further work could also evaluate the transferability of WT models across peatland types with contrasting topography and drainage intensity and develop more refined representations of drainage effects by accounting for ditch density, cumulative drainage influence, and peat properties such as humification, rather than relying solely on distance-to-ditch metrics.

The results of this thesis offer practical implications for peatland management, conservation, and restoration. In Paper I, the predicted hotspots for current and future potential suitable habitats for red-listed peatland plant species help identify areas that should be protected or restored as a priority. This is important because intact peatlands are rare, especially in southern Finland, and vegetation recovery after restoration takes time (Haapalehto et al. 2014; Maanavilja et al. 2014). Knowing where suitable conditions are likely to persist or emerge gives a clear starting point for restoration and conservation planning. Similarly, the GHG maps in Paper II indicate where CO_2, CH_4, and N_2O sinks and sources are located across the landscape, albeit with considerable uncertainty. Rather than providing precise estimates, these maps highlight broad patterns and relative differences in GHG patters among peatland areas. Areas predicted to function as strong potential GHG sinks may therefore indicate peatlands that are more likely to be well functioning and potentially important to safeguard, whereas predicted emission hotspots can be interpreted as locations where restoration could have relatively high climate-mitigation potential. However, these interpretations should be viewed as indicative rather than definitive, and site-level measurements remain necessary to confirm GHG dynamics and guide concrete management actions. In Paper III, the WT modelling showed that frequent WT monitoring can be done cost-effectively with environmental data, satellite, and UAV data, reducing the need for intense fieldworks while still capturing WT spatial and spatiotemporal patterns.

6 Conclusion

This thesis examined how multi-source geospatial data can be used to monitor potential suitable habitat for red-listed peatland plant species, potential GHG sink–source patterns, and WT dynamics. The results show that these data sources can effectively represent peatland conditions at both the national and local scales. Environmental data captured broad-scale drivers such as drainage status, climate, topography, and canopy height, while RS data provided information on vegetation patterns, surface wetness, and their spatial and temporal variability.

Models based on environmental data performed well for most red-listed peatland plant species at the national scale. Drainage and climate variables strongly explained how restoration and climate change influence potential suitable habitats for red-listed species. Restoration can sustain or increase potential suitable habitats, reduce potential habitat loss, moderate northward shifts, and maintain species richness. However, the strength of restoration benefits varied across boreal zones and climate scenarios. Under severe climate conditions, especially towards 2070–2099, restoration was still helpful but could not fully compensate for the negative effects of warming. Although the models performed well, future work should apply ecological constraints such as dispersal and species interactions to produce more realistic projections.

Models using environmental and satellite data were able to predict the occurrence of potential GHG sinks and sources at the national scale. Models using only satellite data had the lowest performance, while models combining environmental and satellite data performed best. Drainage and climate variables strongly explained the occurrence of potential GHG sinks and sources. Maps generated from environmental data alone and from combined datasets were largely similar, whereas satellite-only maps showed different patterns. These results indicate that reliable nationwide estimates of potential peatland GHG sinks and sources cannot be produced with satellite data alone and that combining multiple data sources is recommended for more accurate and realistic spatial predictions.

Combining optical UAV or satellite data with environmental variables improved model performance in both spatial and spatiotemporal WT models at the local scale. In northern patterned aapa mires, topographic variables were especially important, while in the southern drained peatland forest site, tree stand structure played a larger role. These findings show that the most relevant predictors depend on the site conditions, vegetation structure, and scale of the analysis.

Overall, the objectives of this thesis were achieved. The applied methods, combining GIS-based environmental data with RS data across multiple spatial scales, proved suitable for addressing the research questions related to potential peatland red-listed species distribution, potential GHG sinks and sources, and the WT. The usefulness of GIS-based environmental and RS data depends on the object of interest being modelled and the characteristics of the study area. Although each dataset has limitations when used alone, together they provide valuable support for peatland management, restoration planning, and long-term monitoring. No single data source is inherently better than others; instead, its value depends on how well it captures the environmental conditions that affect the variable of interest. By demonstrating how multi-source geospatial data can be combined to model potential suitable habitat for peatland red-listed species distributions, potential GHG sink–source patterns, and WT dynamics across scales, this thesis addresses the practical challenge of monitoring peatlands over large and often inaccessible areas. In this way, the thesis contributes a scalable, data-driven approach that complements field-based measurements and supports the assessment of restoration outcomes under increasing management demands, such as those following the EU Restoration Law.

References

Aalto J (2023) *Climate data from 'fine-grained climate velocities reveal vulnerability of protected areas to climate change' by Heikkinen et al. 2020*. Finnish Meteorological Institute. https://doi.org/10.23728/FMI-B2SHARE.414565C6E993426DBDF4F05FCE8FC28F

Aalto J & Pirinen P (2023) *Bioclimate change across the protected area network of Finland (Version 2)*. Finnish Meteorological Institute. https://doi.org/10.23728/FMI-B2SHARE.0CF61AF0801F4BF3A9D1336FCBBD324E

Abdalla M, Hastings A, Truu J, Espenberg M, Mander Ü & Smith P (2016) Emissions of methane from northern peatlands: a review of management impacts and implications for future management options. *Ecology and Evolution* 6(19): 7080–7102. https://doi.org/10.1002/ece3.2469

Alm J, Wall A, Myllykangas J-P, Ojanen P, Heikkinen J, Henttonen HM, et al. (2023) A new method for estimating carbon dioxide emissions from drained peatland forest soils for the greenhouse gas inventory of finland. *Biogeosciences* 20(18): 3827–3855. https://doi.org/10.5194/bg-20-3827-2023

Andersen R, Farrell C, Graf M, Muller F, Calvar E, Frankard P, et al. (2017) An overview of the progress and challenges of peatland restoration in western europe. *Restoration Ecology* 25(2): 271–282. https://doi.org/10.1111/rec.12415

Araújo MB, Anderson RP, Márcia Barbosa A, Beale CM, Dormann CF, Early R, et al. (2019) Standards for distribution models in biodiversity assessments. *Science Advances* 5(1): eaat4858. https://doi.org/10.1126/sciadv.aat4858
Araújo MB & Guisan A (2006) Five (or so) challenges for species distribution modelling. *Journal of Biogeography* 33(10): 1677–1688. https://doi.org/10.1111/j.1365-2699.2006.01584.x
Araújo MB & Peterson AT (2012) Uses and misuses of bioclimatic envelope modeling. *Ecology* 93(7): 1527–1539. https://doi.org/10.1890/11-1930.1
Asmuß T, Bechtold M & Tiemeyer B (2019) On the potential of sentinel-1 for high resolution monitoring of water table dynamics in grasslands on organic soils. *Remote Sensing* 11(14): 1659. https://doi.org/10.3390/rs11141659
Atkinson J, Brudvig LA, Mallen-Cooper M, Nakagawa S, Moles AT & Bonser SP (2022) Terrestrial ecosystem restoration increases biodiversity and reduces its variability, but not to reference levels: a global meta-analysis. *Ecology Letters* 25(7): 1725–1737. https://doi.org/10.1111/ele.14025
Baltzer JL, Veness T, Chasmer LE, Sniderhan AE & Quinton WL (2014) Forests on thawing permafrost: fragmentation, edge effects, and net forest loss. *Global Change Biology* 20(3): 824–834. https://doi.org/10.1111/gcb.12349
Barbet-Massin M, Jiguet F, Albert CH & Thuiller W (2012) Selecting pseudo-absences for species distribution models: how, where and how many? *Methods in Ecology and Evolution* 3(2): 327–338. https://doi.org/10.1111/j.2041-210X.2011.00172.x
Bechtold M, Schlaffer S, Tiemeyer B & De Lannoy G (2018) Inferring water table depth dynamics from envisat-asar c-band backscatter over a range of peatlands from deeply-drained to natural conditions. *Remote Sensing* 10(4): 536. https://doi.org/10.3390/rs10040536
Belgiu M & Drăguţ L (2016) Random forest in remote sensing: a review of applications and future directions. *ISPRS Journal of Photogrammetry and Remote Sensing* 114: 24–31. https://doi.org/10.1016/j.isprsjprs.2016.01.011
Besson M, Alison J, Bjerge K, Gorochowski TE, Høye TT, Jucker T, et al. (2022) Towards the fully automated monitoring of ecological communities. *Ecology Letters* 25(12): 2753–2775. https://doi.org/10.1111/ele.14123
Beven KJ & Kirkby MJ (1979) A physically based, variable contributing area model of basin hydrology / un modèle à base physique de zone d'appel variable de l'hydrologie du bassin versant. *Hydrological Sciences Bulletin* 24(1): 43–69. https://doi.org/10.1080/02626667909491834
Bhullar GS, Iravani M, Edwards PJ & Olde Venterink H (2013) Methane transport and emissions from soil as affected by water table and vascular plants. *BMC Ecology* 13(1): 32. https://doi.org/10.1186/1472-6785-13-32
Bloom AA, Exbrayat J-F, Van Der Velde IR, Feng L & Williams M (2016) The decadal state of the terrestrial carbon cycle: global retrievals of terrestrial carbon allocation, pools, and residence times. *Proceedings of the National Academy of Sciences* 113(5): 1285–1290. https://doi.org/10.1073/pnas.1515160113
Böhner J & Selige T (2006) Spatial prediction of soil attributes using terrain analysis and climate regionalisation. *Gottinger Geographische Abhandlungen* 115: 13–28.
Bourgeau-Chavez LL, Endres S, Powell R, Battaglia MJ, Benscoter B, Turetsky M, et al. (2017) Mapping boreal peatland ecosystem types from multitemporal radar and optical satellite imagery. *Canadian Journal of Forest Research* 47(4): 545–559. https://doi.org/10.1139/cjfr-2016-0192.
Box JE, Colgan WT, Christensen TR, Schmidt NM, Lund M, Parmentier F-JW, et al. (2019) Key indicators of arctic climate change: 1971–2017. *Environmental Research Letters* 14(4): 045010. https://doi.org/10.1088/1748-9326/aafc1b
Breeuwer A, Robroek BJM, Limpens J, Heijmans MMPD, Schouten MGC & Berendse F (2009) Decreased summer water table depth affects peatland vegetation. *Basic and Applied Ecology* 10(4): 330–339. https://doi.org/10.1016/j.baae.2008.05.005
Breiman L (2001) Random forests. *Machine Learning* 45(1): 5–32. https://doi.org/10.1023/A:1010933404324
Bucklin DN, Basille M, Benscoter AM, Brandt LA, Mazzotti FJ, Romañach SS, et al. (2015) Comparing species distribution models constructed with different subsets of environmental predictors. *Diversity and Distributions* 21(1): 23–35. https://doi.org/10.1111/ddi.12247
Burdun I, Bechtold M, Aurela M, De Lannoy G, Desai AR, Humphreys E, et al. (2023) Hidden becomes clear: optical remote sensing of vegetation reveals water table dynamics in northern peatlands. *Remote Sensing of Environment* 296: 113736. https://doi.org/10.1016/j.rse.2023.113736
Burdun I, Bechtold M, Sagris V, Komisarenko V, De Lannoy G & Mander Ü (2020a) A comparison of three trapezoid models using optical and thermal satellite imagery for water table depth monitoring in estonian bogs. *Remote Sensing* 12(12): 1980. https://doi.org/10.3390/rs12121980
Burdun I, Bechtold M, Sagris V, Lohila A, Humphreys E, Desai AR, et al. (2020b) Satellite determination of peatland water table temporal dynamics by localizing representative pixels of a swir-based moisture index. *Remote Sensing* 12(18): 2936. https://doi.org/10.3390/rs12182936

nordia geographical publications

Byrne B, Liu J, Bowman KW, Pascolini-Campbell M, Chatterjee A, Pandey S, et al. (2024) Carbon emissions from the 2023 Canadian wildfires. *Nature* 633(8031): 835–839. https://doi.org/10.1038/s41586-024-07878-z

Campbell C, Granath G & Rydin H (2021) Climatic drivers of sphagnum species distributions. *Frontiers of Biogeography* 13(4). https://doi.org/10.21425/F5FBG51146

Dieleman CM, Branfireun BA, McLaughlin JW & Lindo Z (2014) Climate change drives a shift in peatland ecosystem plant community: implications for ecosystem function and stability. *Global Change Biology* 21(1): 388–395. https://doi.org/10.1111/gcb.12643

Dronova I, Kislik C, Dinh Z & Kelly M (2021) A review of unoccupied aerial vehicle use in wetland applications: emerging opportunities in approach, technology, and data. *Drones* 5(2): 45. https://doi.org/10.3390/drones5020045

Duan W, Wu M, Peichl M, He H, Roulet N, Noumonvi KD, et al. (2025) Seasonal and diurnal patterns of methane emissions from a northern pristine peatland in the last decade. *Global Biogeochemical Cycles* 39(8): e2025GB008518. https://doi.org/10.1029/2025GB008518

Elith J & Leathwick JR (2009) Species distribution models: ecological explanation and prediction across space and time. *Annual Review of Ecology, Evolution, and Systematics* 40(1): 677–697. https://doi.org/10.1146/annurev.ecolsys.110308.120159

Elith J, Phillips SJ, Hastie T, Dudík M, Chee YE & Yates CJ (2011) A statistical explanation of maxent for ecologists: statistical explanation of maxent. *Diversity and Distributions* 17(1): 43–57. https://doi.org/10.1111/j.1472-4642.2010.00725.x

Elo M, Kareksela S, Ovaskainen O, Abrego N, Niku J, Taskinen S, et al. (2024) Restoration of forestry-drained boreal peatland ecosystems can effectively stop and reverse ecosystem degradation. *Communications Earth & Environment* 5(1): 680. https://doi.org/10.1038/s43247-024-01844-3

Evans CD, Peacock M, Baird AJ, Artz RRE, Burden A, Callaghan N, et al. (2021) Overriding water table control on managed peatland greenhouse gas emissions. *Nature* 593(7860): 548–552. https://doi.org/10.1038/s41586-021-03523-1

Fernandes RF, Scherrer D & Guisan A (2019) Effects of simulated observation errors on the performance of species distribution models. *Diversity and Distributions* 25(3): 400–413. https://doi.org/10.1111/ddi.12868

Finnish Environmental Institute (2009) *Finnish environmental institute spatial drainage stage data on peatlands*. https://www.syke.fi/en-US/Open_information/Spatial_datasets/Downloadable_spatial_dataset (accessed 19 January 2023)

Finnish Environmental Institute (2022) *Forest classification*. https://ckan.ymparisto.fi/dataset/%7B914281ED-C962-4135-8EEA-BF4391DE72AF%7D (accessed 29 December 2025)

Finnish Environmental Institute (2025) *Peatland and mineral soil drainage status*. https://ckan.ymparisto.fi/dataset/%7BC73BC2C1-C2CA-4FCA-9171-B8074F2BC2A3%7D (accessed 29 December 2025)

Frolking S, Talbot J, Jones MC, Treat CC, Kauffman JB, Tuittila E-S, et al. (2011) Peatlands in the earth's 21st century climate system. *Environmental Reviews* 19(NA): 371–396. https://doi.org/10.1139/a11-014

Gao B (1996) NDWI—a normalized difference water index for remote sensing of vegetation liquid water from space. *Remote Sensing of Environment* 58(3): 257–266. https://doi.org/10.1016/S0034-4257(96)00067-3

Golovatskaya EA & Dyukarev EA (2011) Seasonal and diurnal dynamics of co2 emission from oligotrophic peat soil surface. *Russian Meteorology and Hydrology* 36(6): 413–419. https://doi.org/10.3103/S1068373911060094

Gorelick N, Hancher M, Dixon M, Ilyushchenko S, Thau D & Moore R (2017) Google earth engine: planetary-scale geospatial analysis for everyone. *Remote Sensing of Environment* 202: 18–27. https://doi.org/10.1016/j.rse.2017.06.031

Gorham E (1991) Northern peatlands: role in the carbon cycle and probable responses to climatic warming. *Ecological Applications* 1(2): 182–195. https://doi.org/10.2307/1941811

Granlund L, Vesakoski V, Sallinen A, Kolari THM, Wolff F & Tahvanainen T (2022) Recent lateral expansion of sphagnum bogs over central fen areas of boreal aapa mire complexes. *Ecosystems* 25(7): 1455–1475. https://doi.org/10.1007/s10021-021-00726-5

Groendahl L, Friborg T & Soegaard H (2007) Temperature and snow-melt controls on interannual variability in carbon exchange in the high arctic. *Theoretical and Applied Climatology* 88(1–2): 111–125. https://doi.org/10.1007/s00704-005-0228-y

Guisan A, Weiss SB & Weiss AD (1999) GLM versus CCA spatial modeling of plant species distribution. *Plant Ecology* 143(1): 107–122. https://doi.org/10.1023/A:1009841519580

Haapalehto T, Juutinen R, Kareksela S, Kuitunen M, Tahvanainen T, Vuori H, et al. (2017) Recovery of plant communities after ecological restoration of forestry□drained peatlands. *Ecology and Evolution* 7(19): 7848–7858. https://doi.org/10.1002/ece3.3243

Haapalehto T, Kotiaho JS, Matilainen R & Tahvanainen T (2014) The effects of long-term drainage and subsequent restoration on water table level and pore water chemistry in boreal peatlands. *Journal of Hydrology* 519: 1493–1505. https://doi.org/10.1016/j.jhydrol.2014.09.013

Haapalehto TO, Vasander H, Jauhiainen S, Tahvanainen T & Kotiaho JS (2011) The effects of peatland restoration on water-table depth, elemental concentrations, and vegetation: 10 years of changes. *Restoration Ecology* 19(5): 587–598. https://doi.org/10.1111/j.1526-100X.2010.00704.x

Habib W, Ingle R, Saunders M & Connolly J (2024) Quantifying peatland land use and co2 emissions in irish raised bogs: mapping insights using sentinel-2 data and google earth engine. *Scientific Reports* 14(1): 1171. https://doi.org/10.1038/s41598-024-51660-0

Hamedianfar A, Maanavilja L & Sutinen H (2025) Evaluating ensemble machine learning and feature optimization for mapping peatland vegetation using uas-derived data. *International Journal of Applied Earth Observation and Geoinformation* 144: 104901. https://doi.org/10.1016/j.jag.2025.104901

Harris A & Bryant RG (2009) A multi-scale remote sensing approach for monitoring northern peatland hydrology: present possibilities and future challenges. *Journal of Environmental Management* 90(7): 2178–2188. https://doi.org/10.1016/j.jenvman.2007.06.025

Harris A, Charnock R & Lucas RM (2015) Hyperspectral remote sensing of peatland floristic gradients. *Remote Sensing of Environment* 162: 99–111. https://doi.org/10.1016/j.rse.2015.01.029

Heikkinen J, Lång K, Honkanen H & Myllys M (2024) Mitigation of greenhouse gas emissions by optimizing groundwater level in boreal cultivated peatland. *Wetlands* 44(6): 78. https://doi.org/10.1007/s13157-024-01833-4

Heikkinen RK, Leikola N, Aalto J, Aapala K, Kuusela S, Luoto M, et al. (2020) Fine-grained climate velocities reveal vulnerability of protected areas to climate change. *Scientific Reports* 10(1): 1678. https://doi.org/10.1038/s41598-020-58638-8

Heikkinen RK, Luoto M, Araújo MB, Virkkala R, Thuiller W & Sykes MT (2006) Methods and uncertainties in bioclimatic envelope modelling under climate change. *Progress in Physical Geography: Earth and Environment* 30(6): 751–777. https://doi.org/10.1177/0309133306071957

Heiskanen L, Tuovinen J-P, Räsänen A, Virtanen T, Juutinen S, Lohila A, et al. (2021) Carbon dioxide and methane exchange of a patterned subarctic fen during two contrasting growing seasons. *Biogeosciences* 18(3): 873–896. https://doi.org/10.5194/bg-18-873-2021

Hijmans RJ, Phillips S, Leathwick J & Elith J (2010) Dismo: species distribution modeling. https://doi.org/10.32614/CRAN.package.dismo

Hökkä H, Repola J & Laine J (2008) Quantifying the interrelationship between tree stand growth rate and water table level in drained peatland sites within central finland. *Canadian Journal of Forest Research* 38(7): 1775–1783. https://doi.org/10.1139/X08-028.

Holidi H, Armanto ME, Damiri N & Dwi Anugerah Putranto D (2019) Characteristics of selected peatland uses and soil moisture based on tvdi. *Journal of Ecological Engineering* 20(4): 194–200. https://doi.org/10.12911/22998993/102987

Holmgren M, Lin C, Murillo JE, Nieuwenhuis A, Penninkhof J, Sanders N, et al. (2015) Positive shrub–tree interactions facilitate woody encroachment in boreal peatlands. *Journal of Ecology* 103(1): 58–66. https://doi.org/10.1111/1365-2745.12331

Hommeltenberg J, Schmid HP, Drösler M & Werle P (2014) Can a bog drained for forestry be a stronger carbon sink than a natural bog forest? *Biogeosciences* 11(13): 3477–3493. https://doi.org/10.5194/bg-11-3477-2014

Hyvärinen E, Juslén AK, Kemppainen E, Uddström A & Liukko U-M (2019) *The 2019 red list of Finnish species*. Ympäristöministeriö & Suomen ympäristökeskus, Helsinki. http://hdl.handle.net/10138/299501

Hyvönen NP, Huttunen JT, Shurpali, Narasinha J., Lind SE, Marushchak, Maija E., Heitto L, et al. (2013) The role of drainage ditches in greenhouse gas emissions and surface leaching losses from a cutaway peatland cultivated with a perennial bioenergy crop. *Boreal Environment Research* 18: 109–126.

Ikkala L, Ronkanen A-K, Ilmonen J, Similä M, Rehell S, Kumpula T, et al. (2022) Unmanned aircraft system (uas) structure-from-motion (sfm) for monitoring the changed flow paths and wetness in minerotrophic peatland restoration. *Remote Sensing* 14(13): 3169. https://doi.org/10.3390/rs14133169

IPCC (2013) *Climate change 2013: the physical science basis*. Contribution of Working Group I to the Fifth Assessment Report of the Intergovernmental Panel on Climate Change. Cambridge University Press., Cambridge, UK and New York, NY.

Isoaho A, Ikkala L, Marttila H, Hjort J, Kumpula T, Korpelainen P, et al. (2023) Spatial water table level modelling with multi-sensor unmanned aerial vehicle data in boreal aapa mires. *Remote Sensing Applications: Society and Environment* 32: 101059. https://doi.org/10.1016/j.rsase.2023.101059

Isoaho A, Ikkala L, Päkkilä L, Marttila H, Kareksela S & Räsänen A (2024) Multi-sensor satellite imagery reveals spatiotemporal changes in peatland water table after restoration. *Remote Sensing of Environment* 306: 114144. https://doi.org/10.1016/j.rse.2024.114144

Jauhiainen J, Page SE & Vasander H (2016) Greenhouse gas dynamics in degraded and restored tropical peatlands. *Mires and Peat* 17: 1–12.

Jiménez-Valverde A, Lobo JM & Hortal J (2008) Not as good as they seem: the importance of concepts in species distribution modelling. *Diversity and Distributions* 14(6): 885–890. https://doi.org/10.1111/j.1472-4642.2008.00496.x

Joosten H (2009) *The global peatland CO_2 picture: peatland status and drainage related emissions in all countries of the world.* Wetlands International. https://unfccc.int/sites/default/files/draftpeatlandco2report.pdf

Joosten H (2016) Peatlands across the globe. In Bonn A, Allott T, Evans M, Joosten H & Stoneman R (eds) *Peatland restoration and ecosystem services*, 19–43. Cambridge University Press. https://doi.org/10.1017/CBO9781139177788.003

Joosten H & Clarke D (2002) *Wise use of mires and peatlands*. International mire conservation group and international peat society.

Junker J, Blake S, Boesch C, Campbell G, Toit LD, Duvall C, et al. (2012) Recent decline in suitable environmental conditions for african great apes. *Diversity and Distributions* 18(11): 1077–1091. https://doi.org/10.1111/ddi.12005

Junttila S, Kelly J, Kljun N, Aurela M, Klemedtsson L, Lohila A, et al. (2021) Upscaling northern peatland CO_2 fluxes using satellite remote sensing data. *Remote Sensing* 13(4): 818. https://doi.org/10.3390/rs13040818

Kalacska M, Arroyo-Mora JP, Soffer RJ, Roulet NT, Moore TR, Humphreys E, et al. (2018) Estimating peatland water table depth and net ecosystem exchange: a comparison between satellite and airborne imagery. *Remote Sensing* 10(5): 687. https://doi.org/10.3390/rs10050687

Kays R, Crofoot MC, Jetz W & Wikelski M (2015) Terrestrial animal tracking as an eye on life and planet. *Science* 348(6240). https://doi.org/10.1126/science.aaa2478

Keränen K, Isoaho A, Räsänen A, Hjort J, Kumpula T, Korpelainen P, et al. (2024) Multi-resolution remote sensing for flark area detection in boreal aapa mires. *International Journal of Remote Sensing* 45(13): 4324–4343. https://doi.org/10.1080/01431161.2024.2359732

Koch J, Elsgaard L, Greve MH, Gyldenkærne S, Hermansen C, Levin G, et al. (2023) Water-table-driven greenhouse gas emission estimates guide peatland restoration at national scale. *Biogeosciences* 20(12): 2387–2403. https://doi.org/10.5194/bg-20-2387-2023

Kolari THM, Sallinen A, Wolff F, Kumpula T, Tolonen K & Tahvanainen T (2022) Ongoing fen–bog transition in a boreal aapa mire inferred from repeated field sampling, aerial images, and landsat data. *Ecosystems* 25(5): 1166–1188. https://doi.org/10.1007/s10021-021-00708-7

Kolstela J, Aakala T, Maclean I, Niittynen P, Kemppinen J, Luoto M, et al. (2024) Revealing fine-scale variability in boreal forest temperatures using a mechanistic microclimate model. *Agricultural and Forest Meteorology* 350: 109995. https://doi.org/10.1016/j.agrformet.2024.109995

Komulainen V, Tuittila E, Vasander H & Laine J (1999) Restoration of drained peatlands in southern finland: initial effects on vegetation change and co_2 balance. *Journal of Applied Ecology* 36(5): 634–648. https://doi.org/10.1046/j.1365-2664.1999.00430.x

Korhonen K, Ahola A, Heikkinen J, Henttonen H, Hotanen J-P, Ihalainen A, et al. (2021) Forests of Finland 2014–2018 and their development 1921–2018. *Silva Fennica* 55(5). https://doi.org/10.14214/sf.10662

Korkiakoski M, Ojanen P, Tuovinen J-P, Minkkinen K, Nevalainen O, Penttilä T, et al. (2023) Partial cutting of a boreal nutrient-rich peatland forest causes radically less short-term on-site CO_2 emissions than clear-cutting. *Agricultural and Forest Meteorology* 332: 109361. https://doi.org/10.1016/j.agrformet.2023.109361

Korkiakoski M, Tuovinen J-P, Penttilä T, Sarkkola S, Ojanen P, Minkkinen K, et al. (2019) Greenhouse gas and energy fluxes in a boreal peatland forest after clear-cutting. *Biogeosciences* 16(19): 3703–3723. https://doi.org/10.5194/bg-16-3703-2019

Körner C (2007) The use of 'altitude' in ecological research. *Trends in Ecology & Evolution* 22(11): 569–574. https://doi.org/10.1016/j.tree.2007.09.006

Kreyling J, Tanneberger F, Jansen F, Van Der Linden S, Aggenbach C, Blüml V, et al. (2021) Rewetting does not return drained fen peatlands to their old selves. *Nature Communications* 12(1): 5693. https://doi.org/10.1038/s41467-021-25619-y

Kroner Y & Way DA (2016) Carbon fluxes acclimate more strongly to elevated growth temperatures than to elevated CO_2 concentrations in a northern conifer. *Global Change Biology* 22(8): 2913–2928. https://doi.org/10.1111/gcb.13215

Kyrkjeeide MO, Hassel K, Flatberg KI, Shaw AJ, Brochmann C & Stenøien HK (2016) Long□distance dispersal and barriers shape genetic structure of peatmosses (*Sphagnum*) across the northern hemisphere. *Journal of Biogeography* 43(6): 1215–1226. https://doi.org/10.1111/jbi.12716

Lafleur PM, Moore TR, Roulet NT & Frolking S (2005) Ecosystem respiration in a cool temperate bog depends on peat temperature but not water table. *Ecosystems* 8(6): 619–629. https://doi.org/10.1007/s10021-003-0131-2

Laine AM, Mehtätalo L, Tolvanen A, Frolking S & Tuittila E-S (2019a) Impacts of drainage, restoration and warming on boreal wetland greenhouse gas fluxes. *Science of The Total Environment* 647: 169–181. https://doi.org/10.1016/j.scitotenv.2018.07.390

Laine AM, Mäkiranta P, Laiho R, Mehtätalo L, Penttilä T, Korrensalo A, et al. (2019b) Warming impacts on boreal fen CO_2 exchange under wet and dry conditions. *Global Change Biology* 25(6): 1995–2008. https://doi.org/10.1111/gcb.14617

Laine AM, Ojanen P, Lindroos T, Koponen K, Maanavilja L, Lampela M, et al. (2024) Climate change mitigation potential of restoration of boreal peatlands drained for forestry can be adjusted by site selection and restoration measures. *Restoration Ecology* 32(7): e14213. https://doi.org/10.1111/rec.14213

Laine J, Laiho R, Minkkinen K & Vasander H (2006) Forestry and boreal peatlands. *In* Wieder RK & Vitt DH (eds) *Boreal peatland ecosystems*, 331–357. Springer Berlin Heidelberg. https://doi.org/10.1007/978-3-540-31913-9_15

Laine J, Silvola J, Tolonen K, Alm J, Nykänen H, Vasander H, et al. (1996) Effect of water-level drawdown on global climatic warming: northern peatlands. *Ambio* 25(3): 179–184.

Laitinen J, Rehell S, Huttunen A, Tahvanainen T, Heikkilä R & Lindholm T (2007) Mire systems in Finland - special view to aapamires and their water-flow pattern. *Finnish Peatland Society* 58(1): 1–26.

Lees KJ, Artz RRE, Chandler D, Aspinall T, Boulton CA, Buxton J, et al. (2021a) Using remote sensing to assess peatland resilience by estimating soil surface moisture and drought recovery. *Science of The Total Environment* 761: 143312. https://doi.org/10.1016/j.scitotenv.2020.143312

Lees KJ, Khomik M, Quaife T, Clark JM, Hill T, Klein D, et al. (2021b) Assessing the reliability of peatland GPP measurements by remote sensing: from plot to landscape scale. *Science of The Total Environment* 766: 142613. https://doi.org/10.1016/j.scitotenv.2020.142613

Lees KJ, Quaife T, Artz RRE, Khomik M & Clark JM (2018) Potential for using remote sensing to estimate carbon fluxes across northern peatlands – a review. *Science of The Total Environment* 615: 857–874. https://doi.org/10.1016/j.scitotenv.2017.09.103

Lehtonen I, Ruosteenoja K & Jylhä K (2014) Projected changes in European extreme precipitation indices on the basis of global and regional climate model ensembles. *International Journal of Climatology* 34(4): 1208–1222. https://doi.org/10.1002/joc.3758

Leifeld J & Menichetti L (2018) The underappreciated potential of peatlands in global climate change mitigation strategies. *Nature Communications* 9(1): 1071. https://doi.org/10.1038/s41467-018-03406-6

Leppiniemi O, Karjalainen O, Aalto J, Luoto M & Hjort J (2025) Environmental drivers of palsa and peat plateau occurrences: a regional comparison across the northern hemisphere. *Permafrost and Periglacial Processes* 36(1): 37–50. https://doi.org/10.1002/ppp.2253

Levy P, Clement R, Cowan N, Keane B, Myrgiotis V, Van Oijen M, et al. (2022) Challenges in scaling up greenhouse gas fluxes: experience from the uk greenhouse gas emissions and feedbacks program. *Journal of Geophysical Research: Biogeosciences* 127(5): e2021JG006743. https://doi.org/10.1029/2021JG006743

Liu C, White M & Newell G (2013) Selecting thresholds for the prediction of species occurrence with presence-only data. *Journal of Biogeography* 40(4): 778–789. https://doi.org/10.1111/jbi.12058

Long KD, Flanagan LB & Cai T (2010) Diurnal and seasonal variation in methane emissions in a northern canadian peatland measured by eddy covariance. *Global Change Biology* 16(9): 2420–2435. https://doi.org/10.1111/j.1365-2486.2009.02083.x

Lopatin J, Kattenborn T, Galleguillos M, Perez-Quezada JF & Schmidtlein S (2019) Using aboveground vegetation attributes as proxies for mapping peatland belowground carbon stocks. *Remote Sensing of Environment* 231: 111217. https://doi.org/10.1016/j.rse.2019.111217

Ma X, Xu H, Cao Z, Shu L & Zhu R (2022) Will climate change cause the global peatland to expand or contract? evidence from the habitat shift pattern of *Sphagnum* mosses. *Global Change Biology* 28(21): 6419–6432. https://doi.org/10.1111/gcb.16354

Maanavilja L, Aapala K, Haapalehto T, Kotiaho JS & Tuittila E-S (2014) Impact of drainage and hydrological restoration on vegetation structure in boreal spruce swamp forests. *Forest Ecology and Management* 330: 115–125. https://doi.org/10.1016/j.foreco.2014.07.004

Maanavilja L, Riutta T, Aurela M, Pulkkinen M, Laurila T & Tuittila E-S (2011) Spatial variation in co2 exchange at a northern aapa mire. *Biogeochemistry* 104(1–3): 325–345. https://doi.org/10.1007/s10533-010-9505-7

Mäkiranta P, Laiho R, Mehtätalo L, Straková P, Sormunen J, Minkkinen K, et al. (2018) Responses of phenology and biomass production of boreal fens to climate warming under different water□ table level regimes. *Global Change Biology* 24(3): 944–956. https://doi.org/10.1111/gcb.13934

Maljanen M, Sigurdsson BD, Guðmundsson J, Óskarsson H, Huttunen JT & Martikainen PJ (2010) Greenhouse gas balances of managed peatlands in the nordic countries – present knowledge and gaps. *Biogeosciences* 7(9): 2711–2738. https://doi.org/10.5194/bg-7-2711-2010

Malmer N, Albinsson C, Svensson BM & Wallén B (2003) Interferences between *sphagnum* and vascular plants: effects on plant community structure and peat formation. *Oikos* 100(3): 469–482. https://doi.org/10.1034/j.1600-0706.2003.12170.x

Manzoor SA, Griffiths G & Lukac M (2018) Species distribution model transferability and model grain size – finer may not always be better. *Scientific Reports* 8(1): 7168. https://doi.org/10.1038/s41598-018-25437-1

McFeeters SK (1996) The use of the normalized difference water index (ndwi) in the delineation of open water features. *International Journal of Remote Sensing* 17(7): 1425–1432. https://doi.org/10.1080/01431169608948714

Meingast KM, Falkowski MJ, Kane ES, Potvin LR, Benscoter BW, Smith AMS, et al. (2014) Spectral detection of near-surface moisture content and water-table position in northern peatland ecosystems. *Remote Sensing of Environment* 152: 536–546. https://doi.org/10.1016/j.rse.2014.07.014

Menberu MW, Marttila H, Tahvanainen T, Kotiaho JS, Hokkanen R, Kløve B, et al. (2017) Changes in pore water quality after peatland restoration: assessment of a large-scale, replicated before-after-control-impact study in Finland. *Water Resources Research* 53(10): 8327–8343. https://doi.org/10.1002/2017WR020630

Menberu MW, Tahvanainen T, Marttila H, Irannezhad M, Ronkanen A, Penttinen J, et al. (2016) Water□ table□ dependent hydrological changes following peatland forestry drainage and restoration: analysis of restoration success. *Water Resources Research* 52(5): 3742–3760. https://doi.org/10.1002/2015WR018578

Mendes WDS & Sommer M (2023) Advancing soil organic carbon and total nitrogen modelling in peatlands: the impact of environmental variable resolution and vis-nir spectroscopy integration. *Agronomy* 13(7): 1800. https://doi.org/10.3390/agronomy13071800

Mendes WDS, Sommer M, Koszinski S & Wehrhan M (2022) Peatlands spectral data influence in global spectral modelling of soil organic carbon and total nitrogen using visible-near-infrared spectroscopy. *Journal of Environmental Management* 317: 115383. https://doi.org/10.1016/j.jenvman.2022.115383

Merow C, Smith MJ & Silander JA (2013) A practical guide to maxent for modeling species' distributions: what it does, and why inputs and settings matter. *Ecography* 36(10): 1058–1069. https://doi.org/10.1111/j.1600-0587.2013.07872.x

Minasny B, Berglund Ö, Connolly J, Hedley C, De Vries F, Gimona A, et al. (2019) Digital mapping of peatlands – a critical review. *Earth-Science Reviews* 196: 102870. https://doi.org/10.1016/j.earscirev.2019.05.014

Minayeva TY & Sirin AA (2012) Peatland biodiversity and climate change. *Biology Bulletin Reviews* 2(2): 164–175. https://doi.org/10.1134/S207908641202003X

Minkkinen K, Ojanen P, Koskinen M & Penttilä T (2020) Nitrous oxide emissions of undrained, forestry-drained, and rewetted boreal peatlands. *Forest Ecology and Management* 478: 118494. https://doi.org/10.1016/j.foreco.2020.118494

Minkkinen K, Ojanen P, Penttilä T, Aurela M, Laurila T, Tuovinen J-P, et al. (2018) Persistent carbon sink at a boreal drained bog forest. *Biogeosciences* 15(11): 3603–3624. https://doi.org/10.5194/bg-15-3603-2018

Murphy PNC, Ogilvie J & Arp P (2009) Topographic modelling of soil moisture conditions: a comparison and verification of two models. *European Journal of Soil Science* 60(1): 94–109. https://doi.org/10.1111/j.1365-2389.2008.01094.x

Murphy PNC, Ogilvie J, Meng F & Arp P (2008) Stream network modelling using lidar and photogrammetric digital elevation models: a comparison and field verification. *Hydrological Processes* 22(12): 1747–1754. https://doi.org/10.1002/hyp.6770

National Land Survey of Finland (2025) *Orthophotos and terrain height profiles*. https://kartta.paikkatietoikkuna.fi/?lang=en (accessed 16 January 2026)

Nichols JE & Peteet DM (2019) Rapid expansion of northern peatlands and doubled estimate of carbon storage. *Nature Geoscience* 12(11): 917–921. https://doi.org/10.1038/s41561-019-0454-z

Nimr OA, Marttila H, Batelaan O, Partington D & Ala-Aho P (2026) *How does rewetting propagate through restored peatlands? an integrated surface–subsurface modelling analysis of water–table dynamics*. SSRN. https://doi.org/10.2139/ssrn.6265631

O'Connell JL, Johnson LA, Beas BJ, Smith LM, McMurry ST & Haukos DA (2013) Predicting dispersal-limitation in plants: optimizing planting decisions for isolated wetland restoration in agricultural landscapes. *Biological Conservation* 159: 343–354. https://doi.org/10.1016/j.biocon.2012.10.019

Ojanen P & Minkkinen K (2020) Rewetting offers rapid climate benefits for tropical and agricultural peatlands but not for forestry-drained peatlands. *Global Biogeochemical Cycles* 34(7): e2019GB006503. https://doi.org/10.1029/2019GB006503

Ojanen P, Minkkinen K, Alm J & Penttilä T (2010) Soil–atmosphere co2, ch4 and n2o fluxes in boreal forestry-drained peatlands. *Forest Ecology and Management* 260(3): 411–421. https://doi.org/10.1016/j.foreco.2010.04.036

Ojanen P, Minkkinen K, Alm J & Penttilä T (2018) Corrigendum to "soil–atmosphere co2, ch4 and n2o fluxes in boreal forestry-drained peatlands" [for. ecol. manage. 260 (2010) 411–421]. *Forest Ecology and Management* 412: 95–96. https://doi.org/10.1016/j.foreco.2018.01.020

Ojanen P, Minkkinen K, Lohila A, Badorek T & Penttilä T (2012) Chamber measured soil respiration: a useful tool for estimating the carbon balance of peatland forest soils? *Forest Ecology and Management* 277: 132–140. https://doi.org/10.1016/j.foreco.2012.04.027

Ojanen P, Minkkinen K & Penttilä T (2013) The current greenhouse gas impact of forestry-drained boreal peatlands. *Forest Ecology and Management* 289: 201–208. https://doi.org/10.1016/j.foreco.2012.10.008

Ojanen P, Penttilä T, Tolvanen A, Hotanen J-P, Saarimaa M, Nousiainen H, et al. (2019) Long-term effect of fertilization on the greenhouse gas exchange of low-productive peatland forests. *Forest Ecology and Management* 432: 786–798. https://doi.org/10.1016/j.foreco.2018.10.015

Oke TA & Hager HA (2017) Assessing environmental attributes and effects of climate change on sphagnum peatland distributions in north america using single- and multi-species models. *PLOS ONE* 12(4): e0175978. https://doi.org/10.1371/journal.pone.0175978

Päivänen J (1969) The bulk density of peat and its determination. *Silva Fennica* 3(1). https://doi.org/10.14214/sf.a14569

Pang Y, Räsänen A, Juselius-Rajamäki T, Aurela M, Juutinen S, Väliranta M, et al. (2023) Upscaling field-measured seasonal ground vegetation patterns with sentinel-2 images in boreal ecosystems. *International Journal of Remote Sensing* 44(14): 4239–4261. https://doi.org/10.1080/01431161.2023.2234093

Parkkari M, Parviainen M, Ojanen P & Tolvanen A (2017) Spatial modelling provides a novel tool for estimating the landscape level distribution of greenhouse gas balances. *Ecological Indicators* 83: 380–389. https://doi.org/10.1016/j.ecolind.2017.08.014

Parmesan C (2006) Ecological and evolutionary responses to recent climate change. *Annual Review of Ecology, Evolution, and Systematics* 37(1): 637–669. https://doi.org/10.1146/annurev.ecolsys.37.091305.110100

Parmesan C, Root TL & Willig MR (2000) Impacts of extreme weather and climate on terrestrial biota[*]. *Bulletin of the American Meteorological Society* 81(3): 443–450. https://doi.org/10.1175/1520-0477(2000)081%3C0443:IOEWAC%3E2.3.CO;2

Parviainen M, Zimmermann NE, Heikkinen RK & Luoto M (2013) Using unclassified continuous remote sensing data to improve distribution models of red-listed plant species. *Biodiversity and Conservation* 22(8): 1731–1754. https://doi.org/10.1007/s10531-013-0509-1

Pasquarella VJ, Brown CF, Czerwinski W & Rucklidge WJ (2023) *Comprehensive quality assessment of optical satellite imagery using weakly supervised video learning*. IEEE, Vancouver, BC, Canada. https://doi.org/10.1109/CVPRW59228.2023.00206

Peacock M, Audet J, Bastviken D, Futter MN, Gauci V, Grinham A, et al. (2021) Global importance of methane emissions from drainage ditches and canals. *Environmental Research Letters* 16(4): 044010. https://doi.org/10.1088/1748-9326/abeb36

Pearson RG, Dawson TP & Liu C (2004) Modelling species distributions in britain: a hierarchical integration of climate and land-cover data. *Ecography* 27(3): 285–298. https://doi.org/10.1111/j.0906-7590.2004.03740.x

Phillips SJ, Anderson RP, Dudík M, Schapire RE & Blair ME (2017) Opening the black box: an open□ source release of maxent. *Ecography* 40(7): 887–893. https://doi.org/10.1111/ecog.03049

Phillips SJ, Anderson RP & Schapire RE (2006) Maximum entropy modeling of species geographic distributions. *Ecological Modelling* 190(3–4): 231–259. https://doi.org/10.1016/j.ecolmodel.2005.03.026

Phillips SJ & Dudík M (2008) Modeling of species distributions with maxent: new extensions and a comprehensive evaluation. *Ecography* 31(2): 161–175. https://doi.org/10.1111/j.0906-7590.2008.5203.x.

Pirinen P, Simola H, Aalto J, Kaukoranta J-P, Karlsson P & Ruuhela R (2012) *Climatological statistics of Finland 1981–2010*. Finnish Meteorological Institute, Helsinki. https://helda.helsinki.fi/server/api/core/bitstreams/17a2b5c8-f148-4baf-9ce8-4b74d18b6456/content

Pitkänen TP, Balazs A & Tuominen S (2024) Automatized sentinel-2 mosaicking for large area forest mapping. *International Journal of Applied Earth Observation and Geoinformation* 127: 103659. https://doi.org/10.1016/j.jag.2024.103659

Post E, Alley RB, Christensen TR, Macias-Fauria M, Forbes BC, Gooseff MN, et al. (2019) The polar regions in a 2°c warmer world. *Science Advances* 5(12): eaaw9883. https://doi.org/10.1126/sciadv.aaw9883

Potvin LR, Kane ES, Chimner RA, Kolka RK & Lilleskov EA (2015) Effects of water table position and plant functional group on plant community, aboveground production, and peat properties in a peatland mesocosm experiment (peatcosm). *Plant and Soil* 387(1–2): 277–294. https://doi.org/10.1007/s11104-014-2301-8

Purre A-H, Penttilä T, Ojanen P, Minkkinen K, Aurela M, Lohila A, et al. (2019) Carbon dioxide fluxes and vegetation structure in rewetted and pristine peatlands in finland and estonia. *Boreal Environment Research* 24: 243–261.

Qiu C, Zhu D, Ciais P, Guenet B, Krinner G, Peng S, et al. (2018) ORCHIDEE-peat (revision 4596), a model for northern peatland CO_2, water, and energy fluxes on daily to annual scales. *Geoscientific Model Development* 11(2): 497–519. https://doi.org/10.5194/gmd-11-497-2018

Qiu C, Zhu D, Ciais P, Guenet B, Peng S, Krinner G, et al. (2019) Modelling northern peatland area and carbon dynamics since the holocene with the orchidee-peat land surface model (svn r5488). *Geoscientific Model Development* 12(7): 2961–2982. https://doi.org/10.5194/gmd-12-2961-2019

R Core Team (2025) *R: a language and environment for statistical computing*. R Foundation for Statistical Computing, Vienna, Austria. https://www.R-project.org/.

Raney PA & Leopold DJ (2018) Fantastic wetlands and where to find them: modeling rich fen distribution in new york state with maxent. *Wetlands* 38(1): 81–93. https://doi.org/10.1007/s13157-017-0958-5

Rantanen M, Karpechko AYu, Lipponen A, Nordling K, Hyvärinen O, Ruosteenoja K, et al. (2022) The arctic has warmed nearly four times faster than the globe since 1979. *Communications Earth & Environment* 3(1): 168. https://doi.org/10.1038/s43247-022-00498-3

Räsänen A, Aurela M, Juutinen S, Kumpula T, Lohila A, Penttilä T, et al. (2020) Detecting northern peatland vegetation patterns at ultra-high spatial resolution. *Remote Sensing in Ecology and Conservation* 6(4): 457–471. https://doi.org/10.1002/rse2.140

Räsänen A, Manninen T, Korkiakoski M, Lohila A & Virtanen T (2021) Predicting catchment-scale methane fluxes with multi-source remote sensing. *Landscape Ecology* 36(4): 1177–1195. https://doi.org/10.1007/s10980-021-01194-x

Räsänen A, Tolvanen A & Kareksela S (2022) Monitoring peatland water table depth with optical and radar satellite imagery. *International Journal of Applied Earth Observation and Geoinformation* 112: 102866. https://doi.org/10.1016/j.jag.2022.102866

Räsänen A & Virtanen T (2019) Data and resolution requirements in mapping vegetation in spatially heterogeneous landscapes. *Remote Sensing of Environment* 230: 111207. https://doi.org/10.1016/j.rse.2019.05.026

Renou-Wilson F, Barry C, Müller C & Wilson D (2014) The impacts of drainage, nutrient status and management practice on the full carbon balance of grasslands on organic soils in a maritime temperate zone. *Biogeosciences* 11(16): 4361–4379. https://doi.org/10.5194/bg-11-4361-2014

Richardson CJ, Flanagan NE, Wang H & Ho M (2022) Annual carbon sequestration and loss rates under altered hydrology and fire regimes in southeastern USA pocosin peatlands. *Global Change Biology* 28(21): 6370–6384. https://doi.org/10.1111/gcb.16366

Rochefort L (2000) *Sphagnum* —a keystone genus in habitat restoration. *The Bryologist* 103(3): 503–508. https://doi.org/10.1639/0007-2745(2000)103%5B0503:SAKGIH%5D2.0.CO;2

Roulet N, Moore T, Bubier J & Lafleur P (1992) Northern fens: methane flux and climatic change. *Tellus B: Chemical and Physical Meteorology* 44(2): 100. https://doi.org/10.3402/tellusb.v44i2.15429

Rouse JW, Haas RH, Schell JA & Deering DW (1974) *Monitoring vegetation systems in the great plains with erts*. NASA.

Rydin H & Jeglum JK (2006) *The biology of peatlands*. Oxford University Press. https://doi.org/10.1093/acprof:oso/9780198528722.001.0001

Rydin H & Jeglum JK (2013) *The biology of peatlands*. Oxford University Press. https://doi.org/10.1093/acprof:osobl/9780199602995.001.0001

Saarimaa M, Aapala K, Tuominen S, Karhu J, Parkkari M & Tolvanen A (2019) Predicting hotspots for threatened plant species in boreal peatlands. *Biodiversity and Conservation* 28(5): 1173–1204. https://doi.org/10.1007/s10531-019-01717-8

Sadeghi M, Jones SB & Philpot WD (2015) A linear physically-based model for remote sensing of soil moisture using short wave infrared bands. *Remote Sensing of Environment* 164: 66–76. https://doi.org/10.1016/j.rse.2015.04.007

Salmivaara A (2023) Cartographic depth-to-water (dtw) index map. 2m. CSC – IT Center for Science. http://urn.fi/urn:nbn:fi:att:770f345e-58d4-45e5-b4e7-3fdbd858872f

Sarkkola S, Hökkä H, Koivusalo H, Nieminen M, Ahti E, Päivänen J, et al. (2010) Role of tree stand evapotranspiration in maintaining satisfactory drainage conditions in drained peatlands. *Canadian Journal of Forest Research* 40(8): 1485–1496. https://doi.org/10.1139/X10-084

Sarkkola S, Nieminen M, Koivusalo H, Laurén A, Ahti E, Launiainen S, et al. (2013) Domination of growing-season evapotranspiration over runoff makes ditch network maintenance in mature peatland forests questionable. *Mires & Peat* 11.

Schwieger S, Kreyling J, Couwenberg J, Smiljanić M, Weigel R, Wilmking M, et al. (2021) Wetter is better: rewetting of minerotrophic peatlands increases plant production and moves them towards carbon sinks in a dry year. *Ecosystems* 24(5): 1093–1109. https://doi.org/10.1007/s10021-020-00570-z

Seabrook L, McAlpine C, Rhodes J, Baxter G, Bradley A & Lunney D (2014) Determining range edges: habitat quality, climate or climate extremes? *Diversity and Distributions* 20(1): 95–106. https://doi.org/10.1111/ddi.12152

Similä M, Aapala K & Penttinen J (eds) (2014) *Ecological restoration in drained peatlands: best practices from Finland*. Metsähallitus, Natural Heritage Services, Vantaa.

Small E (1972) Photosynthetic rates in relation to nitrogen recycling as an adaptation to nutrient deficiency in peat bog plants. *Canadian Journal of Botany* 50(11): 2227–2233. https://doi.org/10.1139/b72-289

Smith B, Wårlind D, Arneth A, Hickler T, Leadley P, Siltberg J, et al. (2014) Implications of incorporating n cycling and n limitations on primary production in an individual-based dynamic vegetation model. *Biogeosciences* 11(7): 2027–2054. https://doi.org/10.5194/bg-11-2027-2014

Stickley SF & Fraterrigo JM (2023) Microclimate species distribution models estimate lower levels of climate-related habitat loss for salamanders. *Journal for Nature Conservation* 72: 126333. https://doi.org/10.1016/j.jnc.2023.126333

Strack M (2023) *Peatlands and climate change*. 2nd ed. International Peat Society.

Strack M & Price JS (2009) Moisture controls on carbon dioxide dynamics of peat- *Sphagnum* monoliths. *Ecohydrology* 2(1): 34–41. https://doi.org/10.1002/eco.36

Sun S, Zhang Y, Huang D, Wang H, Cao Q, Fan P, et al. (2020) The effect of climate change on the richness distribution pattern of oaks (quercus l.) in china. *Science of The Total Environment* 744: 140786. https://doi.org/10.1016/j.scitotenv.2020.140786

Swindles GT, Morris PJ, Mullan DJ, Payne RJ, Roland TP, Amesbury MJ, et al. (2019) Widespread drying of european peatlands in recent centuries. *Nature Geoscience* 12(11): 922–928. https://doi.org/10.1038/s41561-019-0462-z

Thuiller W, Lavorel S, Araújo MB, Sykes MT & Prentice IC (2005) Climate change threats to plant diversity in Europe. *Proceedings of the National Academy of Sciences* 102(23): 8245–8250. https://doi.org/10.1073/pnas.0409902102

Tolvanen A, Saarimaa M, Tuominen S & Aapala K (2020) Is 15% restoration sufficient to safeguard the habitats of boreal red-listed mire plant species? *Global Ecology and Conservation* 23: e01160. https://doi.org/10.1016/j.gecco.2020.e01160

UNEP (2022) *Global peatlands assessment: the state of the world's peatlands—evidence for action toward the conservation, restoration, and sustainable management of peatlands*. Global Peatlands Initiative. United Nations Environment Programme, Nairobi. https://wedocs.unep.org/20.500.11822/41222

Urban MC, Bocedi G, Hendry AP, Mihoub J-B, Pe'er G, Singer A, et al. (2016) Improving the forecast for biodiversity under climate change. *Science* 353(6304): aad8466. https://doi.org/10.1126/science.aad8466

Urbanová Z, Bárta J & Picek T (2013) Methane emissions and methanogenic archaea on pristine, drained and restored mountain peatlands, central europe. *Ecosystems* 16(4): 664–677. https://doi.org/10.1007/s10021-013-9637-4

Van Breemen N (1995) How sphagnum bogs down other plants. *Trends in Ecology & Evolution* 10(7): 270–275. https://doi.org/10.1016/0169-5347(95)90007-1

Vasander H (ed.) (1996) *Peatlands in Finland*. Finnish Peatland Society, Helsinki.

Vasander H, Tuittila E-S, Lode E, Lundin L, Ilomets M, Sallantaus T, et al. (2003) Status and restoration of peatlands in northern europe. *Wetlands Ecology and Management* 11(1–2): 51–63. https://doi.org/10.1023/A:1022061622602

Virtanen R, Luoto M, Rämä T, Mikkola K, Hjort J, Grytnes J, et al. (2010) Recent vegetation changes at the high-latitude tree line ecotone are controlled by geomorphological disturbance, productivity and diversity. *Global Ecology and Biogeography* 19(6): 810–821. https://doi.org/10.1111/j.1466-8238.2010.00570.x

Wei Y, Zhang L, Wang J, Wang W, Niyati N, Guo Y, et al. (2021) Chinese caterpillar fungus (ophiocordyceps sinensis) in China: current distribution, trading, and futures under climate change and overexploitation. *Science of The Total Environment* 755: 142548. https://doi.org/10.1016/j.scitotenv.2020.142548

Weiss A (2011) *Topographic position and landforms analysis*. https://env761.github.io/assets/files/tpi-poster-tnc_18x22.pdf (Accessed 14 May 2025)

Wilkinson SL, Andersen R, Moore PA, Davidson SJ, Granath G & Waddington JM (2023) Wildfire and degradation accelerate northern peatland carbon release. *Nature Climate Change* 13(5): 456–461. https://doi.org/10.1038/s41558-023-01657-w

Wilson D, Blain D, Couwenberg J, Evans CD, Murdiyarso D, Page SE, et al. (2016) Greenhouse gas emission factors associated with rewetting of organic soils. *Mires and Peat* 17: 1–28. https://doi.org/10.19189/MAP.2016.OMB.222

Wilson D, Mackin F, Tuovinen J, Moser G, Farrell C & Renou-Wilson F (2022) Carbon and climate implications of rewetting a raised bog in ireland. *Global Change Biology* 28(21): 6349–6365. https://doi.org/10.1111/gcb.16359

Wu H, Zhang Z, Xue Z, Zhao W, Sang L, Wu H, et al. (2025) Predicting the potential geographical distribution of peatlands in northeast China based on the ensemble model. *Global and Planetary Change* 252: 104866. https://doi.org/10.1016/j.gloplacha.2025.104866

Wu J & Roulet NT (2014) Climate change reduces the capacity of northern peatlands to absorb the atmospheric carbon dioxide: the different responses of bogs and fens. *Global Biogeochemical Cycles* 28(10): 1005–1024. https://doi.org/10.1002/2014GB004845

Xu J, Morris PJ, Liu J & Holden J (2018) PEATMAP: refining estimates of global peatland distribution based on a meta-analysis. *CATENA* 160: 134–140. https://doi.org/10.1016/j.catena.2017.09.010

Yu Z, Loisel J, Brosseau DP, Beilman DW & Hunt SJ (2010) Global peatland dynamics since the last glacial maximum. *Geophysical Research Letters* 37(13): 2010GL043584. https://doi.org/10.1029/2010GL043584

Zanatta F, Engler R, Collart F, Broennimann O, Mateo RG, Papp B, et al. (2020) Bryophytes are predicted to lag behind future climate change despite their high dispersal capacities. *Nature Communications* 11(1): 5601. https://doi.org/10.1038/s41467-020-19410-8

Zhu J, Li H, He H, Zhang F, Yang Y & Li Y (2022) Interannual characteristics and driving mechanism of co2 fluxes during the growing season in an alpine wetland ecosystem at the southern foot of the qilian mountains. *Frontiers in Plant Science* 13: 1013812. https://doi.org/10.3389/fpls.2022.1013812

Zoltai SC & Vitt DH (1995) Canadian wetlands: environmental gradients and classification. *Vegetatio* 118(1–2): 131–137. https://doi.org/10.1007/BF00045195